UNIVERSITÀ DI PARMA

UNIVERSITÀ DEGLI STUDI DI PARMA

Dottorato di Ricerca in Scienze Chimiche

Ciclo XXXVI

# Innovative analytical strategies for food safety: biorecognition platforms and emerging mass spectrometry-based techniques


Coordinatore:

Chiar.ma Prof.ssa Alessia Bacchi

Tutor:

Chiar.ma Prof.ssa Monica Mattarozzi

Dottorando:

Lorenzo Toma


Anni accademici 2020/21 – 2023/24

UNIVERSITÀ DI PARMA

UNIVERSITÀ DEGLI STUDI DI PARMA

Ph.D. Course in Chemical Sciences

Cycle XXXVI

# Innovative analytical strategies for food safety: biorecognition platforms and emerging mass spectrometry-based techniques


Coordinator:

Prof. Alessia Bacchi

Tutor:

Prof. Monica Mattarozzi

Ph.D. candidate:

Lorenzo Toma


Academic years 2020/21 – 2023/24

## INDEX Page

# Abstract (eng)

The present PhD Thesis explores innovative analytical methods for the detection of hidden allergens from food or food-related samples. Hidden allergens in food pose a significant food safety concern, leading to a wide range of hypersensitivity reactions in adult and child consumers. When food allergens, commonly proteins or glicoproteins, are deliberately added to food but not declared on product labels or are present unintentionally due to cross-contamination, they become hidden allergens. Compliance with food labeling regulations, such as EU Regulation No. 1169/2011, is vital to prevent adverse reactions and misuse of precautionary labels, despite the lack of specific regulation for hidden allergens. Currently, there is no cure for food allergy, necessitating the careful avoidance of allergenic foods. In this context, there is a call for sensitive and reliable methods for the determination of allergenic components in food. Innovative mass spectrometry techniques and biorecognition platforms, also based on micro- and nanosized materials, emerged as important analytical advancements with potential in the field of food allergens [1].

A general introduction (Chapter 1) about new trends and perspectives in analytical chemistry, with particular attention to ambient mass spectrometry and biosensing platforms, is followed by two chapters (Chapter 2 and Chapter 3) both focalized on lysozyme from chicken egg as case study of an allergenic protein.

Chapter 2 was aimed at investigating the potentialities of aptamers as emerging biomimetic receptors for selective and high-affinity recognition of allergenic proteins [2]. A critical assessment of potentialities and limits of anti-lysozyme aptamers, depending on different conditions that influence binding to the target, is performed by means of a properly devised multi-technique approach, which involved fluorescence titration, circular dichroism, electrochemical apta-assay, and asymmetrical flow field-flow fractionation [3,4]. To the best of our knowledge, this represents one of the first studies that critically determines the actual potentialities of aptamers throughout a “multifaceted analytical approach” [5], and the first of its kind regarding anti-lysozyme aptamers.

Chapter 3 was aimed at investigating the potentialities of Swab Touch Spray-Mass Spectrometry (Swab TS-MS), an Ambient Mass Spectrometry (AMS) technique, for the detection of surface-contaminating allergenic proteins. Since Swab TS-MS exploits the swab used for sampling as a probe for direct ionization [6], this technique resulted particularly suitable for the intended purpose. After preliminary experiments proving Swab TS-MS feasibility for the detection of proteins (after digestion), a study of the experimental conditions was performed; analytical quality parameters were assessed carrying out experiments also with egg white powder matrix. In parallel, swabbing strategies were studied by conventional hyphenated LC-ESI-MS/MS method, developing an *in situ*

*digestion/swabbing* strategy to be directly coupled with Swab TS-MS approach. To the best of our knowledge, this represent the first time Swab TS-MS is exploited for detection of proteins, developing a method that could be used for the development of cleaning procedures. In addition, potentialities of Paper Spray-MS (PS-MS) were investigated as an alternative AMS method for protein detection.

## Bibliography


(1) Martins, R. O.; de Araújo, G. L.; de Freitas, C. S.; Silva, A. R.; Simas, R. C.; Vaz, B. G.; Chaves, A. R. Miniaturized Sample Preparation Techniques and Ambient Mass Spectrometry as Approaches for Food Residue Analysis. *J Chromatogr A* **2021**, *1640*. https://doi.org/10.1016/j.chroma.2021.461949.

(2) Mattarozzi, M.; Toma, L.; Bertucci, A.; Giannetto, M.; Careri, M. Aptamer-Based Assays: Strategies in the Use of Aptamers Conjugated to Magnetic Micro- and Nanobeads as Recognition Elements in Food Control. *Anal Bioanal Chem* **2022**, *414* (1), 63-74. https://doi.org/10.1007/s00216-021-03501-6.

(3) Marassi, V.; Mattarozzi, M.; Toma, L.; Giordani, S.; Ronda, L.; Roda, B.; Zattoni, A.; Reschiglian, P.; Careri, M. FFF-Based High-Throughput Sequence Shortlisting to Support the Development of Aptamer-Based Analytical Strategies. *Anal Bioanal Chem* **2022**, *414* (18), 5519-5527. https://doi.org/10.1007/s00216-022-03971-2.

(4) Toma, L.; Mattarozzi, M.; Ronda, L.; Marassi, V.; Zattoni, A.; Fortunati, S.; Giannetto, M.; Careri, M. Are Aptamers Really Promising as Receptors for Analytical Purposes? Insights into Anti-Lysozyme DNA Aptamers through a Multi-Technique Study. *Anal Chem*, *in press* (accepted on 17 January **2024**).

(5) Bottari, F.; Daems, E.; De Vries, A. M.; Van Wielendaele, P.; Trashin, S.; Blust, R.; Sobott, F.; Madder, A.; Martins, J. C.; De Wael, K. Do Aptamers Always Bind? The Need for a Multifaceted Analytical Approach When Demonstrating Binding Affinity between Aptamer and Low Molecular Weight Compounds. *J Am Chem Soc* **2020**, *142* (46), 19622–19630. https://doi.org/10.1021/jacs.0c08691.

(6) Jarmusch, A. K.; Pirro, V.; Logsdon, D. L.; Cooks, R. G. Direct Ion Generation from Swabs. *Talanta* **2018**, *184*, 356–363. https://doi.org/10.1016/j.talanta.2018.02.105.

# Abstract (ita)

La presente Tesi di Dottorato riguarda l'investigazione di strategie analitiche innovative per la rivelazione di allergeni nascosti negli alimenti e in prodotti ad essi correlati. La tematica degli allergeni è di particolare interesse nell'ambito della sicurezza alimentare, in quanto possono provocare reazioni di ipersensibilità con conseguenze molto gravi per i consumatori. Quando gli allergeni alimentari, comunemente proteine o glicoproteine, vengono deliberatamente aggiunti al cibo ma non dichiarati nelle etichette dei prodotti o sono presenti involontariamente a causa di cross-contaminazione, vengono denominati "allergeni nascosti". L'ottemperanza al Regolamento Europeo N. 1169/2011 sull'etichettatura degli alimenti è di enorme importanza per prevenire reazioni avverse e una scorretta etichettatura dei prodotti alimentari, nonostante sia assente un regolamento specifico per gli allergeni nascosti. Attualmente, non esiste una cura per le allergie alimentari, il che rende fondamentale evitare il consumo di ingredienti allergenici. In questo ambito, sono necessari metodi analitici affidabili per la determinazione di proteine allergeniche in alimenti. Tecniche innovative basate sulla spettrometria di massa o sull'uso di elementi di bioriconoscimento, in associazione a micro- e nanomateriali, sono emerse negli ultimi anni come importanti sviluppi analitici, con un notevole potenziale nel campo di applicazione degli allergeni alimentari [1].

La Tesi è composta da tre capitoli: nel Capitolo 1 è presente una introduzione generale riguardo le nuove tendenze e prospettive in chimica analitica, con un particolare focus sulla spettrometria di massa e le piattaforme biosensoristiche; i seguenti due capitoli riguardano le attività di ricerca svolte durante il periodo del Dottorato di ricerca, entrambe aventi come caso di studio la proteina allergenica lisozima da bianco d'uovo.

Il Capitolo 2 riguarda l'investigazione delle potenzialità degli aptameri come elementi di riconoscimento biomimetico ad alta affinità e selettività di un determinato target [2]. In particolare, viene effettuata una valutazione critica delle potenzialità e dei limiti di aptameri selezionati per riconoscere con alta affinità il lisozima; la valutazione tiene in considerazione le differenti condizioni che influenzano il legame al target, attraverso un approccio multi-tecnica, che comprende le tecniche di spettroscopia di fluorescenza, dicroismo circolare, apta-saggio elettrochimico, frazionamento in campo flusso - flusso asimmetrico (AF4) [3,4]. Il presente studio si inserisce tra i primi volti ad evidenziare alcune rilevanti criticità associate ad aptameri già ampiamente utilizzati in letteratura [5], focalizzando l'attenzione sugli aptameri anti-lisozima.

Il Capitolo 3 riporta la valutazione delle potenzialità della tecnica Swab Touch Spray-Mass Spectrometry (Swab TS-MS), facente parte del gruppo di tecniche *Ambient Mass Spectrometry* (AMS), per la rivelazione di residui di proteine allergeniche su superfici di lavoro. Poichè la tecnica

Swab TS-MS sfrutta lo swab utilizzato per il campionamento da superficie come un supporto per la ionizzazione [6], questa tecnica è particolarmente adatta per lo scopo previsto. Dopo esperimenti preliminari che dimostrano la capacità della tecnica Swab TS-MS nel rilevare le proteine (in seguito a digestione enzimatica), è stato condotto uno studio sulle condizioni sperimentali da utilizzare per l'analisi; i parametri di qualità analitica sono stati valutati effettuando anche analisi su matrice di bianco d'uovo in polvere. In parallelo, sono state studiate delle strategie di campionamento con swab con rivelazione attraverso tecnica LC-ESI-MS/MS, che ha permesso di sviluppare una procedura di digestione *in situ* seguita da campionamento per il diretto accoppiamento con la tecnica Swab TS-MS. Al meglio delle nostre conoscenze, questa rappresenta la prima volta in cui la tecnica Swab TS-MS viene sfruttata per la rivelazione di proteine, sviluppando un metodo che potrebbe essere utilizzato per lo sviluppo di nuove procedure di pulizia di superfici di lavoro. Inoltre, sono state indagate le potenzialità della tecnica Paper Spray-MS (PS-MS) come metodo AMS alternativo per la rivelazione di proteine.

## Bibliography


(1) Martins, R. O.; de Araújo, G. L.; de Freitas, C. S.; Silva, A. R.; Simas, R. C.; Vaz, B. G.; Chaves, A. R. Miniaturized Sample Preparation Techniques and Ambient Mass Spectrometry as Approaches for Food Residue Analysis. *J Chromatogr A* **2021**, *1640*. https://doi.org/10.1016/j.chroma.2021.461949.

(2) Mattarozzi, M.; Toma, L.; Bertucci, A.; Giannetto, M.; Careri, M. Aptamer-Based Assays: Strategies in the Use of Aptamers Conjugated to Magnetic Micro- and Nanobeads as Recognition Elements in Food Control. *Anal Bioanal Chem* **2022**, *414* (1), 63-74. https://doi.org/10.1007/s00216-021-03501-6.

(3) Marassi, V.; Mattarozzi, M.; Toma, L.; Giordani, S.; Ronda, L.; Roda, B.; Zattoni, A.; Reschiglian, P.; Careri, M. FFF-Based High-Throughput Sequence Shortlisting to Support the Development of Aptamer-Based Analytical Strategies. *Anal Bioanal Chem* **2022**, *414* (18), 5519-5527. https://doi.org/10.1007/s00216-022-03971-2.

(4) Toma, L.; Mattarozzi, M.; Ronda, L.; Marassi, V.; Zattoni, A.; Fortunati, S.; Giannetto, M.; Careri, M. Are Aptamers Really Promising as Receptors for Analytical Purposes? Insights into Anti-Lysozyme DNA Aptamers through a Multi-Technique Study. *Anal Chem*, *in press* (accepted on 17 January **2024**).

(5) Bottari, F.; Daems, E.; De Vries, A. M.; Van Wielendaele, P.; Trashin, S.; Blust, R.; Sobott, F.; Madder, A.; Martins, J. C.; De Wael, K. Do Aptamers Always Bind? The Need for a Multifaceted Analytical Approach When Demonstrating Binding Affinity between Aptamer and Low Molecular Weight Compounds. *J Am Chem Soc* **2020**, *142* (46), 19622–19630. https://doi.org/10.1021/jacs.0c08691.

(6) Jarmusch, A. K.; Pirro, V.; Logsdon, D. L.; Cooks, R. G. Direct Ion Generation from Swabs. *Talanta* **2018**, *184*, 356–363. https://doi.org/10.1016/j.talanta.2018.02.105.

# Abbreviations and acronyms

| | |
|---|---|
| AF4 | Asymmetrical Flow Field-Flow Fractionation |
| AMS | Ambient Mass Spectrometry |
| CD | Circular Dichroism |
| DDA | Data-Dependent Acquisition |
| DPV | Differential Pulse Voltammetry |
| ESI | Electrospray Ionization |
| GAC | Green Analytical Chemistry |
| HRMS | High-Resolution Mass Spectrometry |
| LC | Liquid chromatography |
| MB | Magnetic Bead |
| MP | Magnetic Particle |
| MSPE | Magnetic Solid-Phase Extraction |
| PS-MS | Paper Spray–Mass Spectrometry |
| Q | Quadrupole |
| SELEX | Systematic Evolution of Ligands by Exponential Enrichment |
| SPE | Solid-Phase Extraction |
| Swab TS–MS | Swab Touch Spray–Mass Spectrometry |
| TS | Touch Spray |

# Objectives and structure of the Thesis

The present PhD Thesis explores innovative analytical methods for detection of hidden allergens from food or food-related samples. Hidden allergens in food pose a significant food safety concern, leading to a wide range of hypersensitivity reactions in adult and child consumers. When food allergens, commonly proteins or glicoproteins, are deliberately added to food but not declared on product labels, or are present unintentionally due to cross-contamination, they become hidden allergens. Compliance with food labeling regulations, such as EU Regulation No. 1169/2011, is vital to prevent adverse reactions and misuse of precautionary labels, despite the lack of specific regulation for hidden allergens. Currently, there is no cure for food allergies, necessitating the careful avoidance of allergenic foods. In this context, there is a call for sensitive and reliable methods for specific determination of allergenic components in food. Innovative mass spectrometry techniques and biorecognition platforms, also based on micro- and nanosized materials, emerged as important analytical advancements with potentialities in the field of food allergens.

The present dissertation consists in three chapters, here described:

- Chapter 1: a starting introduction about new trends and perspectives in analytical chemistry, with particular attention to ambient mass spectrometry (AMS) and strategies based on the use of bioreceptors [1]. The role of aptamers, single stranded DNA or RNA molecules used for binding with high affinity a particular target, is discussed, in view of the possible analytical application of these bioreceptors for the development of biosensing devices and miniaturized sample treatment techniques. A relevant analytical advancement in this context is represented by the use of micro- and nanosized materials, such as magnetic beads (MBs), with potential in the food allergen field of application [2]. AMS represents another new trend in analytical chemistry, enabling rapid and direct analysis, especially for screening and qualitative investigation, in which High Resolution MS could enable performing selective and high-throughput analysis, also *in situ* in case of having a portable mass spectrometer. Accordance with Green Analytical Chemistry (GAC) principles is a characteristic of miniaturized sample treatment procedure as well as of AMS techniques [1];
- Chapter 2: potentialities of DNA anti-lysozyme aptamers as biomimetic receptors for selective/specific and high-affinity recognition of lysozyme were assessed with the perspective of the development of competitive aptasensors and magnetic bead-based sample treatment step for enrichment of the protein from food samples [4]. A critical assessment of potentialities of the investigated anti-lysozyme aptamers, depending on different conditions that influence binding to the target, was performed by means of a multitechnique approach which involved fluorescence titration, circular dicroism (CD), electrochemical apta-assay, and asymmetrical flow field-flow fractionation

(AF4). To the best of our knowledge, this represents one of the first studies that critically determines the actual potentialities of aptamers throughout a "multifaceted analytical approach", as prompted by Bottari et al. in 2020 [5], and the first of its kind regarding lysozyme as target;

- Chapter 3: activities regarded the development of a Swab Touch Spray-MS (Swab TS-MS) method for the analysis of lysozyme from chicken egg, followed by the assessment of the analytical quality parameters. Swab TS-MS belongs to AMS techniques and is particularly suited for rapid analysis of surface residues, since it exploits a nasopharyngeal swab for sampling from a surface or a tissue, and then immediately converted into a support for ionization from the tip [6]. In this case, for the first time, potentialities of the Swab TS-MS technique were investigated to develop a rapid, direct and high-throughput analysis for determination of allergenic proteins residues on food preparation surfaces by swabbing test. For this reason, activities focused also on investigating swabbing strategies by LC-ESI-MS/MS method. Moreover, suitability of Paper Spray–MS was investigated for detection of proteins or tryptic peptides, as a possible alternative to Swab TS-MS.

The experimental activities concerning the AMS techniques were carried out during the 6-months visiting period at the University of Barcelona (Spain), under the supervision of Professor Encarnación Moyano Morcillo.

Chapters 2 and 3 are constituted of a specific introduction, then presenting experimental section, different experimental groups, and final conclusions.

## Bibliography

(1) Martins, R. O.; de Araújo, G. L.; de Freitas, C. S.; Silva, A. R.; Simas, R. C.; Vaz, B. G.; Chaves, A. R. Miniaturized Sample Preparation Techniques and Ambient Mass Spectrometry as Approaches for Food Residue Analysis. *J Chromatogr A* **2021**, *1640*. https://doi.org/10.1016/j.chroma.2021.461949.

(2) Mattarozzi, M.; Toma, L.; Bertucci, A.; Giannetto, M.; Careri, M. Aptamer-Based Assays: Strategies in the Use of Aptamers Conjugated to Magnetic Micro- and Nanobeads as Recognition Elements in Food Control. *Anal Bioanal Chem* **2022**, *414* (1), 63-74. https://doi.org/10.1007/s00216-021-03501-6.

(3) Marassi, V.; Mattarozzi, M.; Toma, L.; Giordani, S.; Ronda, L.; Roda, B.; Zattoni, A.; Reschiglian, P.; Careri, M. FFF-Based High-Throughput Sequence Shortlisting to Support the

Development of Aptamer-Based Analytical Strategies. *Anal Bioanal Chem* **2022**, *414* (18), 5519-5527. https://doi.org/10.1007/s00216-022-03971-2.

(4) Toma, L.; Mattarozzi, M.; Ronda, L.; Marassi, V.; Zattoni, A.; Fortunati, S.; Giannetto, M.; Careri, M. Are Aptamers Really Promising as Receptors for Analytical Purposes? Insights into Anti-Lysozyme DNA Aptamers through a Multi-Technique Study. *Anal Chem*, *in press* (accepted on 17 January **2024**).

(5) Bottari, F.; Daems, E.; De Vries, A. M.; Van Wielendaele, P.; Trashin, S.; Blust, R.; Sobott, F.; Madder, A.; Martins, J. C.; De Wael, K. Do Aptamers Always Bind? The Need for a Multifaceted Analytical Approach When Demonstrating Binding Affinity between Aptamer and Low Molecular Weight Compounds. *J Am Chem Soc* **2020**, *142* (46), 19622–19630. https://doi.org/10.1021/jacs.0c08691.

(6) Jarmusch, A. K.; Pirro, V.; Logsdon, D. L.; Cooks, R. G. Direct Ion Generation from Swabs. *Talanta* **2018**, *184*, 356–363. https://doi.org/10.1016/j.talanta.2018.02.105.

# 1. Analytical trends in food quality and safety

Within contemporary hot topics in analytical chemistry, relevant advancements were performed in food safety. In fact, the new challenges in the food production such as the reduction of environmental impact and the simultaneous demand increase, due to the worldwide population growth, led industry towards relevant changes in all steps of the food chain [1]. Analytical chemistry plays a key-role in this context for many purposes such as quality control, safety for human health, and environmental sustainability [2]. Many parallel steps were moved towards the increase of analytical performance and, in parallel, the reduction of the environmental impact [3,4]. In the last two decades the "Green Analytical Chemistry" and its principles became a new reference to face during the method development [5]. As a result, new procedures were developed towards the reduction of sample and extractant volumes, energy consumption, waste production, limited use of disposable components and replacement of polluting solvents with greener alternatives [6]. Most of these goals were achieved thanks to miniaturization of instruments and approaches, which is still a contemporary trend that can be intended also as the opportunity to fully exploit their potential [7].

Mass spectrometry and biosensors were within the techniques who benefitted more from these changes. In fact, both were improved in terms of analytical performance with the simultaneous miniaturization of their dimension, in compliance with the GAC requirements cited before [8]. A second huge advantage of biosensors and mass spectrometry is their high selectivity/specificity that make them suitable for direct analysis (especially for sensors [9] but also for some MS-based techniques like Ambient-MS [10]) or for procedure with streamlined sample preparation (common in dilute-and-shoot LC-MS metabolomics and HS-SPME-GC-MS flavoromics [11]). The visual roadmap reported in **Figure 1.1** addresses all these key themes, that are explored in the present Thesis.

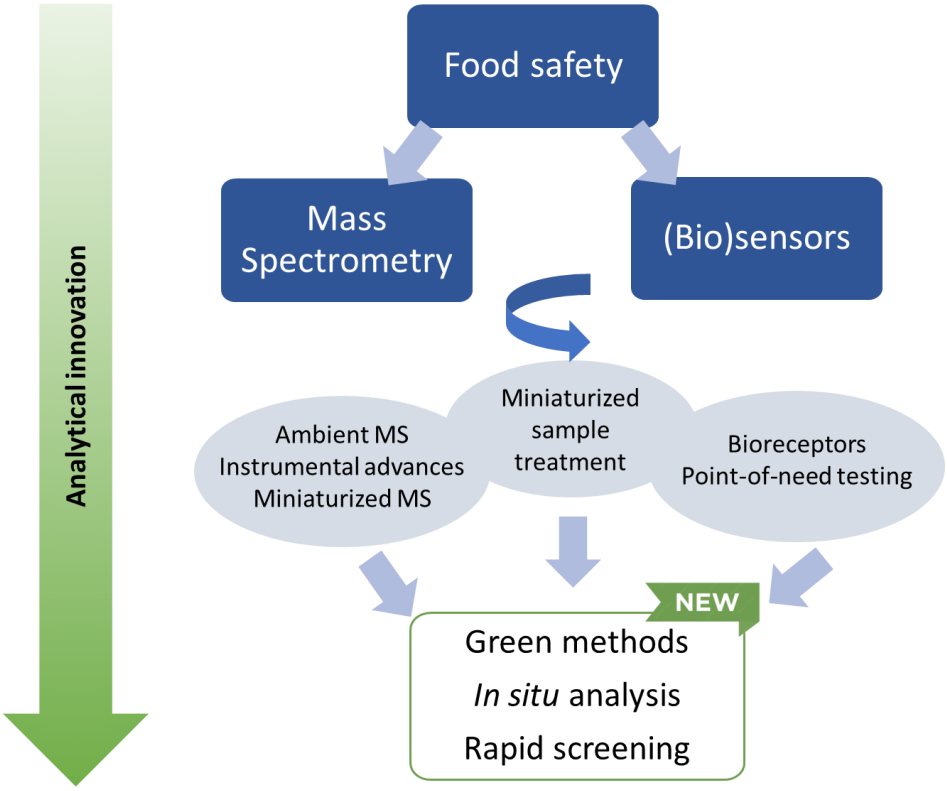


**Figure 1.1**. Visual roadmap on the current innovation in analytical chemistry in the field of food safety

In particular, MS-based techniques have undergone continuous development, reaching unrivalled sensibility, selectivity, and versatility for qualitative and quantitative chemical analysis. For this reason, MS finds applications in many fields of science, spanning from omics to rigorous quantitative procedures to imaging, through untargeted or target approaches [12]. MS versatility is the reason of its use in the most diverse fields of applications, from food safety concerns to environmental analysis, not to mention forensic medicine, clinical investigation, and defense. Nowadays, both GC-MS and LC-MS techniques are the gold standard for food safety and food quality purpose, especially for complex food matrices [13]. However, the availability of portable miniaturized mass spectrometers and the development of ambient ionization techniques (Ambient-MS or AMS) are boosting the application of on-site analyses, such as detection systems for explosives and useful instruments for space missions [14–17]. Another technology that deserves to be mentioned is the coupling of mass spectrometry with ion mobility systems (IMS-MS), that allows separation of gaseous ions according to their mobility through an inert gas under the influence of an electric field [18]; IMS-MS provides an additional separation dimension in combination with the high versatility, selectivity, sensitivity and structural characterization potential of mass spectrometry, resulting in a very powerful tool, both for target and untarget analysis [19]. The new separation dimension of IMS-MS further strengthens the potential of direct, chromatography-free approaches like Ambient-MS [20,21], with particular relevance

for imaging mass spectrometry [22,23]. In Ambient-MS, analytes are submitted to the ionization process directly from samples in their native state or after deposition onto an ionization support. With Ambient-MS it is possible to directly analyze a sample with no (or a simple) sample preparation, minimal solvent consumption for extraction without chromatographic separation, and it can be also intended as a non-destructive technique. In all cases, in Ambient-MS the identification of compounds in the mixture is only based on their *m/z* ratio, so it can strongly benefit from high-resolution analyzers and/or IMS-MS [24]. On the other hand, Ambient-MS is not suitable for accurate compound discovery, accurate quantification, presenting also lower sensitivity and precision in comparison with conventional hyphenated MS techniques, especially when moving to complex matrices [25]. Ambient-MS is mostly famous for the direct detection of explosives and drugs in the forensic field, but some interesting applications were performed in food safety for the detection of hazardous residues [26,27], and in food authenticity for discovering some frauds [28].

In addition to the use of advanced instrumental configurations and acquisition modes, analytical selectivity can be achieved also by the incorporation into the analytical platform of a biological recognition element, such as enzyme, antibody, or aptamer, able to interact selectively with the target for its determination [29]. Over the past 15 years, biosensors research has attracted enormous interest in analytical chemistry, leading to the development of analytical devices that integrate a biological recognition element with a transduction element able to convert the biorecognition event into a measurable signal. Biosensors cover a wide range of applications in food, environmental, medicine and biology fields [9,30,31]. To meet the increasing demand for *in-situ* analysis, such as point-of-need or point-of-care testing (POC), and improve analytical performance, in the recent decade the miniaturization trend has strongly influenced the biosensing research, boosting the use of micro- and nanomaterials, micro-and nano- fabrication technologies, even towards microfluidic devices [32]. Biorecognition elements in combination with micro- and nanomaterial supports can be exploited not only for the development of biosensors, but also to devise sample treatment techniques aimed at improving efficiency of analyte pre-concentration and enrichment; this can be fundamental to reach adequate sensitivity and selectivity, especially in complex matrices. The exploitation of these micro- and nanomaterials facilitates the downscaling of conventional analytical and bioanalytical systems, that involves reducing volumes for samples, solvents, and waste, resulting in greener and cost-effective analytical processes [5,7,33,34]. Downscaling of miniaturized supports from sample treatment contributes to the greenness of (bio)sensors, that already present several green characteristics: although not providing the maximum specificity and accuracy compared to other methods, sensors generate little or no waste, require minimal amounts of sample volume, reducing quantities of reagents or solvents, provide a rapid analysis, that can be performed on-site for remote monitoring.

Basically, the concept of sensor involves a cheap, small, and easy-to-use device, giving great relevance to portability; all of these characteristics meet GAC principles [35].

The present introduction will examine some of the main trends in analytical chemistry: (i) biorecognition platforms based on the interaction between the bioreceptor and the target analyte for biosensing or sample treatment purposes. In particular, the focus is paid on aptamers as emerging biomimetic receptors; (ii) evolution of innovative Ambient Mass spectrometry techniques, taking into account the recent advancements connected to miniaturization of mass spectrometers, leading to a shift toward *in situ* analysis.
The theme of Green Analytical chemistry will be discussed throughout the whole section, keeping a particular focus on food safety field of application, especially for detection and quantification of allergenic proteins from foods.

## 1.1. Aptamers as biorecognition elements

Different analytical approaches, especially biosensors but also some sample treatment procedures, are based on the exploitation of biorecognition elements capable of recognizing analyte with high affinity and selectivity. Biorecognition elements include antibodies, enzymes, aptamers, and molecularly imprinted polymers (MIPs), each of them presenting different characteristics that influence performances of analytical methods [29]. In the present dissertation, particular attention will be given to aptamers, bioinspired molecules that recently gained attention in scientific community as bioreceptors, taking into consideration possible applications, as well as discussing the limits reported in literature.
The term "aptamer", deriving from the Latin "apto" (to fit) and the Greek "meros" (part), was first used in 1990 by Ellington and Szostak to describe RNA molecules that bound a small organic dye [36]. Aptamers are short single-stranded RNA or DNA molecules (~ 20-100 bases) having a stable tridimensional structure, whose sequence is selected from an oligonucleotide library, by means of a SELEX (Systematic Evolution of Ligands by Exponential Enrichment) procedure to bind a predefined target [36–38]. Aptamers are reported to recognize and interact to targets that cover a high range of dimensions (**Figure 1.2**), such as metallic ions, small molecules, proteins and even cells. Due to their promising analytical, diagnostic and therapeutic performance and antibody-like properties in terms of affinity, in the last years an increasing number of aptamer sequences has been reported in literature as biomimetic receptors, with dissociation constants ($K_D$) from micro- to picomolar level [39].

The growing interest towards aptamers relies on several advantages showed over antibodies, such as:

- simple and inexpensive *in vitro* synthesis;
- lesser scale;
- low or absent immunogenicity;
- high reproducibility between different batches;
- easy binding of certain functional groups or chemical molecules;
- possibility of conformational change, to be exploited for specific applications;
- deep penetration into tissues of interest at a diagnostic and clinical level, given their small size.

Such advantages have been crucial in determining an ever-growing attention and application of aptamers in several areas, especially replacing antibodies, including analytical chemistry [37,39,40].

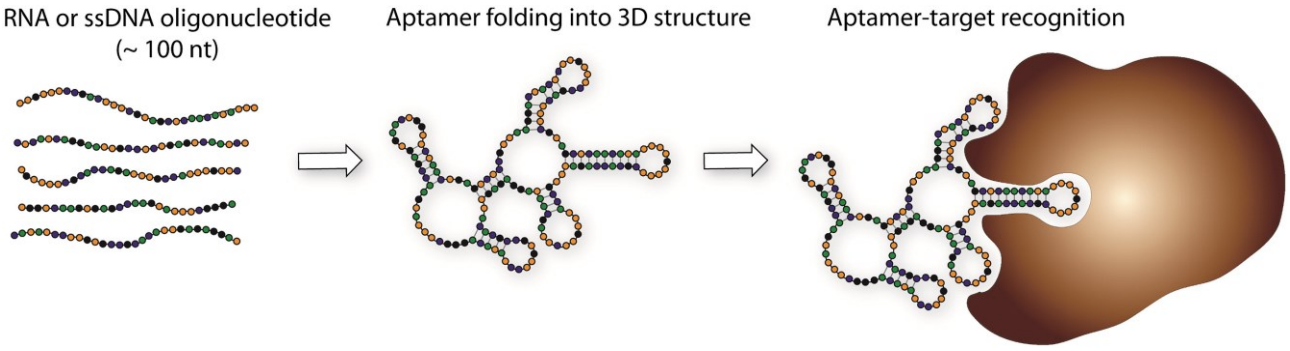


**Figure 1.2**. ssDNA or RNA folding and binding to a target compound. Reprinted from Ref. [37] Copyright © 2023, with permission from Elsevier

To obtain aptamers with high affinity for target molecules, the SELEX method involves iterative steps of binding, separation, dissociation from the target, and amplification. SELEX starts from an oligonucleotide library consisting of about $10^{12}$-$10^{15}$ DNA or RNA oligos. Sequences are composed of a randomized central portion (usually 30-80 base pairs long), differentiating each oligo of the pool, and a constant flanking region of 15-25 base pairs, having the function of primer during the amplification phase for polymerase chain reaction (PCR), fundamental for performing multiple cycles of selection.

Different SELEX variants are known, such as immunoprecipitation-coupled SELEX (IP-SELEX), capture-SELEX, cell-SELEX, capillary electrophoresis-SELEX (CE-SELEX), or even Animal-SELEX, exploiting different techniques and approaches for performing sequence selection, and having peculiar characteristics, advantages and limitations [41].

Although presenting a wide range of variants, all SELEX methods involve four main steps, presented in **Figure 1.3**. First, the target of interest, free or bound to solid supports such as magnetic beads or agarose resins, is incubated with the pool of the library. Then, the target-binding oligonucleotides are separated from the unbound ones. The bound sequences are eluted from the target and amplified by PCR (or RT-PCR, in case of an RNA library), permitting to perform several rounds of selection. At the end, enriched oligonucleotide will be sequenced [41].

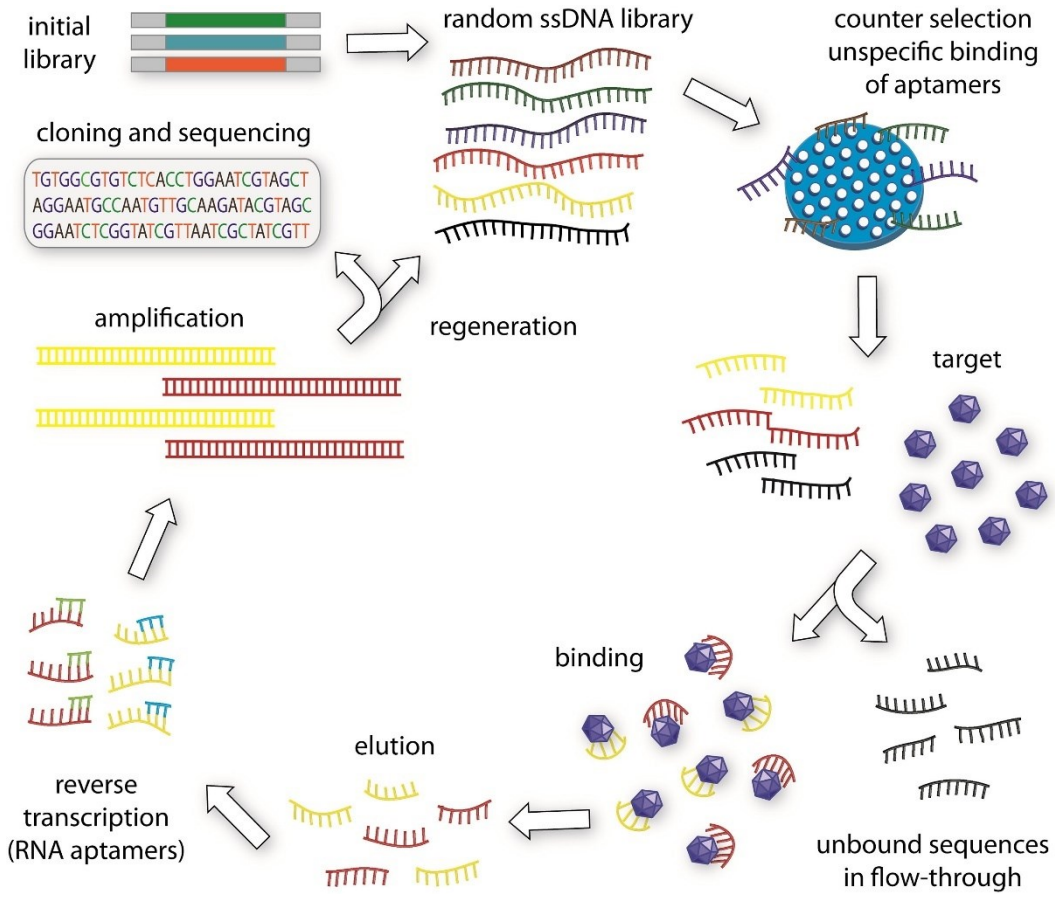


**Figure 1.3.** Schematic representation of SELEX procedure for aptamer selection [37]. Reprinted from Ref. [37] Copyright © 2023, with permission from Elsevier

Design of SELEX ensures that binding of any selected molecule can be attributed only on its specific interactions to the target, which are related to the structural patterns formed, and thus to the sequence of the single aptamer. In fact, selected sequences will present a particular three-dimensional structure that enables binding to the target. From a structural point of view, aptamers are characterized by motifs of secondary and tertiary structure, that include stem-loops, pseudoknots, hairpins, bulges; these elements promote recognition of target molecules by intermolecular interactions, like hydrogen bonds, electrostatic interactions, van der Waals forces, π-π stacking interactions [42] (**Figure 1.4**).

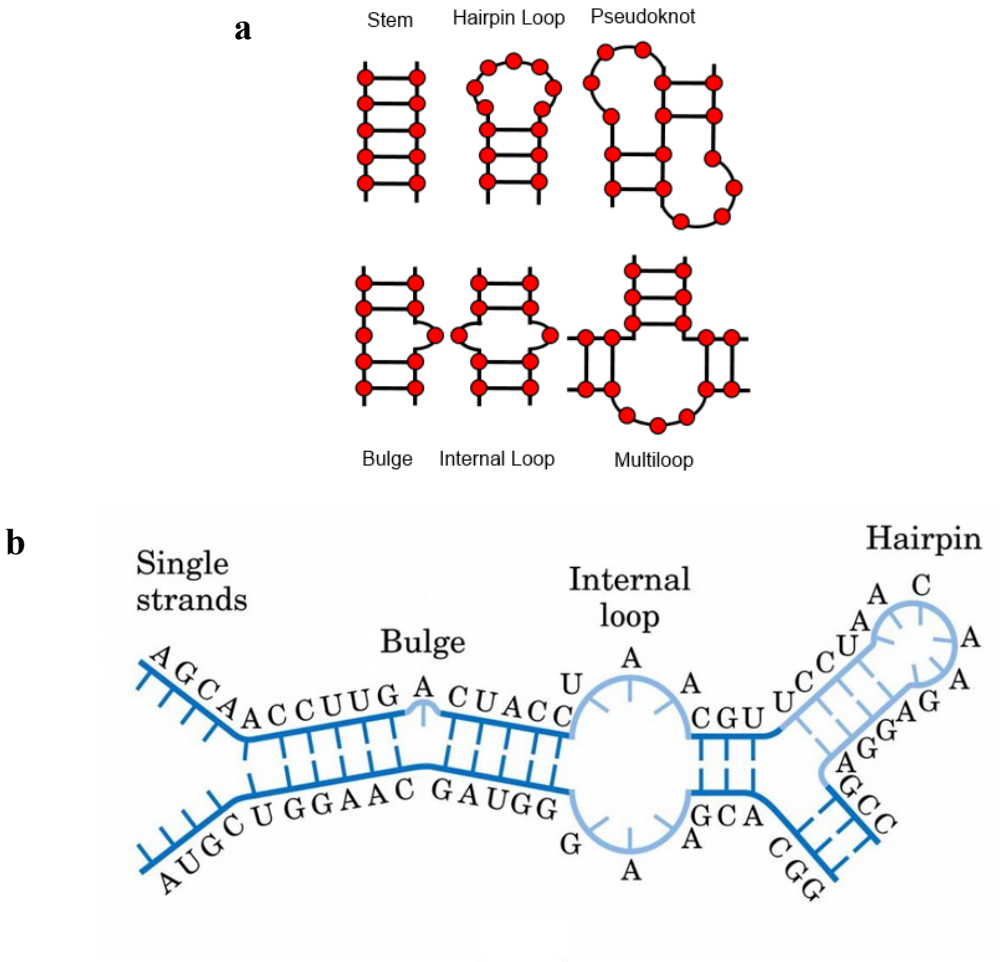


**Figure 1.4. a)** Secondary structure common elements in oligonucleotide sequences. Reprinted from Ref. [43] © 2023; **b)** Typical 2D-structure of an oligonucleotide sequence, that embeds different motifs of secondary structure

The buffer in which SELEX is performed represents a crucial variable for selection of the sequence presenting the best affinity. Typically, selectivity of aptamers for a particular target is hindered by non-specific electrostatic interaction between the negatively charged backbone of oligonucleotides and interfering molecules possibly present. To overcome this limit, selection is done in a binding buffer containing monovalent and bivalent ions ($Na^+$, $K^+$, $Mg^{2+}$, $Ca^{2+}$, etc.), shielding the negatively charged phosphates of oligonucleotides [42]. Other solutions are known, such as utilization of peptide nucleic acids, or addition of chemical modifications on aptamers [29]. This aspect of binding, together with other concerns related to the specificity of binding and the importance of the conditions exploited for recognition of the target, are addressed by a Trend Article written in our research group [32]. In the article, that will be referred more times throughout this dissertation, aptamers are discussed in view of the exploitation as biorecognition elements conjugated to magnetic micro- and nanobeads in food

control field of application. In this perspective, the strict control of binding condition is a critical aspect to take into account when moving from standard solutions exploited in SELEX procedure to real matrix extracts, thus requiring a rigorous characterization of binding performances and dependance of binding from different factors (pH, ionic strength, presence of interferent compounds) [32,44,45].

A perfect example of an aptamer-target system whose binding was carefully investigated by combining data from different techniques is the thrombin binding aptamer (TBA), particularly promising for clinical applications as anticoagulant. First introduced to the scientific community in 1992 [46], investigators have conducted comprehensive studies on its structural attributes, binding sites, and stability in both controlled laboratory settings and within living organisms. In the work conducted by P.-H. Lin et al [47], circular dichroism (CD) technique was employed to study binding parameters (salts concentration, presence of interferent compounds), investigating the effect of these on aptamer conformation. Surface Plasmon Resonance (SPR) and Isothermal Titration Calorimetry (ITC) permitted to obtain information on kinetics and thermodynamics, and finally to infer the mechanism of binding of two distinct aptamers for thrombin [47]. Different critical reviews report and discuss the possible strategies to be employed for studying aptamer-target binding affinity, essential to comprehend effective analytical potentialities of these elements. In addition to the already cited CD, SPR and ITC techniques, different fluorescence analyses can be used, exploiting sensitive and accurate signal detection. Importantly, all of these reviews highlight the importance of considering multiple combinations of different methods, to finally obtain a wide characterization of binding performances of the investigated aptamer [48,49].

### 1.1.1. Applications of aptamers

Aptamers have applications in analytical, diagnostic and therapeutic fields. Biomedicine stands out for the use of aptamers, which are engineered to target cancer biomarkers and identify healthy or cancerous cells. Many aptamers are designed to treat malignant diseases and undergo various stages, from pre-clinical research to Food and Drug Administration (FDA)-approved therapies. Furthermore, preclinical studies in animal models demonstrate aptamers' potential for delivery of nanoparticles, therapeutics, and imaging agents to various cellular targets and molecules [37]. This application is known as *targeted drug delivery,* where aptamers conjugated to chemotherapeutic or diagnostic agents target cancer cell receptors with high specificity and affinity [37,50–52]. In this research field, critical issues such as degradation, structural stability, and nonspecific binding in physiological conditions are highly significant as they affect *in vivo* and clinical applications [50,51].

In analytical chemistry, aptamers are exploited as biorecognition elements for the development of: (i) aptasensors and apta-assays, especially involving electrochemical and optical transduction [32,41,53–59]; (ii) aptamer-based affinity-chromatography for target protein isolation and purification [60–66], and (iii) miniaturized extraction approaches to achieve adequate extraction and pre-concentration of target analytes [32,67–69].

The application of aptamers for sample treatment finds utility in fields such as food safety and environmental monitoring [70], where aptamers are applied for the isolation and determination of several compounds such as persistent organic pollutants (POPs), antibiotics, toxins, allergens and pathogenic microorganisms, in different food matrices [32,68]. For example, Persistent Organic Pollutants, such as bisphenol A [71] and polychlorinated biphenyl [72], were extracted from milk and fish respectively, various antibiotics in milk, honey, fish, meat, and also toxins in peanut, seeds, various grains, flour, beer and rice [61–65,73–77]. Immobilization of aptamers on affinity columns for selective extraction and subsequent analysis by coupling with different detection systems (frequently HPLC-UV) is less common, mainly dealing with determination of aflatoxins in the cases of food safety interest [61–63]. Undoubtedly, the main application of aptamers in analytical chemistry is represented by apta-assays and aptasensors (the latter will be discussed in following paragraph) [32,78]. An example of apta-assay is the one inspired by the Enzyme Linked Immunosorbent Assay (ELISA), here substituting antibodies with aptamers as recognition elements. These Enzyme-Linked Aptamer Assay (ELAA) can employ a direct, sandwich or competitive strategy, as happens in ELISA (**Figure 1.5a, b, c**) [78,79]. In direct ELAA, biotin-conjugated aptamer is incubated with the target, previously immobilized on the surface of the plate, for binding. A streptavidin-enzyme conjugate is added to exploit high-affinity streptavidin-biotin binding. As for the enzyme, horseradish peroxidase (HRP) is frequently used, and the adding of a chromogenic substrate permits colorimetric qualitative or quantitative detection of target (**Figure 1.5a**). In the work by Sun L. et al [80], a competitive direct ELAA strategy is performed for detection of target Aflatoxin B1 (AFB1). In that case, aptamer-HRP was incubated with free AFB1, with the AFB1-BSA conjugate immobilized on the wells: a competition between the free target molecules and the immobilized target will take place for binding with the aptamer conjugated to enzyme (**Figure 1.5b**). In sandwich ELAA configuration (**Figure 1.5c**), the free target binds an antibody or an aptamer immobilized, while another antibody/aptamer-enzyme conjugate is added for detection [81].

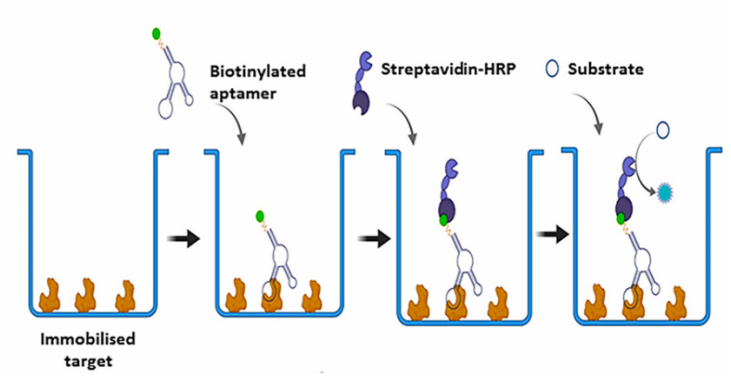


a. Direct ELAA

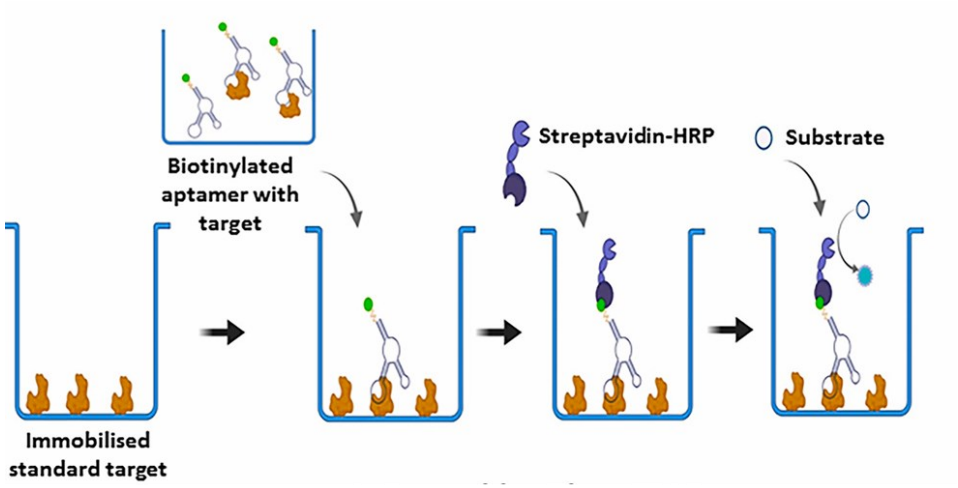


b. Competitive Direct ELAA

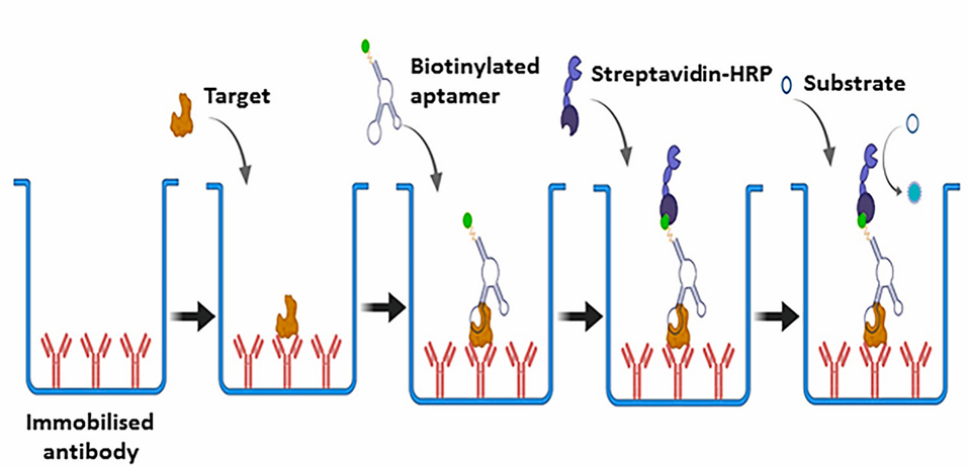


c. Sandwich ELAA

**Figure 1.5.** Scheme of different ELAA approaches. **a)** Direct ELAA; **b)** Competitive Direct ELAA; **c)** Sandwich ELAA. Reprinted and edited from Ref. [78] Copyright © 2023, with permission from Elsevier

### 1.1.2. Aptasensors

Biosensors offer high selectivity/specificity and sensitivity, making it possible to create portable, user-friendly, cost-effective and miniaturized devices capable of *in situ* analysis with no or reduced sample preparation [82]. Typically, biosensors operate through a recognition element that interacts with target molecules; this interaction is converted into a measurable signal by the transducer. When the biorecognition element is an aptamer, the biosensor is usually named as "aptasensor". The advantages and limitations of aptamers, compared to more conventional antibodies, have to be taken in consideration. As can be seen in **Figure 1.6**, aptamers present smaller sizes but, most importantly, the absence of spatial constraints given by disulfide bonds: this results in a greater conformational freedom, that can be exploited for designing aptasensors. Consequently, a fine set-up of working conditions (pH, temperature, ionic strength) has to be reached for performing analysis [83].

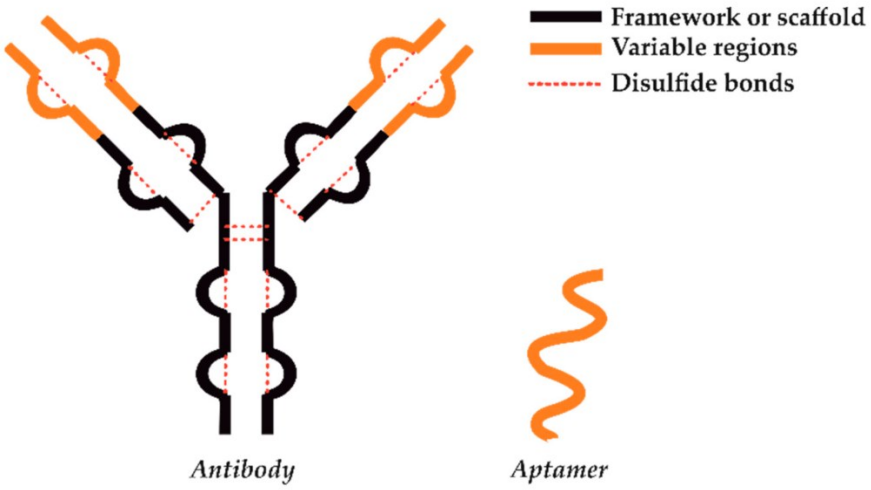


**Figure 1.6.** Structure representation of an antibody, and an aptamer. Representation reflects relative sizes. Spatial constraints are represented by disulfide bonds (dashed lines). Reprinted and edited from. Ref. [83] © 2021 by the authors. Licensee MDPI, Basel, Switzerland

Depending on the type of transducer used, aptasensors can be categorized into various groups, including electrochemical, optical, micromechanical, piezoelectric, etc. Aptamers are commonly functionalized at 3' or 5' end with electroactive or chemical tags, such as fluorophore, depending on the transduction mechanism, necessary for the generation of the signal. In **Figure 1.7** is reported an example of an electrochemical aptasensor, in which the immobilized aptamer presents a redox reporter at one end; the binding to the target induces a conformational change that permits electron transfer [78].

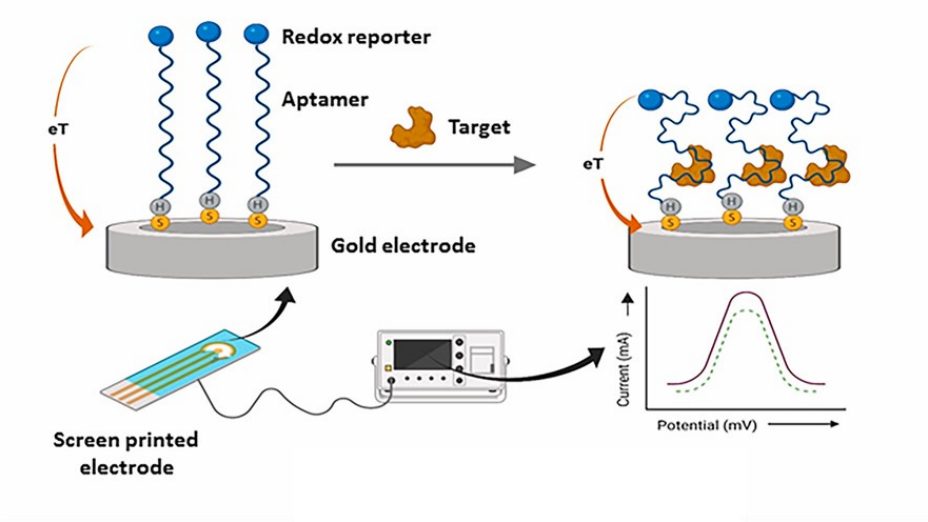


**Figure 1.7.** Representation of an electrochemical aptasensor exploiting a screen-printed gold electrode. Gold particles are functionalized with aptamers that recognize a particular target. Conformational change induced by binding is necessary to induce a biochemical electron transfer that is amplified for detection of an electrical output (eT = electron transfer rate). Reprinted from Ref. [78] Copyright © 2023, with permission from Elsevier

Conformational change is not the only mechanism used in aptasensors: **Figure 1.8** schematizes the different aptasensing mechanisms. A possible way is sandwich mode, in which an aptamer is immobilized, target is added and the complex is formed; then, a labeled aptamer directed to the target is added, in order to bind a different epitope on the target molecule; labeling will enable transduction mechanism (**Figure 1.8a**). In target-induced dissociation (TID) mode (or strand displacement), a labeled aptamer is bound to its complementary immobilized sequence; addition of the target leads to aptamer-target complex formation and displacement of complementary labeled sequence, that is removed with subsequent washing steps, resulting in signal decrease (**Figure 1.8c**). Lastly, a competition for the target is reported in **Figure 1.8d**, named competitive replacement (CR) mode: in this case, immobilized target is recognized by the labeled aptamer, forming the aptamer-target complex; target molecule is added in excess, leading aptamer to preferably bind free target rather than immobilized one. Moreover, signal generation can be obtained by competitive mechanisms, immobilizing the aptamer, in two possible ways: i) after incubation of immobilized aptamer with the target, a second labeled sequence is added, having a sequence partially complementary to the immobilized one; absence or presence of the target will result in signal-on or -off, respectively; ii) an unlabeled aptamer is immobilized, while the analyte present in the sample is put in competition with a labeled homologue at fixed concentration: this will permit to construct a dose-response curve, in which increase in electrochemical signal will be proportional to concentration of analyte present in the sample [32].

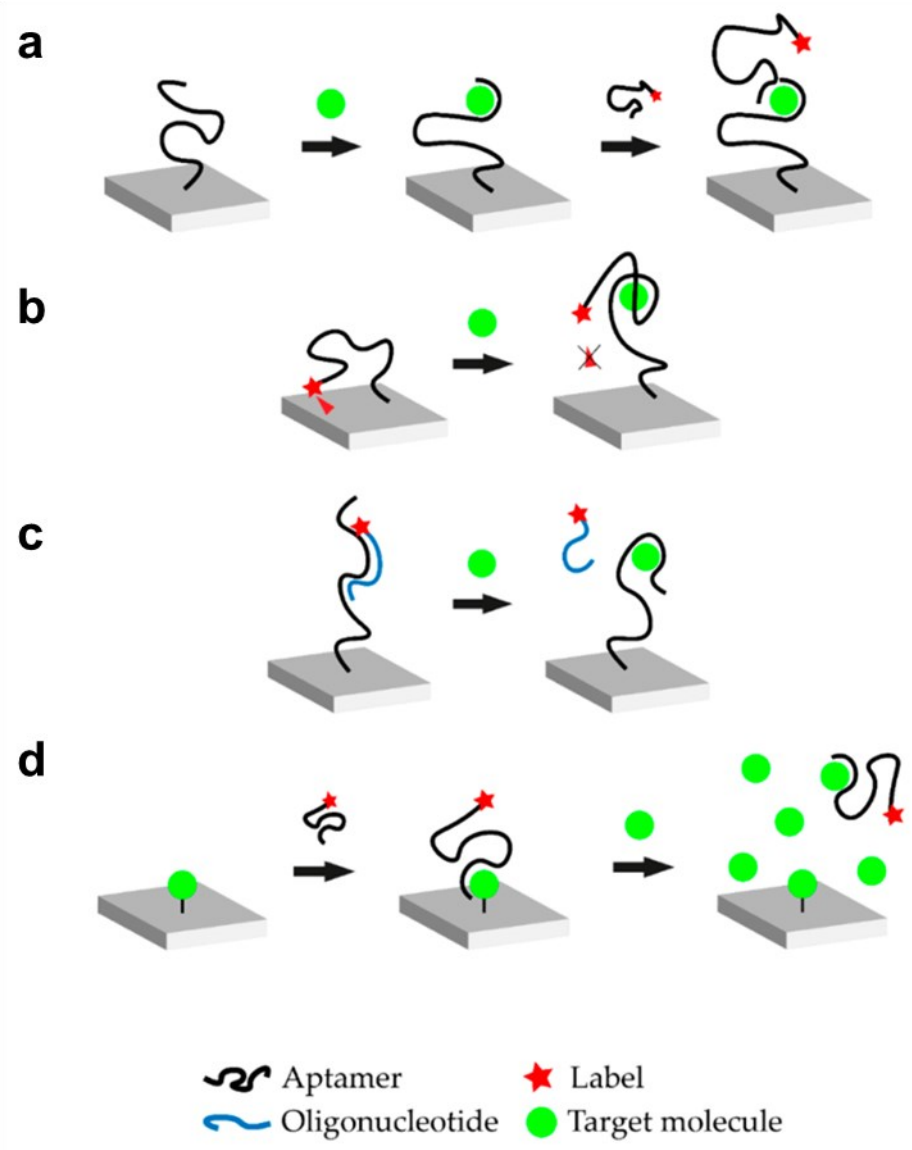


**Figure 1.8.** Scheme of different mechanisms of aptasensor detection. **a)** Sandwich mode; **b)** Conformational change or Target-induce structure switching (TISS) mode; **c)** Strand displacement or target-induced dissociation (TID) mode; **d)** competitive replacement (CR) mode. Reprinted from Ref. [84] © 2020 by the authors. Licensee MDPI, Basel, Switzerland

These applications have practical utility in various fields such as food safety, environmental monitoring and clinics [55,83,85]. For what concerns aptasensors for allergenic proteins, Mishra et al. [86] developed a competitive colorimetric aptamer-based approach for detection of lysozyme in wine samples, in which the target was immobilized onto a magnetic support and biotinylated anti-lysozyme aptamer was added in solution. Competition between the immobilized and the free target possibly

present in the sample was established for binding to the aptamer, as represented in **Figure 1.9**. Finally, streptavidin-alkaline phosphatase was added for colorimetric detection.

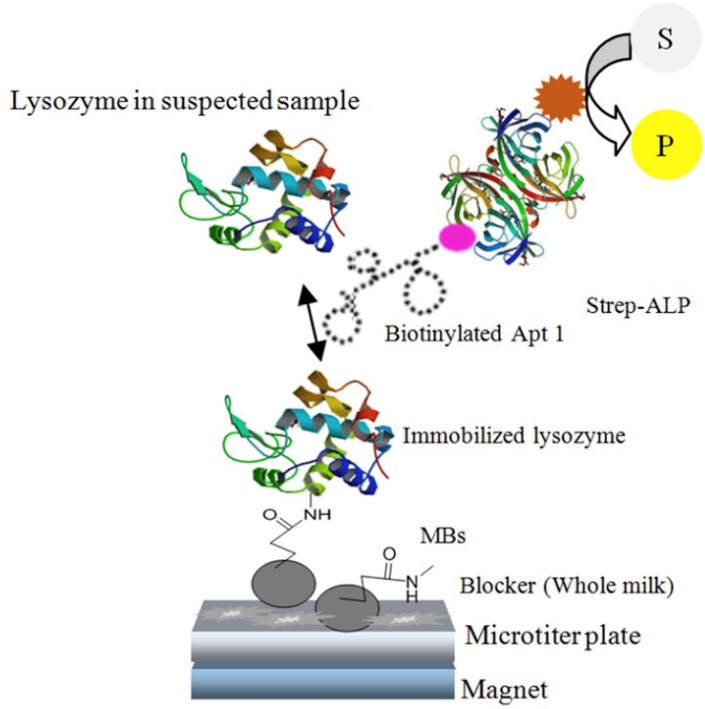


**Figure 1.9.** Colorimetric-based competitive aptasensor for detection of lysozyme from wine samples [86]. Reprinted from Ref. [85] Copyright © 2023, with permission from Elsevier

Additional applications can be found in the literature, particularly concerning the identification of toxins or small molecules of relevant importance in the field of food safety. An interesting application was presented by Dwidar & Yokobayashi who developed an aptasensor for the analysis of histamine in food, demonstrating robustness, stability and performance suitable for its use in a regulatory context [54]. Aptasensor are also used for the determination of Non-Intentionally Added Substances: Jo et al. published a paper focused on the use of a single-stranded DNA aptamer for the detection of Bisphenol A in a sol-gel chip [87]. This sensing system was further improved by Chen et al. who developed an aptasensor with an extended analyte concentration range [88]. Another interesting application of aptamers in biosensing was presented by Naghshabandi et al. who evaluated the use of DNA-aptamer for the detection of fumosin B1 in maize flour [57].

It is worth mentioning that one of the main biosensors (including aptasensors) strength is the possibility to use them without sample preparation, making them suitable for *in vivo* studies as well as for real-time analysis in microfluidic systems. Among the devices developed, a microfluidic electrochemical detector was developed for continuous *in vivo* monitoring, up to 4 hours, of doxorubicin (DOX) and kanamycin in whole human blood and live mice [89]. The detector bases its

activity on the conformational change of the aptamer in presence of its target, with a higher number of bound molecules leading to a stronger electrochemical signal. **Figure 1.10** illustrates the real-time measurement of doxorubicin and kanamycin levels in whole blood during continuous *in vivo* monitoring. The microfluidic electrochemical detector was designed to incorporate an electrochemical aptamer-based sensor for precise measurement, along with a continuous-flow diffusion filter to safeguard the aptamer probes from fouling. Additionally, kinetic differential measurement (KDM) was applied to reduce current drift and enhance the accuracy of real-time measurements [89].

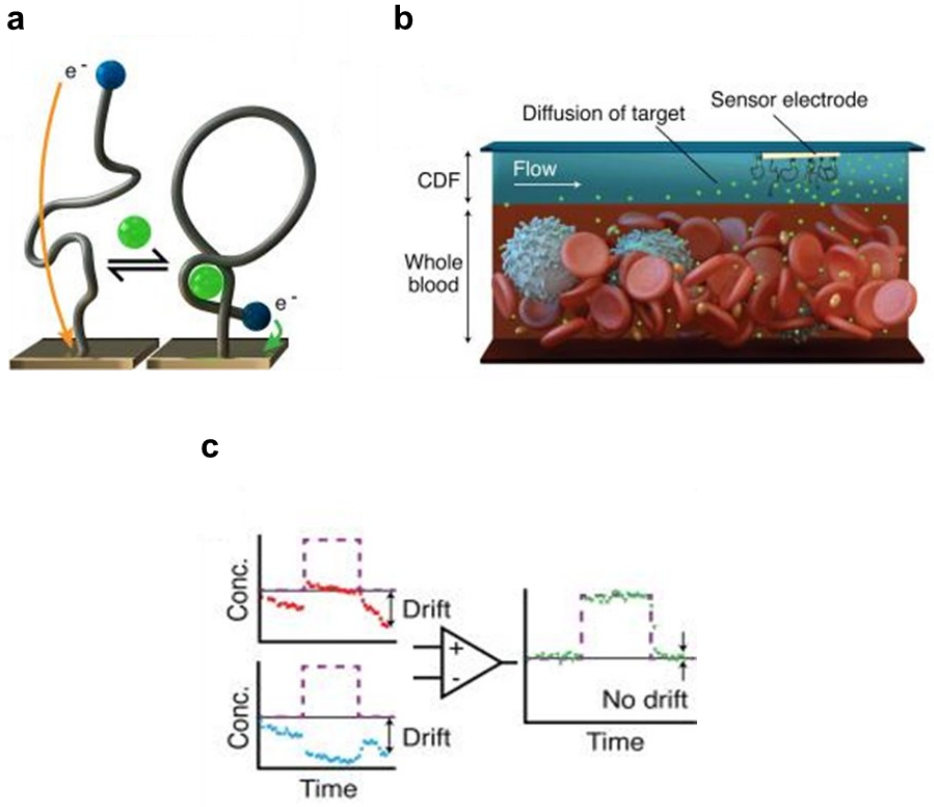


**Figure 1.10. (a)** Aptamer is immobilized on the gold electrode, and binding of the target molecule (green) induces a reversible conformational change, that accelerates electron transfer between the electrochemical redox reporter (blue) and a microfabricated electrode, resulting in a measurable current change over time. **(b)** The microfluidic device is constituted by the continuous-flow diffusion filter (CDF), is formed by vertically stacked laminar flows of buffer (blue) and blood flow (red); target molecules are enabled to diffuse, but not interferent compounds constituting blood. **(c)** Both signal-on (red) and signal-off (blue) responses exhibit noticeable drift in response to a target pulse (dashed purple), but the application of kinetic differential measurement (KDM; green) enhances the accuracy of real-time current measurements by minimizing drift and improving the signal-to-noise ratio. Reprinted from Ref. Reprinted and edited with permission from Ref. [89] Copyright © 2023 American Chemical Society

As said, aptasensors cover most part of application of aptamers in analytical chemistry. A notable trend in aptasensor is the miniaturization of the support on which aptamers can be immobilized, such as the use of magnetic micro- or nano- beads (MBs). MBs will be discussed in the following paragraph, as well as their utilization in aptasensors.

### 1.1.3. Structure, preparation, and coating of magnetic beads

MBs are usually constituted by magnetite ($Fe_3O_4$) or maghemite ($\gamma$-$Fe_2O_3$). After the synthesis of the magnetic core by means of co-precipitation of iron salts in solution, spherical-shaped MPs are coated by appropriate functional units and/or bioreceptors. These coatings are continuously under development thanks to the availability of new technologies or deposition procedures (**Figure 1.11**). The main goal is to obtain adsorbents with maximized analyte affinity, minimal extraction of matrix interferents and possibility of reutilization (resulting in a green application). Targets added to a dispersion containing MBs and recognizing the elements present on their surface can be easily separated from sample solution during washing steps, exploiting the responsiveness of MBs to an external magnetic field; this permits to minimize matrix effect and reduce the analysis time. Actually, the analyte can be purified from its matrix, pre-concentrated, and it is extremely easy to exchange buffer depending on requirements [90–92] .

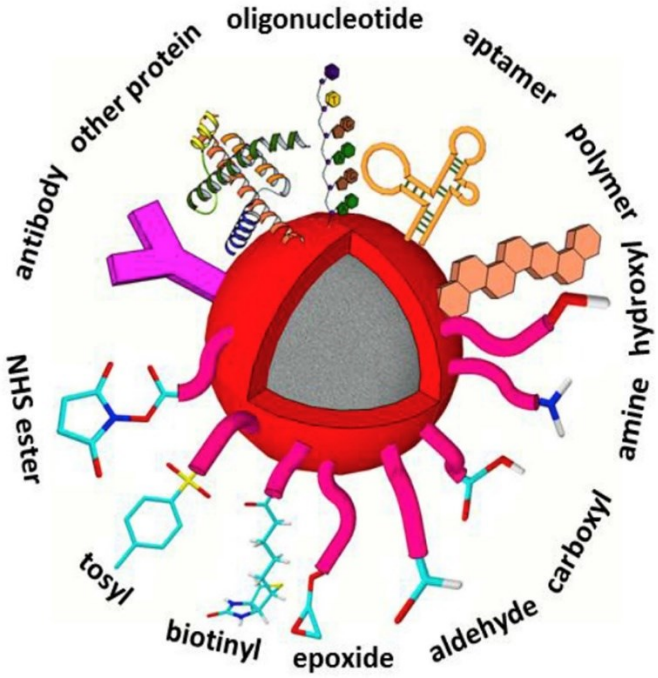


**Figure 1.11:** Scheme of most common magnetic particle modifications and functionalization for analytical purposes. Reprinted from Ref. [90]. Copyright © 2023, with permission from Elsevier

The nature of the chemical group or recognition element exposed on the surface is crucial in modulating interactions and selectivity, which should be reversible and non-covalent. The involved interactions in this mechanism include ionic, dipole-dipole, hydrogen bonds, and Van der Waals bonds. Crucial parameters to be considered in the selection of a suitable material are the nature and polarity of the analyte, its solubility, and possible presence of interferents. Target affinity and non-specific binding of interferents are critical aspects to take into account. In 2016, Pérez-Ruiz et al [93] explored different strategies for MBs functionalization with DNA aptamer against Ara h 1 (a peanut allergen) used as a model system. In particular, four different commercial types of MBs were used for immobilization of anti-Ara h1 aptamer, taking into consideration three distinct parameters: particle surface coverage by immobilized aptamer, specific binding of the immobilized aptamer with thearget and non-specific absorption of the target onto the beads. Results showed that non-specific interactions were dependent on the particle surface (its polarity or hydrophobicity), evidencing the importance of accurate investigation of aptamer-immobilized MBs for subsequent method development.

### 1.1.4. Aptasensors exploiting magnetic beads conjugated to aptamers

In 2022 we published a trend article focused on different analytical strategies involving the use of aptamers conjugated to micro- and nano-MB as recognition elements for food analysis [32]. In the first part of the work, magnetic bead-based electrochemical and optical aptasensors are discussed. The same mechanisms reported in **Figure 1.8** can be transferred to miniaturized magnetic supports.

Integration of MBs into the aptasensors' approach permits to perform bioassays in liquid suspensions, while precisely controlling shaking conditions and incubation temperature. The key advantage of MBs is their easy manipulation, enabling efficient and quick washing steps through straightforward confinement by applying magnetic fields. This not only streamlines the assay process but also enhances performance by regulating the motion of MBs. It is important to highlight that, beyond acting as platforms for immobilizing bioreceptors, MBs can also contribute to the detection mechanism and, in some cases, used as labels.

The advantages of immobilizing aptamer probes on magnetic microbeads and nanobeads, featuring reactive functional groups such as carboxylic and amino units or streptavidin on their surfaces, are numerous. This approach allows for the interaction of the DNA/RNA probe with the target analyte in suspension, taking advantage of an increased active surface area under controlled mechanical stirring and temperature conditions. It's important to highlight that these critical experimental parameters, essential for an efficient aptamer–target interaction, cannot be regulated when the aptasensor relies

on the direct immobilization of the probe on the electrode surface. Following this, aptamer-functionalized magnetic materials present in the sample are subsequently isolated, washed, and transferred onto screen-printed electrodes, without the need for any functionalization with receptors. These procedures can be performed by using a simple magnet [32].

### 1.1.5. Miniaturized approaches for sample treatment - Magnetic Solid-Phase Extraction

Despite recent progress in chromatography and mass spectrometry techniques, sample treatment step remains one of the most critical analytical steps; it involves extraction, purification, and concentration (or dilution) of the analyte while minimizing analyte loss and contamination. Hence, sample preparation enables isolation and enrichment of the target analytes, minimizing their loss and reducing matrix effect by removing interfering compounds [94]. The selection of the appropriate sample treatment technique and, as a consequence, of the ideal sample preparation, depends on analyte's properties, matrix composition, and expected concentration levels.

Sample preparation procedures are continually evolving as they contribute significantly and directly to the analytical performance of the method, thus influencing not only the quality parameters of an analytical method, but also analysis time and cost, which are other fundamental aspects to be considered in the development of the method. This evolution includes not only the advancement of instrumentation, comprising sophisticated and high-performing technologies and miniaturized devices, but also the improvement of sample treatment techniques through the use of miniaturized supports, novel materials, and automation. These developments not only enhance the quality parameters of analytical methods but also align with the principles of Green Analytical Chemistry [34,95]. Different miniaturized versions of SPE have been developed, as *magnetic solid-phase extraction* (MSPE), *microextraction in a packed syringe* (MEPS), *matrix solid phase dispersion* (MSPD), *stir-bar sorptive extraction* (SBSE), *solid phase microextraction* (SPME), and *dispersive SPE* (d-SPE) [96]. All these techniques stand over the same principle (analyte affinity for the sorbent phase) but differ on the analytical route (SPME and SBSE do not include a washing step), automatability, device configuration, type of desorption (thermal-drive or solvent-based), enrichment factor, and suitability to be directly coupled to the instrument. However, despite the technique and thanks to their wide use in routine procedure, many studies focused on the development of new adsorbent/absorbent materials to be used as solid phase [97,98].

One of the main results of the current “green-oriented” trend is the combination of conventional polymeric phases with nanomaterials, combining polymer extraction capabilities with unique properties, such as magnetism. The use of magnetic extractants in some application allows the

elimination of several time-consuming steps like filtration or centrifugation, thereby streamlining the entire analytical process [97]. First introduced by M. Šafařıková et al. in 1999 [99], MSPE relies on the use of micro- or nano-magnetic supports, commonly magnetic beads (MBs or MPs) for the stationary phase. In MSPE, the magnetic beads are dispersed into the sample, and then are easily separated from the matrix sample by applying an external magnetic field, avoiding filtration and centrifugation steps [94]. The miniaturization of the support implies an high surface-to-volume ratio, increasing the efficiency and the sensitivity of the approach, and greatly increases the versatility and ease of operation, facilitating the handling of small volumes.

The mechanism of MSPE (reported in **Figure 1.12**) involves the dispersion of magnetic particles within the sample, the interaction of analytes with the solid phase present on the surface of the magnetic particles, the confinement of the beads on the walls of the reaction tube by external magnetic support, the removal of supernatant and introduction of a new solvent allowing the removal of the analyte, and finally the extract recovery for analysis by confining the magnetic particles, before analyte separation (mostly HPLC) and detection (by MS, UV-Vis or fluorescence). In all the steps, multiple washing cycles are necessary to eliminate non-specifically adsorbed species.

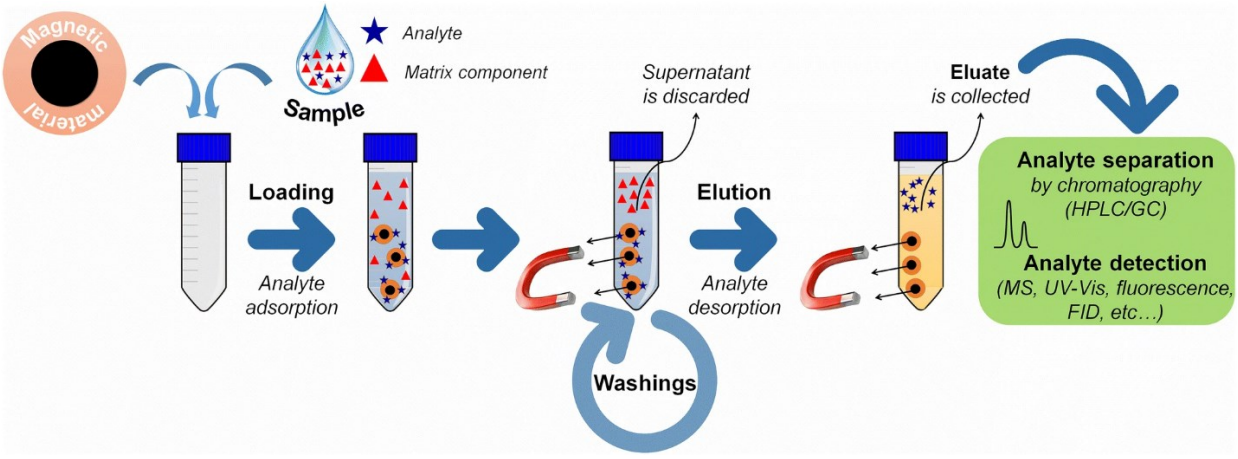


**Figure 1.12.** Schematic representation of the main steps for MSPE. Reprinted from Ref. [94] Copyright © 2023, with permission from Springer

MSPE strengths stand on its fast, effective, and selective extraction offered by the magnetic material, the increased surface-to-area ratio of coated particles compared to other SPE techniques. In order to extend its use in routine practice, recently developed tools allow to automate MSPE. It is worth mentioning again that extracting particles are not disposable and can be used for a high number of analysis after cleaning and reconditioning.

### 1.1.6. Magnetic beads functionalized with aptamers for miniaturized extraction techniques

The application of aptamers in analytical chemistry mainly focuses on the development of aptasensors and apta-assay, while aptamers are rarely used for extraction and enrichment steps in sample treatment procedures, where aptamers are combined with magnetic beads to further increase recoveries and selectivity [32]. MBs immobilized with aptamers can be employed in MSPE to purify, separate or pre-concentrate a particular target starting from a complex matrix [68,100]. Despite the large number of aptamers proposed in literature, their reliable applications in MSPE are still limited to few small molecules, such as mycotoxins or antibiotic residues in food safety field [74,101]. For example, Khodadadi M. et al. [101] and Tu C. et al. [74] performed the determination of Aflatoxin A and chloramphenicol, respectively, from milk samples. In this context, as discussed in Mattarozzi et al [32] and in-depth evaluated during the Ph.D. activities, a careful selection of the experimental conditions is necessary to achieve reliable results. When developing a MSPE protocol based on aptamer-modified beads, there are numerous parameters that require to be considered. To introduce into the discussion, main parameters are summarized in **Figure 1.13**.

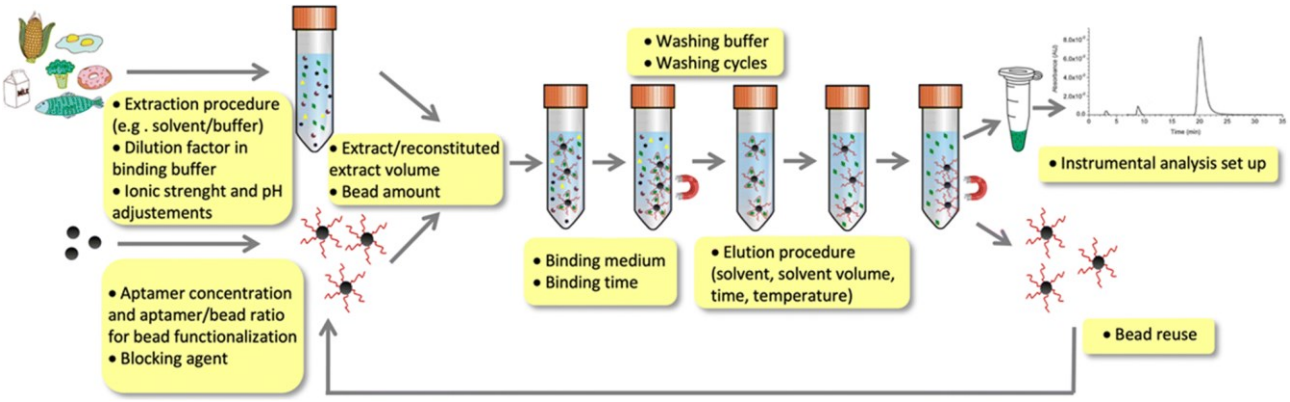


**Figure 1.13.** Schematic representation of the MSPE protocol on aptamer-modified beads, with emphasis on the most critical aspects in each step. Reprinted from Ref. [32], Creative Commons Attribution 4.0 International License

The structure of aptamers is strongly affected by buffer composition, pH conditions and ionic strength; thus, maintaining a strict control of the binding conditions is crucial while moving from standard solutions in binding buffer to matrix extracts, which may contain interfering compounds. In this scenario, the balance between binding conditions to preserve aptamer affinity and selectivity, and extraction buffer/solvent able to ensure satisfactory recovery from complex matrices, becomes

fundamental. When considering a protein as target for aptamer recognition, preservation of its structure represents an additional parameter to be considered.

In order to determine the suitability of aptamer-based methodologies for food samples, a comprehensive evaluation of the aspects described above is essential [32,74,101]. More generally, in the last few years there is a need for a careful evaluation of the performances and applicability of aptamer-based methods, due to the raise of different critical aspects highlighted in their use [100].

### 1.1.7. Critical aspects of aptamers

In the recent years, different authors asserted the need to go beyond the proof of concept for aptamer application in analytical chemistry, evaluating some potentialities and limits of these receptors especially elucidating the binding mechanisms between aptamer and its target [32,44,45,102]. Recent studies dealt with the demonstration of the non-binding capacity of some aptamers widely used in literature through an in-depth characterization of target-aptamer interaction by multi-technique approach [40,103].

As an example, in 2020 Bottari et al. published a relevant work reporting that there is "a lack of a universally accepted and robust quality control protocol for the characterization of aptamer performances coupled with the observation of independent yet inconsistent data sets in the literature", demanding for "multifaceted analytical approach, to unequivocally establish the actual detection potential and performance of aptamers aimed at small organic molecules" [44].

There are several causes behind these considerations:

- a lack of caution in exploiting sequences that are reported in previous works, without confirming the effective aptamer-target binding; the same applies for truncated sequences that are used without a systematic explanation nor verification;
- inattention to binding conditions (buffer nature, pH, ionic strength), often very different from those used to select the aptamer without evaluating the effects of matrix medium; this issue is particularly important when applying aptamers to food samples, for which the matrix can be very complex;
- the lack of negative controls, involving the use of scrambled aptamers (i.e. randomized sequences) or unrelated sequences to evaluate the interaction with other matrix compounds;
- the lack of a previous a multi-technique characterization to evaluate aptamer-target interaction [104].

## 1.2. Ambient Ionization Mass Spectrometry

Since the introduction of the Desorption Electrospray Ionization (DESI) [105,106] and Direct Analysis in Real Time (DART) [107], Ambient Mass Spectrometry (Ambient-MS, or AMS) techniques got an ever-growing attention, leading to an increase in the number of possible approaches. Introduced to reduce time analysis, AMS techniques are all characterized by the sample ionization in its native conditions, avoiding chromatographic separation and reducing or eliminating sample preparation step. If sample preparation is required, it usually involves minimal operations such as gently transferring a sample onto paper or conducting a simple and rapid extraction by dissolving the sample in water or a low-cost solvent [108] (**Figure 1.14**). This peculiarity is essential in enabling a direct and rapid analysis, especially if compared with hyphenated MS techniques, although it could suffer for limits in reproducibility, sensitivity, and possibility to perform quantification approaches [12]. The advancements in performances and frequency of utilization of portable mass spectrometers could favor exploitation of rapid *in situ* AMS analysis.

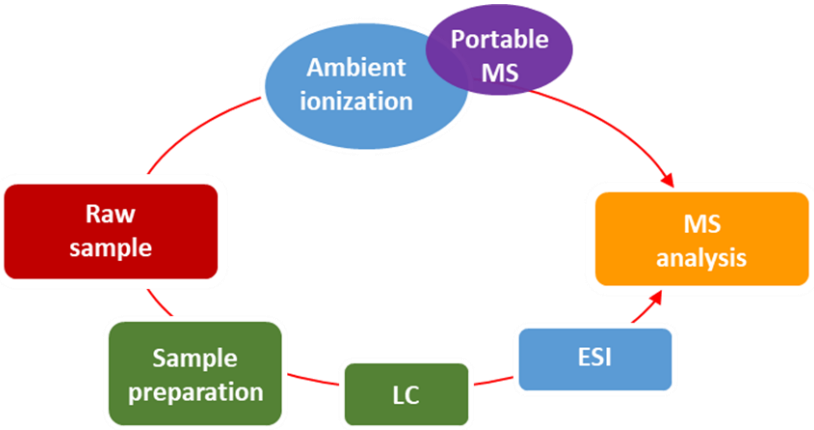


**Figure 1.14.** Common Ambient-MS workflow (upper arrow) versus conventional MS methods (down arrow)

When severe matrix effects and challenging matrix interferences are encountered in high-resolution MS or tandem MS, the use of minimal sample manipulation/treatment is justified.

Nowadays, the advancement of high-resolution MS (HRMS) analyzers, like Orbitrap or Time-of-Flight (TOF), has significantly expanded the capabilities of AMS techniques. Alongside targeted approaches, the integration of AMS with HRMS instruments allows for nontargeted analyses, enabling the detection of numerous suspect contaminants and facilitating sample profiling and identification of biomarkers for sample classification. Moreover, the combination of powerful HRMS with lower-resolution MS analyzers (quadrupoles/ITs combined with Orbitrap or TOF mass

analyzers) enables tandem mass spectrometry experiments, providing valuable structural information for the unequivocal identification of compounds of interest. This integration greatly enhances the potential applications of AMS in modern analytical workflows [109].

The versatility of AMS has led to the emergence of numerous techniques that either utilize or expand upon the core methods, including the above-mentioned DESI and DART, but also new methods like Atmospheric Solid Analysis Probe (ASAP) and Desorption Atmospheric Pressure Photo Ionization (DAPPI). The simplicity of AMS methods allows the easy modification of the already existing ones, to adapt them to both the sample type and the analytical problem. For this reason, many prototypes, homemade new approaches, are continuingly being introduced and explored, extending the application field of ambient ionization technique family. Up to seven different configurations are commercially available and up to one hundred have been developed as bench-scale prototypes [110]. The choice on the most appropriate AMS technique to be utilized depends on factors such as matrix sample type, polarity of the compounds of interest, state of the sample at atmospheric pressure (solid, liquid, or gas), and the compatibility of these characteristics with a specific AMS method [109]. Coupling of AMS techniques with most types of mass spectrometers equipped with an Atmospheric Pressure Ionization (API) source can be easy, as it does not need any modification nor on the ion optics or the vacuum interface [111]. It is worth mentioning that AMS need reduced amount of sample, so it perfectly matches requirements of miniaturized techniques. This is a relevant advantage, together with the absence of preliminary operation and chromatography, towards the GAC compliance. In this context many applications have been developed using miniaturized sample preparation and AMS, especially for the analysis of residue in food [69].

Whatever the actual process of analyte desorption and ionization, in ambient MS it is performed close to the orifice of a standard API interface. The entire interface, from atmospheric pressure source to the mass analyzer operating in vacuum, does not require any adaptation, allowing a rapid and easy switch from conventional API to ambient techniques and making AMS techniques suitable for high-throughput and in situ analysis.

To date, there are several different AMS techniques, which can be classified into three main categories [28,109]: (i) spray or jet ionization, where an electrospray needle generates charged droplets when a high voltage is applied, and droplets are then utilized to ionize the sample; this technique is employed in DESI; (ii) electric discharge ambient ionization, exemplified by DART, involves a corona-to-glow electrical discharge into inert gas (He or $N_2$) that operates at 50-60°C and produces ions, radicals, and excited atoms [112]. This cold plasma is then used for the ionization of the sample; (iii) ambient gas-, heat-, or laser-assisted desorption and ionization, where these media are used to promote the sample vaporization necessary for the following sample ionization [113].

To be more accurate, what really differentiates ambient MS from conventional API-MS techniques is that the sample processing takes place in real time and proximal to ionization, then it would be more correct to say that AMS requires "no additional sample preparation" [111]. Among the developed AMS techniques, the difference relies on the way on how sample processing is combined with well-known ionization mechanisms. For instance, electrospray ionization (ESI), sonic spray ionization (SSI), and photochemical ionization have been coupled in real time with sample processing steps such as liquid extraction, thermal desorption, and laser ablation, among others, depending on the AMS variant exploited.

This introduction will focus on two AMS techniques, Paper Spray (PS) and Swab Touch Spray (Swab TS), both related to the first AMS group (spray ionization) and both consisting in a three-step process.

### 1.2.1. Paper spray–Mass Spectrometry

Paper spray–Mass Spectrometry (PS-MS) makes part of a sub-group of AMS techniques characterized by the generation of an electrospray ionization directly from a solid substrate (paper, leaf, wooden-tip) [114]. It consists in the exploitation of a triangular paper linked to a metal clip, connected to a power supply for the application of a potential. Paper is positioned in front of the orifice of API interface of the mass spectrometer (on-axis position); after the loading of liquid sample, paper (also called substrate) is wetted with a spray solvent which moves to cover the whole surface extracting the analytes; subsequent application of DC high voltage (positive or negative) generates charge droplets at the tip of the paper triangle (**Figure 1.15**).

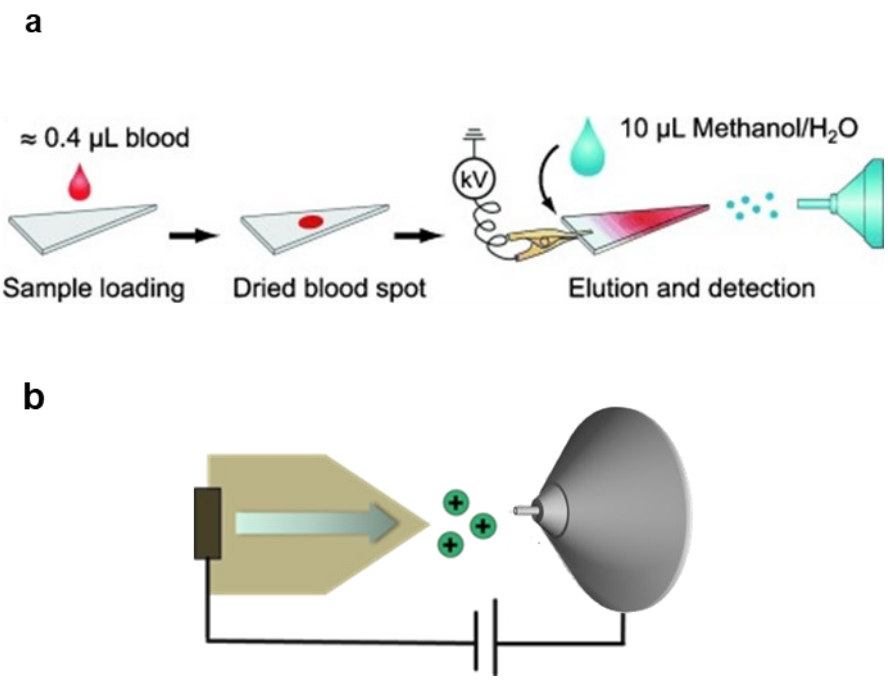


**Figure 1.15. a)** Different steps of PS-MS analysis on dried blood spots. Reprinted from Ref. [115] Copyright © 2023, with permission; **b)** Illustration of PS-MS operation scheme

Solvent acts extracting analytes from the sample spot: in this phase a competition for analytes between stationary phase of paper and liquid phase of the solvent takes place, thus making the choice of solvent and paper material essential for this application. Such extraction permits also a separation of compounds due to different interaction of sample components with substrate, resulting in a real time *in situ* purification. Analytes are thus transported up to the tip, where ionization occurs: for this reason, PS-MS is defined as a 3-step process (extraction, transport, ionization). Sharp corners of the paper are another important parameter that was widely studied: it was observed that the sharper the corner is, the lower is the voltage necessary to generate spray plume formation and, consequently, electrospray ionization. As a result, paper triangles have mostly a 30-45° tip angle [115].

PS-MS is mainly applied in the analysis of drugs, especially in fresh blood samples or dried blood spots. To the best of our knowledge, analysis of proteins by means of this technique is reported only by few works in literature. This can be attributed to the fact that, in case of using cellulose-based paper, van der Waals interactions and hydrogen bonds between proteins and substrate limit analyte migration to the tip. To overcome this limitation, Hal et al (2015) successfully used carbon nanotubes (CNTs)-modified paper spray mass spectrometry (MS) to directly extract, desorb, and ionize intact proteins from gel matrices under ambient conditions. By modifying the paper substrate with CNTs, they achieved larger surface area, smaller pore diameter, and high conductivity, enabling the extraction and migration of proteins to the paper tip via electrophoresis-like behavior for paper spray

ionization [116]. In 2018, Li J. et al [117] had used polystyrene-coated papers for detection of proteins and peptides. In particular, they detected lysozyme as entire protein and the small peptide Angiotensin II (8 aminoacids) depositing MeOH:$H_20$ 1:1 25 µL solvent both on filter paper and polystyrene-impregnated paper. Different solvent conditions were used by Riboni et al (2019) for detection of proteins ($H_2O$:IPA 1:1, HCOOH 1% v/v); interestingly, it was demonstrated that PS elicits detection of noncovalent protein complexes, thus preserving native structure of the molecule [118].

PS-MS is one of the most exploited ambient MS techniques for semi-quantitative or quantitative analysis, possible thanks to the addition of an internal standard, that can be added to the sample or the eluent [115]. The possibility to perform quantitative analysis makes ambient get closer to hyphenated MS methods, in respect of which exhibits a simpler, cheapest and faster analysis, albeit a slightly lower precision. As confirmation of PS-MS potentialities, a high throughput device was developed and now commercially available for fast quantitative analysis of different samples automatically [119,120].

### 1.2.2. Swab Touch Spray–Mass Spectrometry

Swab Touch Spray–MS (Swab TS-MS) is a simple-design and custom AMS technique that involves the use of a nasopharyngeal swab, exploited both as sampling probe and electrospray support and emitter. The analysis consists of the following sequential steps:

1. Sampling of a tissue or contaminated surface by swab tip;
2. Positioning of the swab, that is connected through its metallic body to DC high voltage supply; at the same time, swab tip is connected to a capillary that provides solvent, thus wetting the tip;
3. Application of the potential leads to the formation of ions from the tip throughout an ESI-like mechanism; ions are thus transferred into mass spectrometer to be analyzed [121].

Swab TS-MS shares several similarities with PS-MS, since both can be described as "substrate-spray technologies" [121] and 3-steps method. In fact, the solvent that is continuously added to the tip, acts extracting the analyte and enabling electrospray ionization, as well as happening in PS-MS. Common principle is to create a powerful electric field that surpasses the surface tension of the solution containing the analyte. Therefore, surface tension of the solvent, solvent conductivity and flow rate, and applied voltage are key parameters.

It is worth noting that a metallic body is necessary for enabling potential conduction and hence ionization (even if bamboo-made ones are reported in literature to be effective [122]). After sampling step, the swab is positioned vertically, in contrast to what happens in PS-MS with paper substrate, that is horizontal. This difference is due to the high capacity of the rayon fiber that envelopes the tip, to absorb the solvent: vertical position facilitates solvent streaming down to the tip, where a liquid

hemisphere is formed. When potential is applied, a Taylor cone will emerge originating at the hemisphere, accompanied by a cone-jet electrospray plume, as represented in **Figure 1.16** and **1.17**.

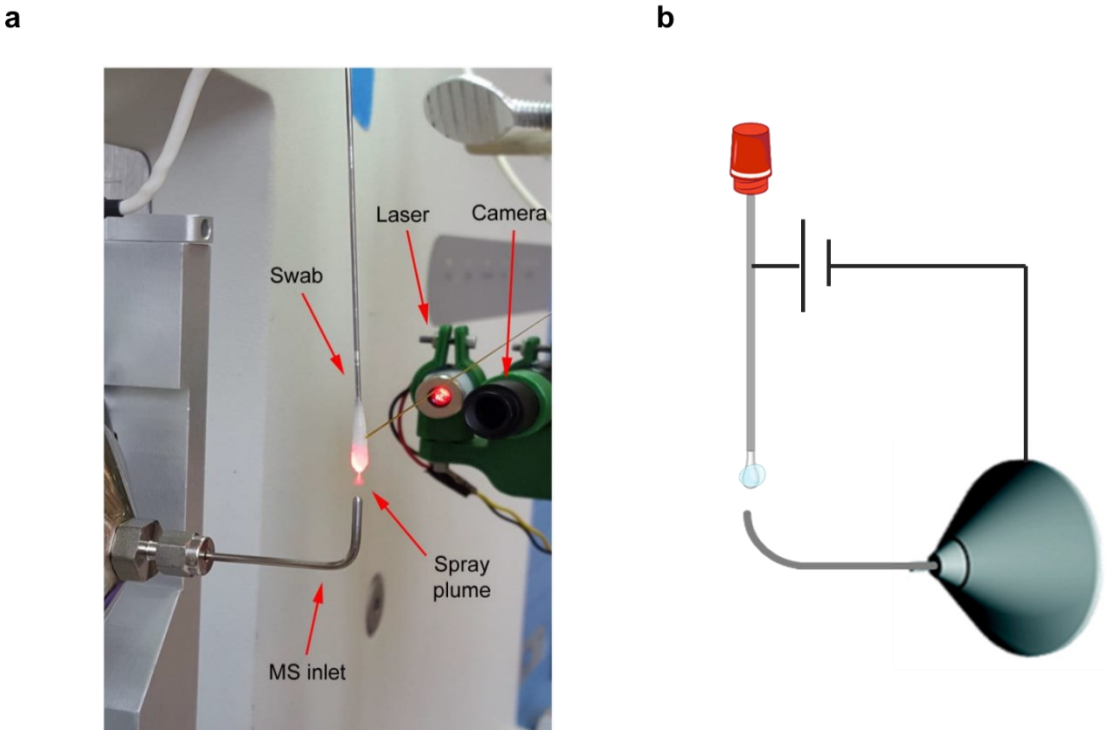


**Figure 1.16. a)** Snapshot on swab tip during ionization. A laser pointer permits to visualize electrospray plume. Reprinted from Ref. [123] Creative Commons Attribution 4.0 International License; **b)** Illustration of Swab TS-MS operation scheme

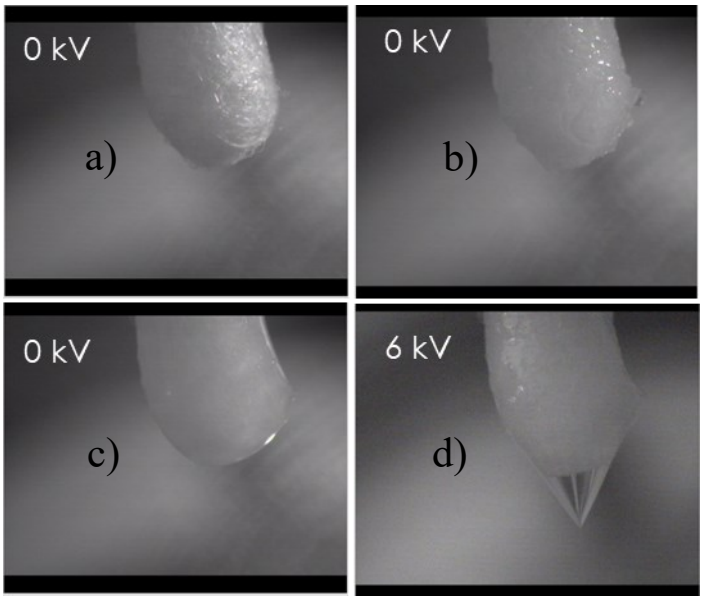


**Figure 1.17.** Zoom on swab tip. Application of the solvent progressively wets the tip (**a-c**). When the solvent comes to form a hemisphere (**c**), potential is applied, starting electrospray ionization and leading to the formation of Taylor cone (**d**)

As can be seen from the **Figure 1.16a**, vertical disposition of the swab makes difficult the use of a classic transfer line for moving ions towards the mass spectrometer. Hence, a modified transfer line configured in an "L" shape is advisable, that significantly improves stability of the signal, although its increased length reduces efficacy in ion transmission to the analyzer.

In Swab TS-MS the solvent role is the extraction of analytes from the matrix and the generation of a stable electrospray when a potential is applied. Therefore, solvent-analyte interaction and its capability to form a Taylor cone, that depends on surface tension of the solvent itself, are key aspects to be considered. Surface tension is also directly related to potential applied: the higher the surface tension is, the greater will be the potential required to exceed Rayleigh limit, form a Taylor cone and enable ionization [121]. Further details about key parameters will be treated in the Chapter 2 (such as surface tension, solvent composition, solvent flow rate, voltage applied, solvent conductivity, ion current).

Swab TS is most suitable for applications that require *in vivo*, quick, minimally invasive sampling of small sample quantities (such as biofluids and tissues) and where swabs are already the preferred method of sampling [121]. For this reason, the technique has been extensively applied in clinical and forensic analysis [122,124–130]. As for clinical investigations, most of the research contribution comes from G. Cooks' laboratory from Purdue University (IN, USA); the methods employed in those analyses were qualitative, relying on detection limits to detect target analytes. Biofluids were sampled *in vivo* using dry swabs, while analytes from dry surfaces were collected by conditioning the swabs with an extractive solvent prior to sampling. Quantitative analysis can be performed by the adding of an internal standard; method validation is frequently conducted by hyphenated-MS confirmative techniques. In this way, Swab TS-MS analysis could represent a rapid and direct screening method in clinical field for point-of-care testing, that exploits a tool, the swab, that is commonly employed for sampling biological fluids and body surfaces in medical applications. The possibility to perform *in vivo* analysis is a significant advantage over DESI-MS technique, that allows *ex vivo* tissue analysis only.

The work from Fedick et al. [128] represents the only contribution of Swab TS-MS technique in forensic field, in particular for detection of organic gunshot residue from different surfaces, which is another situation where swabs are commonly used for sampling. Interestingly, detection of two target analytes after a single shot was performed both on a benchtop LTQ Orbitrap and a portable Mini 12 mass spectrometry, paving the way for possible *in situ* analyses in future.

### 1.2.3. Miniaturized and portable mass spectrometers

Typically, mass spectrometers are primarily utilized as benchtop instruments. These instruments have stringent operating conditions and are affected from many environmental aspects that potentially impact the accuracy and reliability of measurements [108]. With the goal of enhancing the accessibility and practicality of MS analysis, along with the growing interest in performing *in situ* analysis [131], a significant effort was spent to downsize MS instrumentation since the 1970s. The last twenty years saw a swift advancement in portable mass spectrometers, consistently with improvements of electronics and computer science in the miniaturization of devices[15]. In fact, this downsizing passes through improvements in its key components, as ion generation unit, mass analyzer, ion detector and vacuum system. Up to now, portable mass spectrometers are used for research in a broad range of application fields [15,128,132].

Ionization process is directly connected to sample processing and introduction, so the ion source modification is sometimes necessary for portable system. Another issue is the limited resolving power and, in some cases, the impossibility of performing tandem mass spectrometry acquisition [108] that makes in source fragmentation preferred.

Ambient MS ionization techniques perfectly fit portable application requirement, due to the absence of sample treatment and the possibly to perform rapid analysis. As an example, Fedick and Bain [128] conducted a study on the effectiveness of the swab touch spray method in identifying organic gunshot residue (OGSR) on various surfaces. The two targeted analytes were identified using the portable Mini 12 and benchtop LTQ Orbitrap XL after a single shot. Paper spray is also widely used in these applications [15], e. g. in the analysis of therapeutic drugs in dried blood spots [133].

Looking ahead, the relevant innovation taking place in AMS area, that enables direct and streamlined analysis, combined with advancement in technologies for portable MS systems, deserves to be followed up. AMS techniques could be used together with other screening assays like smartphone-based biosensors, in order to improve test reliability, for screening and confirmative purposes [108].

### 1.2.4. Miniaturized devices and Ambient Mass Spectrometry towards Green Analytical Chemistry

Green Chemistry has been outlined “as the utilization of techniques and methodologies that reduce or eliminate the use or generation of feedstocks, products, by-products, solvents, reagents, etc. that are hazardous to human health or the environment” [33]. It emerged in the early 1990s, representing chemistry's contribution to the concept of sustainable development. It brought attention to previously neglected areas within analytical science, such as reducing the use of harmful substances, minimizing

energy consumption and waste generation, and addressing concerns about operator safety and environmental impact [131]. The primary objectives of green analytical chemistry (GAC) strategies encompass the following [95]:

I. Eliminating or reducing the utilization of chemical substances such as solvents, reagents, preservatives, pH-adjusting additives, and others.
II. Minimizing energy consumption during the analytical process.
III. Implementing effective management strategies for analytical waste.
IV. Enhancing operator safety to ensure a secure working environment.

The GAC aligns well with the principles of Ambient Mass Spectrometry. In fact, one principle of GAC is to prioritize *in situ* analysis whenever feasible, eliminating the need for multiple analytical steps. Many critical applications, such as tissue biopsy analysis and therapeutic drug monitoring, would benefit from *in situ* analysis and the use of portable instruments to ensure prompt and accurate assessments. The paradigm shifts towards *in situ* analysis in chemical analysis and mass spectrometry, as opposed to traditional laboratory-based methods, establishes a strong link between green chemistry and AMS. This connection is reinforced by the increasing availability of portable mass spectrometers and the unique characteristics of AMS techniques (**Figure 1.18**).

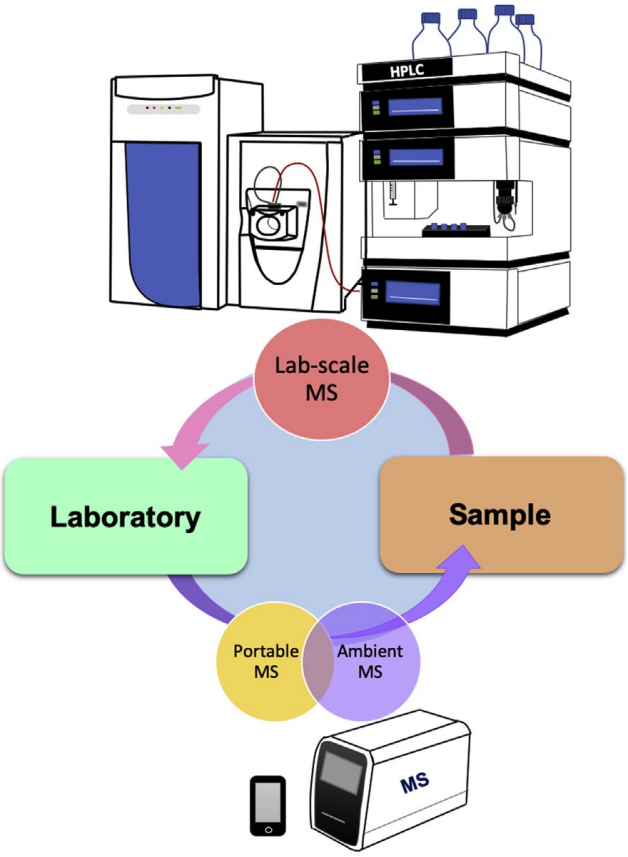


**Figure 1.18.** Shift in Mass Spectrometry from lab-scale to *in situ* analysis. Reprinted from Ref. [131] Copyright © 2023, with permission from Elsevier

For example, the removal (or reduction, at least) of sample processing, peculiar to AMS, as well as the absence of chromatographic separation, automatically leads to a very less consumption of solvents and reagents. Moreover, most part of AMS techniques, such as PS, DESI, DART or TS require a very little amount of sample (~ 5µL in some cases) and solvent volumes (from hundreds µL/min for chromatographic separation to less than a hundred µL/min, or complete absence of volume consumption) to perform a single analysis. A less consumption of gases is another guideline of GAC methods, which is carried out by direct ionization techniques like Paper Spray or Swab Touch Spray-MS, that do not need any gas for the ionization [10,131].

Another principle of GAC is the exploitation of automated methods. Even if most of Ambient MS methods require the presence of the operator for large part of data acquisition and analysis, many example of completed automated methods are reported, thanks to their commercial availability. This is the case of DESI, which also enables development of chemical images by 2D imaging MS, PS and DART [134–136]. Up to now, the most important drawback of AMS in accomplishing green approaches regards operator safety, since exposure to open-air sprays of solvents and high voltages sources is fairly common.

Many of the advancements of Ambient MS rely on enhancing the capabilities of compact, portable mass spectrometers by employing innovative instrumentation solutions that could enable enhanced and more selective acquisition modes; all these progresses will also pave the way for a more common use of AMS techniques, and therefore a larger implementation of GAC methods [131].

## Bibliography


(1) Ali, S.; Rezende, V. T.; Ullah, S.; de Paiva, E. L.; Tonin, F. G.; Abdullah; Corassin, C. H.; Oliveira, C. A. F. de. Food Processing and Challenges in the Food Production and Quality: The Foodomics Approach. *Food Biosci* **2023**, *56*. https://doi.org/10.1016/j.fbio.2023.103217.

(2) Rodrigues, R. C.; Pereira, H. S.; Senra, R. L.; Ribon, A. de O. B.; Mendes, T. A. de O. Understanding the Emerging Potential of Synthetic Biology for Food Science: Achievements, Applications and Safety Considerations. *Food Chemistry Advances* **2023**, *3*. https://doi.org/10.1016/j.focha.2023.100476.

(3) Kannaiah, K. P.; Chanduluru, H. K. Exploring Sustainable Analytical Techniques Using G Score and Future Innovations in Green Analytical Chemistry. *J Clean Prod* **2023**, *428*. https://doi.org/10.1016/j.jclepro.2023.139297.

(4) Hussain, C. M.; Hussain, C. G.; Keçili, R. White Analytical Chemistry Approaches for Analytical and Bioanalytical Techniques: Applications and Challenges. *TrAC - Trends in Analytical Chemistry* **2023**, *159*. https://doi.org/10.1016/j.trac.2022.116905.

(5) Cetinkaya, A.; Kaya, S. I.; Ozkan, S. A. An Overview of the Current Progress in Green Analytical Chemistry by Evaluating Recent Studies Using Greenness Assessment Tools. *TrAC - Trends in Analytical Chemistry* **2023**, *168*. https://doi.org/10.1016/j.trac.2023.117330.

(6) Shi, M.; Zheng, X.; Zhang, N.; Guo, Y.; Liu, M.; Yin, L. Overview of Sixteen Green Analytical Chemistry Metrics for Evaluation of the Greenness of Analytical Methods. *TrAC - Trends in Analytical Chemistry* **2023**, *166*. https://doi.org/10.1016/j.trac.2023.117211.

(7) Agrawal, A.; Keçili, R.; Ghorbani-Bidkorbeh, F.; Hussain, C. M. Green Miniaturized Technologies in Analytical and Bioanalytical Chemistry. *TrAC - Trends in Analytical Chemistry* **2021**, *143*. https://doi.org/10.1016/j.trac.2021.116383.

(8) Carasek, E.; Scur, R.; Bernardi, G. High-Throughput Analytical Methods Employing Microextraction Techniques: Towards Fast Analyses Lasting a Few Seconds. *Advances in Sample Preparation* **2023**, 100095. https://doi.org/10.1016/j.sampre.2023.100095.

(9) Chen, X.; Yao, C.; Li, Z. Microarray-Based Chemical Sensors and Biosensors: Fundamentals and Food Safety Applications. *TrAC - Trends in Analytical Chemistry* **2023**, *158*. https://doi.org/10.1016/j.trac.2022.116785.

(10) Javanshad, R.; Venter, A. R. Ambient Ionization Mass Spectrometry: Real-Time, Proximal Sample Processing and Ionization. *Analytical Methods* **2017**, *9* (34), 4896–4907. https://doi.org/10.1039/c7ay00948h.

(11) Wang, Z.; Zhu, H.; Xiong, W. Advances in Mass Spectrometry-Based Multi-Scale Metabolomic Methodologies and Their Applications in Biological and Clinical Investigations. *Sci Bull (Beijing)* **2023**. https://doi.org/10.1016/j.scib.2023.08.047.

(12) Aszyk, J.; Byliński, H.; Namieśnik, J.; Kot-Wasik, A. Main Strategies, Analytical Trends and Challenges in LC-MS and Ambient Mass Spectrometry–Based Metabolomics. *TrAC Trends in Analytical Chemistry* **2018**, *108*, 278–295. https://doi.org/10.1016/J.TRAC.2018.09.010.

(13) Liu, J.; Zhao, H.; Yin, Z.; Dong, H.; Chu, X.; Meng, X.; Li, Y.; Ding, X. Application and Prospect of Metabolomics-Related Technologies in Food Inspection. *Food Research International* **2023**, *171*. https://doi.org/10.1016/j.foodres.2023.113071.

(14) Costa, C.; van Es, E. M.; Sears, P.; Bunch, J.; Palitsin, V.; Cooper, H.; Bailey, M. J. Exploring a Route to a Selective and Sensitive Portable System for Explosive Detection– Swab Spray Ionisation Coupled to of High-Field Assisted Waveform Ion Mobility Spectrometry (FAIMS). *Forensic Sci Int* **2019**, *1*, 214–220. https://doi.org/10.1016/j.fsisyn.2019.07.009.

(15) Wang, J.; Pursell, M. E.; DeVor, A.; Awoyemi, O.; Valentine, S. J.; Li, P. Portable Mass Spectrometry System: Instrumentation, Applications, and Path to 'omics Analysis. *Proteomics* **2022**, *22* (23–24). https://doi.org/10.1002/pmic.202200112.

(16) Cavazza, A.; Mattarozzi, M.; Franzoni, A.; Careri, M. A Spotlight on Analytical Prospects in Food Allergens: From Emerging Allergens and Novel Foods to Bioplastics and Plant-Based Sustainable Food Contact Materials. *Food Chem* **2022**, *388*. https://doi.org/10.1016/j.foodchem.2022.132951.

(17) Blokland, M. H.; Gerssen, A.; Zoontjes, P. W.; Pawliszyn, J.; Nielen, M. W. F. Potential of Recent Ambient Ionization Techniques for Future Food Contaminant Analysis Using (Trans)Portable Mass Spectrometry. *Food Anal Methods* **2020**, *13* (3), 706–717. https://doi.org/10.1007/s12161-019-01666-6.

(18) Gross, J. H. *Mass Spectrometry*, 3rd edition.; Springer, **2017**.

(19) Moura, P. C.; Vassilenko, V. Contemporary Ion Mobility Spectrometry Applications and Future Trends towards Environmental, Health and Food Research: A Review. *Int J Mass Spectrom* **2023**, *486*, 117012. https://doi.org/10.1016/J.IJMS.2023.117012.

(20) Cooks, R. G.; Ouyang, Z.; Takats, Z.; Wiseman, J. M. Ambient Mass Spectrometry. *Science (1979)* **2006**, *311*, 1566–1570. https://doi.org/10.1126/science.1119426.

(21) Hernández-Mesa, M.; Ropartz, D.; García-Campaña, A. M.; Rogniaux, H.; Dervilly-Pinel, G.; Le Bizec, B. Ion Mobility Spectrometry in Food Analysis: Principles, Current Applications and Future Trends. *Molecules* **2019**, *24* (15). https://doi.org/10.3390/molecules24152706.

(22) Djambazova, K. V.; Van Ardenne, J. M.; Spraggins, J. M. Advances in Imaging Mass Spectrometry for Biomedical and Clinical Research. *TrAC - Trends in Analytical Chemistry* **2023**, *169*. https://doi.org/10.1016/j.trac.2023.117344.

(23) Sans, M.; Feider, C. L.; Eberlin, L. S. Advances in Mass Spectrometry Imaging Coupled to Ion Mobility Spectrometry for Enhanced Imaging of Biological Tissues. *Curr Opin Chem Biol* **2018**, *42*, 138–146. https://doi.org/10.1016/j.cbpa.2017.12.005.

(24) Feider, C. L.; Krieger, A.; Dehoog, R. J.; Eberlin, L. S. Ambient Ionization Mass Spectrometry: Recent Developments and Applications. *Anal Chem* **2019**, *91* (7), 4266–4290. https://doi.org/10.1021/acs.analchem.9b00807.

(25) Lu, H.; Zhang, H.; Chingin, K.; Xiong, J.; Fang, X.; Chen, H. Ambient Mass Spectrometry for Food Science and Industry. *TrAC - Trends in Analytical Chemistry* **2018**, *107*, 99–115. https://doi.org/10.1016/j.trac.2018.07.017.

(26) Martins, R. O.; de Araújo, G. L.; de Freitas, C. S.; Silva, A. R.; Simas, R. C.; Vaz, B. G.; Chaves, A. R. Miniaturized Sample Preparation Techniques and Ambient Mass Spectrometry as Approaches for Food Residue Analysis. *J Chromatogr A* **2021**, *1640*. https://doi.org/10.1016/j.chroma.2021.461949.

(27) Muggli, T. M.; Schürch, S. Analysis of Pesticide Residues on Fruit Using Swab Spray Ionization Mass Spectrometry. *Molecules* **2023**, *28* (18), 6611. https://doi.org/10.3390/molecules28186611.

(28) Black, C.; Chevallier, O. P.; Elliott, C. T. The Current and Potential Applications of Ambient Mass Spectrometry in Detecting Food Fraud. *TrAC - Trends in Analytical Chemistry* **2016**, *82*, 268–278. https://doi.org/10.1016/j.trac.2016.06.005.

(29) Morales, M. A.; Halpern, J. M. Guide to Selecting a Biorecognition Element for Biosensors. *Bioconjug Chem* **2018**, *29* (10), 3231–3239. https://doi.org/10.1021/acs.bioconjchem.8b00592.

(30) Mattarozzi, M.; Giannetto, M.; Careri, M. Electrochemical Immunomagnetic Assay as Biosensing Strategy for Determination of Ovarian Cancer Antigen HE4 in Human Serum. *Talanta* **2020**, *217*. https://doi.org/10.1016/j.talanta.2020.120991.

(31) Naresh, V.; Lee, N. A Review on Biosensors and Recent Development of Nanostructured Materials-Enabled Biosensors. *Sensors (Switzerland)* **2021**, *21* (4), 1–35. https://doi.org/10.3390/s21041109.

(32) Mattarozzi, M.; Toma, L.; Bertucci, A.; Giannetto, M.; Careri, M. Aptamer-Based Assays: Strategies in the Use of Aptamers Conjugated to Magnetic Micro- and Nanobeads as Recognition Elements in Food Control. *Anal Bioanal Chem* **2022**, *414* (1), 63-74. https://doi.org/10.1007/s00216-021-03501-6.

(33) Jurjeva, J.; Koel, M. Implementing Greening into Design in Analytical Chemistry. *Talanta Open* **2022**, *6*, 100136. https://doi.org/10.1016/J.TALO.2022.100136.

(34) Armenta, S.; Esteve-Turrillas, F. A.; Garrigues, S.; de la Guardia, M. Green Analytical Chemistry: The Role of Green Extraction Techniques. In *Comprehensive Analytical Chemistry*; Elsevier, **2017**; pp 7–25.

(35) del Valle, M. Sensors as Green Tools in Analytical Chemistry. *Curr Opin Green Sustain Chem* **2021**, *31*. https://doi.org/10.1016/j.cogsc.2021.100501.

(36) Ellington, A.; Szostak, J. In Vitro Selection of RNA Molecules That Bind Specific Ligands. *Nature* **1990**, *346*, 818–822. https://doi.org/10.1038/346818a0.

(37) Darmostuk, M.; Rimpelova, S.; Gbelcova, H.; Ruml, T. Current Approaches in SELEX: An Update to Aptamer Selection Technology. *Biotechnol Adv* **2014**, *33* (6), 1141–1161. https://doi.org/10.1016/j.biotechadv.2015.02.008.

(38) Tuerk, C.; Gold, L. Systematic Evolution of Ligands by Exponential Enrichment: RNA Ligands to Bacteriophage T4 DNA Polymerase. *Science (1979)* **2012**, *249*, 505–510. https://doi.org/10.1126/science.2200121.

(39) Ilgu, M.; Nilsen-Hamilton, M. Aptamers in Analytics. *Analyst* **2016**, *141* (5), 1551–1558. https://doi.org/10.1039/c5an01824b.

(40) Cho, E. J.; Lee, J. W.; Ellington, A. D. Applications of Aptamers as Sensors. *Annual Review of Analytical Chemistry* **2009**, *2*, 241–264. https://doi.org/10.1146/annurev.anchem.1.031207.112851.

(41) Zhang, Y.; Lai, B. S.; Juhas, M. Recent Advances in Aptamer Discovery and Applications. *Molecules* **2019**, *24* (5). https://doi.org/10.3390/molecules24050941.

(42) Gelinas, A. D.; Davies, D. R.; Janjic, N. Embracing Proteins: Structural Themes in Aptamer-Protein Complexes. *Curr Opin Struct Biol* **2016**, *36*, 122–132. https://doi.org/10.1016/j.sbi.2016.01.009.

(43) Gupta, M. K.; Chheda, N.; Gupta, M. K. RNA as a Permutation, **2014**. https://www.researchgate.net/publication/261030242.

(44) Bottari, F.; Daems, E.; De Vries, A. M.; Van Wielendaele, P.; Trashin, S.; Blust, R.; Sobott, F.; Madder, A.; Martins, J. C.; De Wael, K. Do Aptamers Always Bind? The Need for a Multifaceted Analytical Approach When Demonstrating Binding Affinity between Aptamer and Low Molecular Weight Compounds. *J Am Chem Soc* **2020**, *142* (46), 19622–19630. https://doi.org/10.1021/jacs.0c08691.

(45) Wu, Y.; Belmonte, I.; Sykes, K. S.; Xiao, Y.; White, R. J. Perspective on the Future Role of Aptamers in Analytical Chemistry. *Anal Chem* **2019**, *91* (24), 15335–15344. https://doi.org/10.1021/acs.analchem.9b03853.

(46) Bock, L. C.; Griffin, L. C.; Latham, J. A.; Vermaas, E. H.; Toole, J. J. Selection of Single-Stranded DNA Molecules That Bind and Inhibit Human Thrombin. *Letters to Nature* **1992**, *355*, 564–566. https://doi.org/10.1038/355564a0.

(47) Lin, P. H.; Chen, R. H.; Lee, C. H.; Chang, Y.; Chen, C. S.; Chen, W. Y. Studies of the Binding Mechanism between Aptamers and Thrombin by Circular Dichroism, Surface Plasmon Resonance and Isothermal Titration Calorimetry. *Colloids Surf B Biointerfaces* **2011**, *88* (2), 552–558. https://doi.org/10.1016/j.colsurfb.2011.07.032.

(48) McKeague, M.; De Girolamo, A.; Valenzano, S.; Pascale, M.; Ruscito, A.; Velu, R.; Frost, N. R.; Hill, K.; Smith, M.; McConnell, E. M.; DeRosa, M. C. Comprehensive Analytical Comparison of Strategies Used for Small Molecule Aptamer Evaluation. *Anal Chem* **2015**, *87* (17), 8608–8612. https://doi.org/10.1021/acs.analchem.5b02102.

(49) Thevendran, R.; Citartan, M. Assays to Estimate the Binding Affinity of Aptamers. *Talanta* **2022**, *238*. https://doi.org/10.1016/j.talanta.2021.122971.

(50) Liu, M.; Yu, X.; Chen, Z.; Yang, T.; Yang, D.; Liu, Q.; Du, K.; Li, B.; Wang, Z.; Li, S.; Deng, Y.; He, N. Aptamer Selection and Applications for Breast Cancer Diagnostics and Therapy. *J Nanobiotechnology* **2017**, *15* (1). https://doi.org/10.1186/s12951-017-0311-4.

(51) Zhu, G.; Chen, X. Aptamer-Based Targeted Therapy. *Adv Drug Deliv Rev* **2018**, *134*, 65–78. https://doi.org/10.1016/j.addr.2018.08.005.

(52) Ni, S.; Zhuo, Z.; Pan, Y.; Yu, Y.; Li, F.; Liu, J.; Wang, L.; Wu, X.; Li, D.; Wan, Y.; Zhang, L.; Yang, Z.; Zhang, B. T.; Lu, A.; Zhang, G. Recent Progress in Aptamer Discoveries and Modifications for Therapeutic Applications. *ACS Appl Mater Interfaces* **2021**, *13* (8), 9500–9519. https://doi.org/10.1021/acsami.0c05750.

(53) Melinte, G.; Selvolini, G.; Cristea, C.; Marrazza, G. Aptasensors for Lysozyme Detection: Recent Advances. *Talanta* **2021**, *226*. https://doi.org/10.1016/j.talanta.2021.122169.

(54) Dwidar, M.; Yokobayashi, Y. Development of a Histamine Aptasensor for Food Safety Monitoring. *Sci Rep* **2019**, *9* (1). https://doi.org/10.1038/s41598-019-52876-1.

(55) Phanchai, W.; Srikulwong, U.; Chompoosor, A.; Sakonsinsiri, C.; Puangmali, T. Insight into the Molecular Mechanisms of AuNP-Based Aptasensor for Colorimetric Detection: A Molecular Dynamics Approach. *Langmuir* **2018**, *34* (21), 6161–6169. https://doi.org/10.1021/acs.langmuir.8b00701.

(56) Rezaei, B.; Jamei, H. R.; Ensafi, A. A. An Ultrasensitive and Selective Electrochemical Aptasensor Based on RGO-MWCNTs/Chitosan/Carbon Quantum Dot for the Detection of Lysozyme. *Biosens Bioelectron* **2018**, *115*, 37–44. https://doi.org/10.1016/j.bios.2018.05.012.

(57) Naghshbandi, B.; Adabi, M.; Pooshang Bagheri, K.; Tavakolipour, H. Design of a New Electrochemical Aptasensor Based on Screen Printed Carbon Electrode Modified with Gold Nanoparticles for the Detection of Fumonisin B1 in Maize Flour. *J Nanobiotechnology* **2022**, *20* (1). https://doi.org/10.1186/s12951-022-01745-7.

(58) Malekzad, H.; Jouyban, A.; Hasanzadeh, M.; Shadjou, N.; de la Guardia, M. Ensuring Food Safety Using Aptamer Based Assays: Electroanalytical Approach. *TrAC Trends in Analytical Chemistry* **2017**, *94*, 77–94. https://doi.org/10.1016/J.TRAC.2017.07.001.

(59) Lin, Y.; Sun, Y.; Dai, Y.; Zhu, X.; Liu, H.; Han, R.; Gao, D.; Luo, C.; Wang, X. A Chemiluminescence Assay for Determination of Lysozyme Based on the Use of Magnetic Alginate-Aptamer Composition and Hemin@HKUST-1. *Microchimica Acta* **2020**, *187* (5). https://doi.org/10.1007/s00604-020-04254-2.

(60) Han, B.; Zhao, C.; Yin, J.; Wang, H. High Performance Aptamer Affinity Chromatography for Single-Step Selective Extraction and Screening of Basic Protein Lysozyme. *Journal of Chromatography B* **2012**, *903*, 112–117. https://doi.org/10.1016/J.JCHROMB.2012.07.003.

(61) Liu, H.; Zhao, Y.; Lu, A.; Ye, J.; Wang, J.; Wang, S.; Luan, Y. An Aptamer Affinity Column for Purification and Enrichment of Aflatoxin B1 and Aflatoxin B2 in Agro-Products. *Anal Bioanal Chem* **2020**, *412* (4), 895–904. https://doi.org/10.1007/s00216-019-02300-4.

(62) Liu, H.; Luan, Y.; Lu, A.; Li, B.; Yang, M.; Wang, J. H. An Oligosorbent-Based Aptamer Affinity Column for Selective Extraction of Aflatoxin B2 Prior to HPLC with Fluorometric Detection. *Microchimica Acta* **2018**, *185* (1). https://doi.org/10.1007/s00604-017-2591-7.

(63) Zhao, Y.; Wang, N.; Gao, H. L.; Guo, Z. X.; Lu, A. X.; Guo, X. J.; Lu, J. H.; Luan, Y. X. Determination of Aflatoxin B1 in Lotus Seed by High Performance Liquid Chromatography with Aptamer Affinity Column for Purification and Enrichment. *Chinese Journal of Analytical Chemistry* **2020**, *48* (5), 662–669. https://doi.org/10.1016/S1872-2040(20)60022-6.

(64) Chen, Y.; Ding, X.; Zhu, D.; Lin, X.; Xie, Z. Preparation and Evaluation of Highly Hydrophilic Aptamer-Based Hybrid Affinity Monolith for on-Column Specific Discrimination of Ochratoxin A. *Talanta* **2019**, *200*, 193–202. https://doi.org/10.1016/j.talanta.2019.03.053.

(65) Chi, J.; Chen, M.; Deng, L.; Lin, X.; Xie, Z. A Facile AuNPs@aptamer-Modified Mercaptosiloxane-Based Hybrid Affinity Monolith with an Unusually High Coverage Density of Aptamer for on-Column Selective Extraction of Ochratoxin A. *Analyst* **2018**, *143* (21), 5210–5217. https://doi.org/10.1039/c8an01531g.

(66) Arciszewska, K.; Kowalska, E.; Bartnicki, F.; Bonarek, P.; Banaś, A. K.; Strzałka, W. DNA Aptamer-Based Affinity Chromatography System for Purification of Recombinant Proteins Tagged with Lysine Tag. *J Chromatogr A* **2023**, *1692*. https://doi.org/10.1016/j.chroma.2023.463846.

(67) Garwolinska, D.; Marcinkowska, R.; Namiesnik, J.; Hewelt-Belka, W. Sample Preparation in Foodomics: Miniaturized Solid-Phase Extraction. *Comprehensive Foodomics* **2021**, 566–580. https://doi.org/10.1016/B978-0-08-100596-5.22806-0.

(68) Vergara-Barberán, M.; Lerma-García, M. J.; Moga, A.; Carrasco-Correa, E. J.; Martínez-Pérez-Cejuela, H.; Beneito-Cambra, M.; Simó-Alfonso, E. F.; Herrero-Martínez, J. M. Recent Advances in Aptamer-Based Miniaturized Extraction Approaches in Food Analysis. *TrAC - Trends in Analytical Chemistry* **2021**, *138*. https://doi.org/10.1016/j.trac.2021.116230.

(69) Martins, R. O.; de Araújo, G. L.; de Freitas, C. S.; Silva, A. R.; Simas, R. C.; Vaz, B. G.; Chaves, A. R. Miniaturized Sample Preparation Techniques and Ambient Mass Spectrometry as Approaches for Food Residue Analysis. *J Chromatogr A* **2021**, *1640*. https://doi.org/10.1016/j.chroma.2021.461949.

(70) Wang, Y.; Zhai, H.; Yin, J.; Guo, Q.; Zhang, Y.; Sun, X.; Guo, Y.; Yang, Q.; Li, F.; Zhang, Y. Recent Advances and Future Prospects of Aptamer-Based Biosensors in Food Safety Analysis. *Int J Electrochem Sci* **2022**, *17*. https://doi.org/10.20964/2022.01.07.

(71) Xu, Z.; Chen, Y.; Tang, Y.; Chen, M.; Chen, W.; Cheng, Y. Aptamer-Enhanced Fluorescence Determination of Bisphenol A after Magnetic Solid-Phase Extraction Using Fe3O4@SiO2@aptamer. *Analytical Methods* **2020**, *12* (36), 4479–4486. https://doi.org/10.1039/d0ay01124j.

(72) Lin, S.; Gan, N.; Zhang, J.; Qiao, L.; Chen, Y.; Cao, Y. Aptamer-Functionalized Stir Bar Sorptive Extraction Coupled with Gas Chromatography-Mass Spectrometry for Selective Enrichment and Determination of Polychlorinated Biphenyls in Fish Samples. *Talanta* **2016**, *149*, 266–274. https://doi.org/10.1016/j.talanta.2015.11.062.

(73) Guo, Y.; Wei, W.; Zhang, Y.; Dai, Y.; Wang, W.; Wang, A. Determination of Sulfadimethoxine in Milk with Aptamer-Functionalized Fe3O4/Graphene Oxide as Magnetic Solid-Phase Extraction Adsorbent Prior to HPLC. *J Sep Sci* **2020**, *43* (17), 3499–3508. https://doi.org/10.1002/jssc.202000277.

(74) Tu, C.; Guo, Y.; Dai, Y.; Wei, W.; Wang, W.; Wu, L.; Wang, A. Determination of Chloramphenicol in Honey and Milk by HPLC Coupled with Aptamer-Functionalized Fe3O4/Graphene Oxide Magnetic Solid-Phase Extraction. *J Food Sci* **2019**, *84* (12), 3624–3633. https://doi.org/10.1111/1750-3841.14955.

(75) Liu, X.; Ren, J.; Su, L.; Gao, X.; Tang, Y.; Ma, T.; Zhu, L.; Li, J. Novel Hybrid Probe Based on Double Recognition of Aptamer-Molecularly Imprinted Polymer Grafted on Upconversion

Nanoparticles for Enrofloxacin Sensing. *Biosens Bioelectron* **2017**, *87*, 203–208. https://doi.org/10.1016/j.bios.2016.08.051.

(76) Zhang, Q.; Zhou, Q.; Yang, L.; Wang, X.; Zheng, Y.; Bao, L. Covalently Bonded Aptamer-Functionalised Magnetic Mesoporous Carbon for High-Efficiency Chloramphenicol Detection. *J Sep Sci* **2020**, *43* (13), 2610–2618. https://doi.org/10.1002/jssc.201901189.

(77) Nasirian, V.; Chabok, A.; Barati, A.; Rafienia, M.; Arabi, M. S.; Shamsipur, M. Ultrasensitive Aflatoxin B1 Assay Based on FRET from Aptamer Labelled Fluorescent Polymer Dots to Silver Nanoparticles Labeled with Complementary DNA. *Microchimica Acta* **2017**, *184* (12), 4655–4662. https://doi.org/10.1007/s00604-017-2508-5.

(78) Kalita, J. J.; Sharma, P.; Bora, U. Recent Developments in Application of Nucleic Acid Aptamer in Food Safety. *Food Control* **2023**, *145*. https://doi.org/10.1016/j.foodcont.2022.109406.

(79) Banu, K.; Mondal, B.; Rai, B.; Monica, N.; Hanumegowda, R. Prospects for the Application of Aptamer Based Assay Platforms in Pathogen Detection. *Biocybern Biomed Eng* **2022**, *42* (3), 934–949. https://doi.org/10.1016/j.bbe.2022.07.005.

(80) Sun, L.; Zhao, Q. Competitive Horseradish Peroxidase-Linked Aptamer Assay for Sensitive Detection of Aflatoxin B1. *Talanta* **2018**, *179*, 344–349. https://doi.org/10.1016/j.talanta.2017.11.048.

(81) Jing, L.; Li, J.; Qin, M.; Song, Y.; Zhang, J.; Chen, Q.; Xia, X.; Han, Q. Development and Characterization of Sandwich-Type Enzyme-Linked Aptamer Assay for the Detection of Rongalite in Food. *Anal Biochem* **2018**, *563*, 25–34. https://doi.org/10.1016/j.ab.2018.09.019.

(82) Chen, L.; Yang, G.; Qu, F. Advances of Aptamer-Based Small-Molecules Sensors in Body Fluids Detection. *Talanta* **2023**, 125348. https://doi.org/10.1016/j.talanta.2023.125348.

(83) Ziółkowski, R.; Jarczewska, M.; Górski, Ł.; Malinowska, E. From Small Molecules toward Whole Cells Detection: Application of Electrochemical Aptasensors in Modern Medical Diagnostics. *Sensors (Switzerland)* **2021**, *21* (3), 1–49. https://doi.org/10.3390/s21030724.

(84) Prante, M.; Segal, E.; Scheper, T.; Bahnemann, J.; Walter, J. Aptasensors for Point-of-Care Detection of Small Molecules. *Biosensors (Basel)* **2020**, *10* (9). https://doi.org/10.3390/bios10090108.

(85) Khedri, M.; Ramezani, M.; Rafatpanah, H.; Abnous, K. Detection of Food-Born Allergens with Aptamer-Based Biosensors. *TrAC - Trends in Analytical Chemistry* **2018**, *103*, 126–136. https://doi.org/10.1016/j.trac.2018.04.001.

(86) Mishra, R. K.; Hayat, A.; Mishra, G. K.; Catanante, G.; Sharma, V.; Marty, J. L. A Novel Colorimetric Competitive Aptamer Assay for Lysozyme Detection Based on Superparamagnetic Nanobeads. *Talanta* **2017**, *165*, 436–441. https://doi.org/10.1016/j.talanta.2016.12.083.

(87) Jo, M.; Ahn, J. Y.; Lee, J.; Lee, S.; Hong, S. W.; Yoo, J. W.; Kang, J.; Dua, P.; Lee, D. K.; Hong, S.; Kim, S. Development of Single-Stranded DNA Aptamers for Specific Bisphenol a Detection. *Oligonucleotides* **2011**, *21* (2), 85–91. https://doi.org/10.1089/oli.2010.0267.

(88) Chen, M. L.; Chen, J. H.; Ding, L.; Xu, Z.; Wen, L.; Wang, L. B.; Cheng, Y. H. Study of the Detection of Bisphenol A Based on a Nano-Sized Metal-Organic Framework Crystal and an Aptamer. *Analytical Methods* **2017**, *9* (6), 906–909. https://doi.org/10.1039/c6ay03151j.

(89) Ferguson, B. S.; Hoggarth, D. A.; Maliniak, D.; Ploense, K.; White, R. J.; Woodward, N.; Hsieh, K.; Bonham, A. J.; Eisenstein, M.; Kippin, T. E.; Plaxco, K. W.; Soh, H. T. Real-Time, Aptamer-Based Tracking of Circulating Therapeutic Agents in Living Animals. *Sci Transl Med* **2013**, *5* (213). https://doi.org/10.1126/scitranslmed.3007095.

(90) Kudr, J.; Klejdus, B.; Adam, V.; Zitka, O. Magnetic Solids in Electrochemical Analysis. *TrAC - Trends in Analytical Chemistry* **2018**, *98*, 104–113. https://doi.org/10.1016/j.trac.2017.10.023.

(91) Faraji, M.; Shirani, M.; Rashidi-Nodeh, H. The Recent Advances in Magnetic Sorbents and Their Applications. *TrAC - Trends in Analytical Chemistry* **2021**, *141*. https://doi.org/10.1016/j.trac.2021.116302.

(92) Wang, L.; Huang, X.; Wang, C.; Tian, X.; Chang, X.; Ren, Y.; Yu, S. Applications of Surface Functionalized Fe3O4 NPs-Based Detection Methods in Food Safety. *Food Chem* **2021**, *342*. https://doi.org/10.1016/j.foodchem.2020.128343.

(93) Pérez-Ruiz, E.; Lammertyn, J.; Spasic, D. Evaluation of Different Strategies for Magnetic Particle Functionalization with DNA Aptamers. *N Biotechnol* **2016**, *33* (6), 755–762. https://doi.org/10.1016/j.nbt.2016.06.1459.

(94) Capriotti, A. L.; Cavaliere, C.; La Barbera, G.; Montone, C. M.; Piovesana, S.; Laganà, A. Recent Applications of Magnetic Solid-Phase Extraction for Sample Preparation. *Chromatographia* **2019**, *82* (8), 1251–1274. https://doi.org/10.1007/s10337-019-03721-0.

(95) Gałuszka, A.; Migaszewski, Z.; Namieśnik, J. The 12 Principles of Green Analytical Chemistry and the SIGNIFICANCE Mnemonic of Green Analytical Practices. *TrAC Trends in Analytical Chemistry* **2013**, *50*, 78–84. https://doi.org/10.1016/J.TRAC.2013.04.010.

(96) Samanidou, V. *Solid Phase Extraction State of the Art and Future Perspectives Molecules*; **2019**. www.mdpi.com/journal/molecules.

(97) Lucena, R.; Cárdenas Aranzana, M. S. Analytical Sample Preparation with Nano- and Other High-Performance Materials. **2021**.

(98) Suseela, M. N. L.; Viswanadh, M. K.; Mehata, A. K.; Priya, V.; Vikas; Setia, A.; Malik, A. K.; Gokul, P.; Selvin, J.; Muthu, M. S. Advances in Solid-Phase Extraction Techniques: Role of

Nanosorbents for the Enrichment of Antibiotics for Analytical Quantification. *J Chromatogr A* **2023**, *1695*. https://doi.org/10.1016/j.chroma.2023.463937.

(99) Šafaříková, M.; Šafařík, I. Magnetic Solid-Phase Extraction. *J Magn Magn Mater* **1999**, *194* (1–3), 108–112. https://doi.org/10.1016/S0304-8853(98)00566-6.

(100) Piqueras-García, N.; Vergara-Barberán, M.; Lerma-García, M. J.; Herrero-Martínez, J. M. Aptamer-Functionalized Magnetic Supports for Sample Preparation. *Advances in Sample Preparation* **2023**, *7*. https://doi.org/10.1016/j.sampre.2023.100083.

(101) Khodadadi, M.; Malekpour, A.; Mehrgardi, M. A. Aptamer Functionalized Magnetic Nanoparticles for Effective Extraction of Ultratrace Amounts of Aflatoxin M1 Prior Its Determination by HPLC. *J Chromatogr A* **2018**, *1564*, 85–93. https://doi.org/10.1016/J.CHROMA.2018.06.022.

(102) Miller, A. A.; Rao, A. S.; Nelakanti, S. R.; Kujalowicz, C.; Shi, T.; Rodriguez, T.; Ellington, A. D.; Stovall, G. M. Systematic Review of Aptamer Sequence Reporting in the Literature Reveals Widespread Unexplained Sequence Alterations. *Anal Chem* **2022**, *94* (22), 7731–7737. https://doi.org/10.1021/acs.analchem.1c04407.

(103) Zong, C.; Liu, J. The Arsenic-Binding Aptamer Cannot Bind Arsenic: Critical Evaluation of Aptamer Selection and Binding. *Anal Chem* **2019**, *91* (16), 10887–10893. https://doi.org/10.1021/acs.analchem.9b02789.

(104) Mattarozzi, M.; Toma, L.; Bertucci, A.; Giannetto, M.; Careri, M. Aptamer-Based Assays: Strategies in the Use of Aptamers Conjugated to Magnetic Micro- and Nanobeads as Recognition Elements in Food Control. *Anal Bioanal Chem* **2022**, *414* (1), 63-74. https://doi.org/10.1007/s00216-021-03501-6.

(105) Takáts, Z.; Wiseman, J. M.; Cooks, R. G. Ambient Mass Spectrometry Using Desorption Electrospray Ionization (DESI): Instrumentation, Mechanisms and Applications in Forensics, Chemistry, and Biology. *Journal of Mass Spectrometry* **2005**, *40* (10), 1261–1275. https://doi.org/10.1002/jms.922.

(106) Takáts, Z.; Wiseman, J. M.; Gologan, B.; Graham Cooks, R. Mass Spectrometry Sampling Under Ambient Conditions with Desorption Electrospray Ionization. *Ind. Eng. Chem. Process Des. Dev* **1998**, *297* (2), 209. https://doi.org/10.1126/science.1104404.

(107) Cody, R. B.; Laramée, J. A.; Durst, H. D. Versatile New Ion Source for the Analysis of Materials in Open Air under Ambient Conditions. *Anal Chem* **2005**, *77* (8), 2297–2302. https://doi.org/10.1021/ac050162j.

(108) Birse, N.; Broadbent, J. A.; Bose, U.; Hamzelou, S.; Nelis, J. L. D. Benchmarking Screening Assays Using Ambient Mass Spectrometry; **2023**. https://doi.org/10.1016/bs.coac.2023.01.002.

(109) Arrizabalaga-Larrañaga, A.; Ayala-Cabrera, J. F.; Seró, R.; Santos, J. F.; Moyano, E. Ambient Ionization Mass Spectrometry in Food Analysis. In *Food Toxicology and Forensics*; Elsevier, **2020**; pp 271–312. https://doi.org/10.1016/B978-0-12-822360-4.00006-6.

(110) Rankin-Turner, S.; Reynolds, J. C.; Turner, M. A.; Heaney, L. M. Applications of Ambient Ionization Mass Spectrometry in 2021: An Annual Review. *Analytical Science Advances* **2022**, *3* (3–4), 67–89. https://doi.org/10.1002/ansa.202100067.

(111) Seró, R.; Núñez; Moyano, E. Ambient Ionisation-High-Resolution Mass Spectrometry. Environmental, Food, Forensic and Doping Analysis. *Comprehensive Analytical Chemistry* **2016**, *71*, 51–88. https://doi.org/10.1016/bs.coac.2016.01.003.

(112) Gross, J. H. Direct Analysis in Real Time-a Critical Review on DART-MS. *Anal Bioanal Chem* **2014**, *406* (1), 63–80. https://doi.org/10.1007/s00216-013-7316-0.

(113) Tose, L. V.; Murgu, M.; Vaz, B. G.; Romão, W. Application of Atmospheric Solids Analysis Probe Mass Spectrometry (ASAP-MS) in Petroleomics: Analysis of Condensed Aromatics Standards, Crude Oil, and Paraffinic Fraction. *J Am Soc Mass Spectrom* **2017**, *28* (11), 2401–2407. https://doi.org/10.1007/s13361-017-1764-2.

(114) McBride, E. M.; Mach, P. M.; Dhummakupt, E. S.; Dowling, S.; Carmany, D. O.; Demond, P. S.; Rizzo, G.; Manicke, N. E.; Glaros, T. Paper Spray Ionization: Applications and Perspectives. *TrAC - Trends in Analytical Chemistry* **2019**, *118*, 722–730. https://doi.org/10.1016/j.trac.2019.06.028.

(115) Klampfl, C. W.; Himmelsbach, M. Direct Ionization Methods in Mass Spectrometry: An Overview. *Anal Chim Acta* **2015**, *890*, 44–59. https://doi.org/10.1016/J.ACA.2015.07.012.

(116) Han, F.; Yang, Y.; Ouyang, J.; Na, N. Direct Analysis of In-Gel Proteins by Carbon Nanotubes-Modified Paper Spray Ambient Mass Spectrometry. *Analyst* **2015**, *140* (3), 710–715. https://doi.org/10.1039/c4an01688b.

(117) Jin, L.; Yajun, Z.; Wei, M.; Theoneste, M.; Zhiping, Z. Polystyrene-Impregnated Paper Substrates for Direct Mass Spectrometric Analysis of Proteins and Peptides in Complex Matrices. *Analytical Methods* **2018**, *10*, 2803–2811. https://doi.org/10.1039/C8AY01081A.

(118) Zhang, Y.; Ju, Y.; Huang, C.; Wysocki. Vicky H. Paper Spray Ionization of Noncovalent Protein Complexes. *Anal Chem* **2014**, *86*, 1342–1346. https://doi.org/10.1021/ac403383d.

(119) Conaway, M. P.; Scientific, T. F. *The World Leader in Serving Science Rapid Biofluid Analysis Using the Prosolia Velox 360™ PaperSpray ® System and Mass Spectrometry*.

(120) Shen, L.; Zhang, J.; Yang, Q.; Manicke, N. E.; Ouyang, Z. High Throughput Paper Spray Mass Spectrometry Analysis. *Clinica Chimica Acta* **2013**, *420*, 28–33. https://doi.org/10.1016/J.CCA.2012.10.025.

(121) Jarmusch, A. K.; Pirro, V.; Logsdon, D. L.; Cooks, R. G. Direct Ion Generation from Swabs. *Talanta* **2018**, *184*, 356–363. https://doi.org/10.1016/j.talanta.2018.02.105.

(122) Yang, B. C.; Wang, F.; Yang, X.; Zou, W.; Wang, J. C.; Zou, Y.; Liu, F. Y.; Liu, H.; Huang, O. P. Medical Swab Touch Spray-Mass Spectrometry for Newborn Screening of Nicotine and Cotinine in Meconium. *Journal of Mass Spectrometry* **2016**, *51* (12), 1237–1242. https://doi.org/10.1002/jms.3892.

(123) Pirro, V.; Llor, R. S.; Jarmusch, A. K.; Alfaro, C. M.; Cohen-Gadol, A. A.; Hattab, E. M.; Cooks, R. G.; Cooks, R. G. Analysis of Human Gliomas by Swab Touch Spray-Mass Spectrometry: Applications to Intraoperative Assessment of Surgical Margins and Presence of Oncometabolites - *Electronic Supplementary Material (ESI)*. *Analyst* **2017**. https://doi.org/10.1039/c7an01334e.

(124) Pirro, V.; Llor, R. S.; Jarmusch, A. K.; Alfaro, C. M.; Cohen-Gadol, A. A.; Hattab, E. M.; Cooks, R. G. Analysis of Human Gliomas by Swab Touch Spray-Mass Spectrometry: Applications to Intraoperative Assessment of Surgical Margins and Presence of Oncometabolites. *Analyst* **2017**, *142* (21), 4058–4066. https://doi.org/10.1039/c7an01334e.

(125) Jarmusch, A. K.; Pirro, V.; Kerian, K. S.; Cooks, R. G. Detection of Strep Throat Causing Bacterium Directly from Medical Swabs by Touch Spray-Mass Spectrometry. *Analyst* **2014**, *139* (19), 4785–4789. https://doi.org/10.1039/c4an00959b.

(126) Morato, N. M.; Pirro, V.; Fedick, P. W.; Cooks, R. G. Quantitative Swab Touch Spray Mass Spectrometry for Oral Fluid Drug Testing. *Anal Chem* **2019**, *91* (11), 7450–7457. https://doi.org/10.1021/acs.analchem.9b01637.

(127) Pirro, V.; Jarmusch, A. K.; Vincenti, M.; Cooks, R. G. Direct Drug Analysis from Oral Fluid Using Medical Swab Touch Spray Mass Spectrometry. *Anal Chim Acta* **2015**, *861*, 47–54. https://doi.org/10.1016/j.aca.2015.01.008.

(128) Fedick, P. W.; Bain, R. M. Swab Touch Spray Mass Spectrometry for Rapid Analysis of Organic Gunshot Residue from Human Hand and Various Surfaces Using Commercial and Fieldable Mass Spectrometry Systems. *Forensic Chemistry* **2017**, *5*, 53–57. https://doi.org/10.1016/j.forc.2017.06.005.

(129) Kerian, K. S.; Jarmusch, A. K.; Pirro, V.; Koch, M. O.; Masterson, T. A.; Cheng, L.; Cooks, R. G. Differentiation of Prostate Cancer from Normal Tissue in Radical Prostatectomy Specimens by Desorption Electrospray Ionization and Touch Spray Ionization Mass Spectrometry. *Analyst* **2015**, *140* (4), 1090–1098. https://doi.org/10.1039/c4an02039a.

(130) Snyder, D. T.; Szalwinski, L. J.; Schrader, R. L.; Pirro, V.; Hilger, R.; Cooks, R. G. Precursor and Neutral Loss Scans in an RF Scanning Linear Quadrupole Ion Trap. *J Am Soc Mass Spectrom* **2018**, *29* (7), 1345–1354. https://doi.org/10.1007/s13361-018-1920-3.

(131) Molina-Díaz, A.; Beneito-Cambra, M.; Moreno-González, D.; Gilbert-López, B. Ambient Mass Spectrometry from the Point of View of Green Analytical Chemistry. *Curr Opin Green Sustain Chem* **2019**, *19*, 50–60. https://doi.org/10.1016/J.COGSC.2019.05.005.

(132) Pu, F.; Chiang, S.; Zhang, W.; Ouyang, Z. Direct Sampling Mass Spectrometry for Clinical Analysis. *Analyst* **2019**, *144* (4), 1034–1051. https://doi.org/10.1039/c8an01722k.

(133) Zhang, Z.; Xu, W.; Manicke, N. E.; Cooks, R. G.; Ouyang, Z. Silica Coated Paper Substrate for Paper-Spray Analysis of Therapeutic Drugs in Dried Blood Spots. *Anal Chem* **2012**, *84* (2), 931–938. https://doi.org/10.1021/ac202058w.

(134) *DART SVP Hardware and Network Installation Manual For DART SVP Source and Controllers*; **2014**.

(135) Conaway, M. P.; Scientific, T. F. *The World Leader in Serving Science Rapid Biofluid Analysis Using the Prosolia Velox 360™ PaperSpray ® System and Mass Spectrometry*.

(136) Towers, M.; Reid, L.; Murray, P.; Ballantyne, J.; Chipperfield, J. *DESI XS – Designed to Deliver*. www.waters.com.

# 2. Aptamer potentialities for biomimetic protein recognition for food safety issues: the case of anti-lysozyme aptamers

## 2.1. Introduction

Among bioreceptors, which are molecules that exhibit high affinity and selectivity for specific analytes even in presence of interfering compounds, aptamers stand out as synthetic, biologically inspired bio-recognition elements of great interest. As discussed in the general Introduction section, these oligonucleotides can recognize specific molecules with high affinity and selectivity through various molecular interactions.

Since their introduction more than 30 years ago, aptamers looked very promising to the scientific community for the possibility to exploit them in different fields: as bioreceptors for drug delivery and therapeutics [1], and as biorecognition elements in the analytical field, mainly for the development of aptasensors [2,3]. In the analytical chemistry field, predominant aptamer utilization regards biosensing platforms, with limited applications in separation techniques (such as affinity chromatography) and sample treatment techniques [4,5]. The integration of these bioreceptors with magnetic micro- and nanomaterial supports, widely employed in the design of biosensing strategies, could also prove valuable in the development of selective sample treatment methodologies, such as magnetic solid-phase extraction (MSPE)[2], as recently discussed by our research group [2]. Up to now, a wide list of aptamers has been selected for different targets, including small organic molecules, metal ions, proteins, and even entire cells, leading to many papers published in the field [5] (more than 33,000 results from Science Direct database search, from year 2000 to 2023).

Actually, there is an increasing criticism regarding the application of aptamers. In fact, although some innovations on SELEX procedure have led to the selection of aptamers for a wide range of molecular targets in the last years, only a few of them are successfully integrated into analytical platforms [4,5]. In addition, some aptamers have recently been shown to be unsuitable for effective target binding and practical analytical applications, despite having been widely used in several analytical contexts and sensing applications [5–8]. The failure of some aptamer sequences is often ascribable to an insufficient attention by the scientific community to a rigorous characterization of aptamer performance and aptamer/target interaction; consequently, affinity, selectivity/specificity and robustness of some aptamers remain misleading [3].

In this context, following an initial enthusiasm towards analytical capabilities of aptamers, in the last few years the scientific community realized the need to improve the rigor of studies dealing with

these bioreceptors, leading to an increasing number of publications that criticized the effective analytical potentialities of some of the selected aptamers, widely used in literature. An in-depth characterization of aptamer/target systems is being claimed by different research groups, based on the investigation also of the experimental variables that influence the interaction between aptamer and its target [2,5].

In Mattarozzi et al. [2], our research group focused the attention on the use of aptamers as recognition elements conjugated to magnetic micro- and nanobeads to be exploited in electrochemical and optical apta-assays, and miniaturized extraction techniques for food control. In this work, challenges to be overcome for assessing potentialities and reliability of aptamers as bioreceptors are explained in three points: i) understanding specificity of binding and the role of binding conditions, such as pH and ionic strength, that can vary when moving from buffer to real matrix extract. As an example, a matrix extract could contain organic solvents, denaturant agents or interferents used for analyte extraction, that could influence specificity of binding; ii) use of negative control sequences for assessing real capabilities of the investigated method; in the case of aptamers, negative controls can be randomly scrambled sequences , unrelated oligos, or even homogeneous ssDNA or ssRNA (e.g. polythymine); iii) a rigorous multifaceted characterization of aptamer/target binding by means of a multi-technique approach is requested, to fill the gap between aptamer selection and analytical applications [3]; as interestingly observed by McKeague et al., since different techniques have distinct limitations, a combination of multiple methods would be fundamental to critically evaluate aptamer suitability for the intended application [9]. These aspects are not discussed in most published research articles in which aptamers are used as biorecognition elements.

A relevant comprehensive multi-technique approach for the characterization of aptamer/target binding was conducted by Bottari et al. [5], including isothermal titration calorimetry (ITC), $^{1}$H-nuclear magnetic resonance spectroscopy ($^{1}$H NMR) and native nano-electrospray ionization mass spectrometry (nESI-MS); in particular, this approach was devised to validate or disproving the binding affinity of three anti-ampicillin aptamers, which had been extensively used in literature. The authors selected three distinct techniques that did not require immobilization on a substrate of any component (aptamer or target), thus permitting to directly evaluate aptamer-target binding characteristics and performance. Their findings revealed that none of the three anti-ampicillin aptamers exhibited any specific binding with their intended target. Likewise, another recent study demonstrated that an aptamer widely used in the detection of As(III) actually showed no specific binding to As(III) [7].

The scientific community also examined the range of causes that led to the previously explained issues. In 2022, Zhao and colleagues collected and discussed several recent studies that raised

concerns about the inability of some aptamers to effectively bind to their intended targets. They highlighted that one of the primary reasons of binding failures of aptamers is the unjustified truncation of the original sequence on the 3' and/or 5' sides, without proper validation of their binding capacity [8]. In this regard, Miller et al. [10], systematically reviewed 780 publications, uncovering that 41% of these papers reported unexplained sequence modifications or omitted sequences, that were catalogued into ten alteration categories such as deletions, substitutions and insertions, among others. The authors asked for a careful report of the following essential information: 1) the reporting of complete sequences investigated, thus considering central portion and flanking regions; abbreviations of sequences' name have to be reported in the same way in subsequent publications: greater rigor and clarity in nomenclature may result in a lower propagation of errors through works of different groups 2) comprehensive descriptions of binding and experimental conditions; 3) the incorporation of proper negative and positive controls for both aptamers and targets. Then, Zhao et al. [8] also encouraged researchers to publish also negative results to avoid further ambiguities and misleading information within the field of aptamers, fully aware that the difficulties of demonstrating non-binding are more than demonstrating binding.

### 2.1.1. Lysozyme as target protein

Lysozyme from chicken egg white (also named muramidase, Lyz, Gal d 4) is an enzyme capable of catalyzing the cleavage of the β-1,4-glycosidic bond between N-acetyluramic acid (NAM) and N-acetylglucosamine (NAG) of the bacterial cell wall (Enzyme Commission N. 3.2.1.17). It is a protein with a relatively low molecular weight (14.6 kDa), basic (pI= 11.35), consisting of a single polypeptide chain of 129 amino acid residues whose sequence in FASTA format is the following:

>sp|P00698|LYSC_CHICK Lysozyme C OS=Gallus gallus OX=9031 GN=LYZ PE=1 SV=1
MRSLLILVLCFLPLAALGKVFGRCELAAAMKRHGLDNYRGYSLGNWVCAAKFESNFNTQATN
RNTDGSTDYGILQINSRWWCNDGRTPGSRNLCNIPCSALLSSDITASVNCAKKIVSDGNGMNAW
VAWRNRCKGTDVQAWIRGCRL

Thanks to its antibacterial action, lysozyme is used in many fields, especially food, medicine and health care products. For example, it is used for the preparation of wine, cheese, and in some drugs such as eye drops.

Egg lysozyme is a recognized allergenic food protein. Allergic reactions to chicken eggs are a common condition that primarily impacts around 1–2% of children globally, ranking as the second most frequent food allergy in children, following cow's milk allergy. Egg allergy is primarily induced by hypersensitivity to four allergenic proteins present in egg whites: ovomucoid, ovalbumin, ovotransferrin, and lysozyme [11,12]. In egg white, lysozyme accounts for 3.5% of the total proteins,

triggering adverse reactions in sensitive people even if present at trace level. Consequently, the development of analytical methods for lysozyme detection and determination in foods is very important to safeguard consumer health. For this reason, lysozyme is a widely investigated target analyte and various biosensing strategies have been devised for its determination in food samples [13]. For this purpose, beyond antibodies, anti-lysozyme aptamers have attracted attention as biorecognition elements [14–20].

### 2.1.2. Anti-lysozyme aptamers

Two independent studies selected aptamer sequences targeting lysozyme from chicken egg white, from which the mostly widespread anti-lysozyme aptamers derive:

1. In 2001, Cox and Ellington [21] developed an automated system for the selection of ssRNA aptamers, and subsequently applied it to target the egg white lysozyme protein. The original RNA oligonucleotide library was estimated to comprise $1.1\times10^{14}$ sequences. The selection was conducted using magnetic beads functionalized with streptavidin to which the biotinylate lysozyme was bound (exploiting the strong streptavidin-biotin interaction). The selection buffer had the following composition: 20mM Tris, 100mM NaCl, 5mM $MgCl_2$ (pH=7.5). SELEX was interrupted after 12 selection cycles and the aptamers were sequenced, observing that only 6 sequences remained from the initial pool; in **Figure 2.1**, DNA sequences used as templates for RNA synthesis are reported. Clone 1 is the one of the sequences that demonstrates the greatest binding capacity and alone represents 61% of the final pool of aptamers. *In vitro* studies have shown its ability to inhibit the enzymatic action of lysozyme. The estimated Kd is 31 nM, that was determined using the RNA sequence tagged with a radioactive isotope and filtering the solution through two membranes: the nitrocellulose membrane captured the RNA-protein complex while the nylon membrane captured the unbound RNA. The radioactivity of the two membranes was measured and the percentage of aptamer bound calculated as a ratio. The Kd was finally obtained through a binding curve.

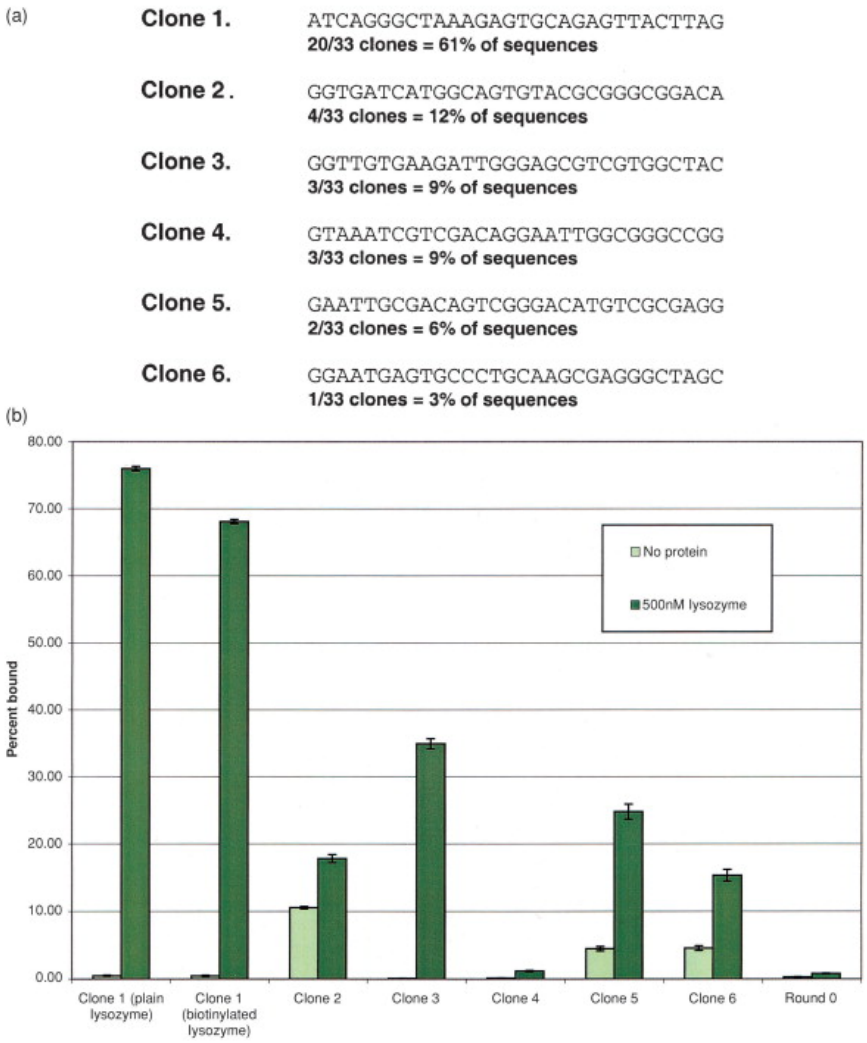


**Figure 2.1.** Selection of anti-lysozyme aptamers from SELEX procedure: **(a)** list of clones retained following 12 rounds of selection; it is displayed only the 30-nucleotide random region. **(b)** binding capabilities of the selected aptamers, where light green bars indicate the percentage of binding in the absence of the protein, while dark green bars depict the percentage of binding when exposed to 500nM lysozyme. Reprinted from Ref. [21]. Copyright © 2023, with permission from Elsevier

2. Tran et al. [22] in 2010 selected aptamers for lysozyme from a DNA oligonucleotide library, using the CE-SELEX (Capillary Electrophoresis-SELEX) variant. Compared to the method adopted by Cox and Ellington [21], CE-SELEX has the advantage of better separation and less non-specific binding, being carried out in solution. The binding buffer used is TGK pH 8.3, with the following composition: 25mM Trizma base, 192mM glycine and 5mM $K_2HPO_4$. At the end of SELEX only five sequences were isolated and identified, whose variable portions are shown in **Figure 2.2**. Of these aptamers, only Apta1, Apta3 and Apta8 were selected, due to their greater relative abundance.

| Clone ID | Sequence of random region (5' to 3') |
|---|---|
| Apta1 | GCAGCTAAGCAGGCGGCTCACAAAACCATTCGCATGCGGC |
| Apta2 | GCGTGGGCAGCTAGCACCGATGGTTCTATCGTGGGCTCCG |
| Apta3 | GCGGGTCGGTTGCTCGCTTCGCCCGATCGGTCTAAGGGTG |
| Apta4 | GCGCAAGGTCATCGCATCGCGTCGGAATGGGCTACAGGTG |
| Apta8 | GCACCTTGATGACATGATAGTCGTTGTGTATGCAGTTGGC |

**Figure 2.2**. Central random portion (40-mer) of five aptamer variants isolated by Tran et al. [22] Reprinted from Ref. [22] © 2010 by the authors; licensee Molecular Diversity Preservation International, Basel, Switzerland

The affinities of Apta1, Apta3 and Apta8 were initially evaluated by Affinity Capillary Electrophoresis (ACE), obtaining Kd of 52.9 ± 9.1 nM, 47.1 ± 16.3 nM and 52.1 ± 12.7 nM, respectively. Since the Kd values were very similar and the secondary structure of Apta1 was found to be energetically favored than the other two aptamers, only for Apta1 the Kd was determined by other techniques as well. Using fluorescence anisotropy (FA), an estimated Kd of 2.8 ± 0.3 nM was obtained, while surface plasmon resonance (SPR) yielded a Kd of 6.1 ± 0.5 nM. The authors considered more reliable the value of Kd determined by FA, for its higher accuracy compared with other techniques. The study concluded with an evaluation of the selectivity of the three aptamers against lysozyme, where ovomucoid, ovotransferrin and Bovine Serum Albumin (BSA) were used as interfering proteins. For all three aptamers, the affinity measured with ACE technique for lysozyme has been shown to be 2 to 4 orders of magnitude higher respect to that towards the investigated interferents.

### 2.1.3. Aptasensors for lysozyme determination

Recent reviews deal with the advancements in lysozyme detection and determination by electrochemical and optical aptasensors, uniquely utilizing DNA aptamers [13,19]. The mechanisms proposed for lysozyme determination in aptasensors mainly rely on (i) competition events utilizing complementary oligosequences, (ii) changes in recorded signals resulting from conformational changes in aptamers following interaction with the target. For electrochemical transduction, the strategy can also involve alterations in electrochemical impedance. It is important to note that aptasensors based on target-induced conformational change of the aptamer are often designed without proving and characterizing the potential conformational variation with independent techniques.

In most cases there is a lack of clarity in the literature regarding the rationale for selecting a particular anti-lysozyme sequence and the binding buffer when developing aptasensors. These choices should

ideally be aligned with the specific assay setup, the buffer used in SELEX selection, and the sample matrix. Additionally, even for the same aptamer, published works often use different types of buffers with variations in salt concentration, divalent cations, and pH levels for the biorecognition event, regardless of the buffer used during the SELEX process [15,16,18,23,24]. As far as we know, the only research that compared two different anti-lysozyme aptamers in developing an aptasensor for lysozyme determination was conducted by Ocaña et al. [24]. As mentioned above, Miller et al. conducted a systematic review of aptamer sequence reported in the literature, revealing a common trend of modifying and using sequences without providing any rationale [10]; the authors dedicated part of the article to the case of the "Clone 1" aptamer, that is a SELEX-selected sequence as ssRNA anti-lysozyme aptamer [21] : surprisingly, the author verified that only 4 publications out of the 61 reviewed utilized the correct oligonucleotide sequence, whereas the other reported different types of unexplained alteration (like insertion, modification, or deletion).

## 2.2. Aim of the work

The research activities described in the present chapter are part of a project (PRIN 2017, grant: 2017YER72K funded by the Italian Ministry for Education, University and Research (MIUR)), aimed at the development of innovative analytical methods for hidden allergen determination. In particular, one of the aims was the development of innovative sample treatment strategies and a novel competitive aptasensor based on aptamer-modified magnetic beads (MBs) for lysozyme determination. In this context, potentialities and limitations of aptamers as biomimetic receptors for interaction with the allergenic protein lysozyme from chicken egg white were critically assessed through a multi-technique approach, which includes electrochemical apta-assay, circular dichroism (CD), fluorescence titration, and asymmetrical flow field-flow fractionation - UV (AF4-UV) [25]. The combination of multiple approaches was intended to provide distinct and complementary information about aptamer-target binding. A combination of results from different techniques could permit to obtain a critical evaluation of the performance of the system investigated. Conditions that influence aptamer-target binding were explored, such as such as buffer composition. Negative controls were used to assess specificity of the interaction.

Part of the obtained results led to the following publications:

- Marassi, V.; Mattarozzi, M.; Toma, L.; Giordani, S.; Ronda, L.; Roda, B.; Zattoni, A.; Reschiglian, P.; Careri, M. FFF-Based High-Throughput Sequence Shortlisting to Support the Development of Aptamer-Based Analytical Strategies. *Anal Bioanal Chem* **2022**, *414* (18), 5519-5527. https://doi.org/10.1007/s00216-022-03971-2 [26];
- Toma, L.; Mattarozzi, M.; Ronda, L.; Marassi, V.; Zattoni, A.; Fortunati, S.; Giannetto, M.; Careri, M. Are aptamers really promising as receptors for analytical purposes? Insights into anti-lysozyme DNA aptamers through a multi-technique study. *Anal Chem*, *in press* (accepted on 17 January **2024**) [25].

## 2.3. Materials and methods

**Chemicals.** The following chemical reagents and materials were procured from specified suppliers. Magnesium chloride ($MgCl_2$), ammonium bicarbonate ($NH_4HCO_3$), L-glycine, Trizma® base, Tween-20, ethanolamine (EA), N-(3-dimethylaminopropyl)-N'-ethylcarbodiimide hydrochloride (EDC), N-hydroxysuccinimide (NHS), bovine serum albumin (BSA), iodoacetamide (IAA), DL-dithiothreitol (DTT), sodium hydroxide, sodium chloride, 4-morpholineethanesulfonic acid monohydrate (MES), hydrochloric acid, formic acid (FA), acetonitrile (ACN), streptavidin-alkaline phosphatase from *Streptomyces avidinii* conjugate (Strep-ALP), and lysozyme from chicken egg white were all purchased from Merck (Milan, Italy). Monobasic potassium phosphate ($KH_2PO_4$), di-potassium hydrogen phosphate ($K_2HPO_4$), sodium phosphate dibasic dodecahydrate ($Na_2HPO_4 \cdot 12H_2O$) and potassium chloride were purchased from Carlo Erba (Cornaredo, Milan, Italy). Hydroquinone diphosphate (HQDP) was sourced from Metrohm Italiana (Origgio, Varese, Italy).

Deionized water was obtained using a Milli-Q element A10 system (Millipore, San Francisco, CA, USA) and was utilized for the preparation of buffer solutions.

The buffer compositions were as follows. MES buffer: 25 mM MES (pH 5); Tris Buffer (TRIS): 0.1 M Trizma® Base, 5 mM $MgCl_2$ (pH 7.4); Tris Buffered Saline-Tween (TRIS-T): 0.1 M Trizma® Base, 5 mM $MgCl_2$, 0.05% w/v Tween® 20 (pH 7.4); Tris Buffered Saline (TRIS saline): 20 mM Trizma® Base, 5 mM $MgCl_2$, 0.1 M NaCl (pH 7.4); Phosphate Buffer Saline containing Magnesium ions (PBS-$Mg^{2+}$): 1.5 mM $KH_2PO_4$, 8 mM $Na_2HPO_4$, 137 mM NaCl, 2.7 mM KCl, 1 mM $MgCl_2$ (pH 7.4); Phosphate Buffered Saline (PBS) was purchased as dry-blended powder from Thermo Fisher Scientific (Waltham, MA, USA), having the following composition after dissolution: 0.1 M $Na_2HPO_4$, 0.15M NaCl (pH 7.2); Tris Glycine Potassium (TGK): 25 mM Trizma® Base, 192 mM L-glycine, 5 mM $K_2HPO_4$ (pH 8.3).

**Aptamers.** All single-stranded DNA sequences were custom synthesized by Biomers.net (Ulm, Germany) and delivered in a dried state. To prevent repetitive freeze/thaw cycles, they were appropriately aliquoted. The lyophilized aliquots were reconstituted in Milli-Q water to achieve a stock final concentration of 100 µM and were stored at -20 °C, following the supplier's recommendations. The specific DNA sequences used in the study are detailed in **Table 2.1**. Depending on the experiment, various end modifications were introduced. An aminolink-C6 modification was added at the 5'-end to enable crosslinking with carboxylic groups on the surface of magnetic beads. Biotin conjugation at 3'-end was employed to exploit the high-affinity interaction

between biotin and streptavidin. Cy3 and Dansyl-X conjugation at 3'-end was implemented for analysis via fluorescence spectroscopy.

**Table 2.1.** ssDNA aptamer sequences used in the present study. Central variable regions are in bold, flanking regions are underlined.

| *Name* | *Sequence (5'-3')* | *Number of bases* |
|---|---|---|
| A80 | AGCAGCACAGAGGTCAGATG**GCAGCTAAGCAGGCGGCTCACAAAA CCATTCGCATGCGGC**CCTATGCGTGCTACCGTGAA | 80 |
| A40 | **GCAGCTAAGCAGGCGGCTCACAAAACCATTCGCATGCGGC** | 40 |
| A80R | AGCAGCACAGAGGTCAGATG**ACTATGTCGGCCGCAATGCCCAGAG GCCACATACAAGCGG**CCTATGCGTGCTACCGTGAA | 80 |
| C80 | GGGAATGGATCCACATCTACGAATTC**ATCAGGGCTAAAGAGTGCA GAGTTACTTAG**TTCACTGCAGACTTGACGAAGCTT | 80 |
| C30 | **ATCAGGGCTAAAGAGTGCAGAGTTACTTAG** | 30 |
| C42 | ATCTACGAATTC**ATCAGGGCTAAAGAGTGCAGAGTTACTTAG** | 42 |
| C80R | GGGAATGGATCCACATCTACGAATTC**AAGTGGATTAACTGTGTAGA CCGATAGACG**TTCACTGCAGACTTGACGAAGCTT | 80 |
| PolyT40 | TTTTTTTTTTTTTTTTTTTTTTTTTTTTTTTTTTTT | 40 |

**Biotinylation of lysozyme.** Biotinylation of lysozyme was carried out using the EZ-Link NHS-PEG4-Biotinylation Kit from Thermo Scientific according to manufacturer instructions. Briefly, the biotinylation reaction was conducted in PBS buffer with 1:5 lysozyme:biotinylating agent ratio, at room temperature, under gentle stirring for one hour. The biotinylated protein was subsequently purified through dialysis, using a regenerated cellulose membrane (10 kDa molecular weight cut-off), under gentle stirring for four hours, refreshing PBS buffer after two hours. The protein solution was then centrifuged at 4 °C, 10,000 rpm for 10 minutes, and the supernatant was collected.

The concentration of biotinylated lysozyme was determined through spectrophotometric analysis, utilizing a UV-vis/NIR Lambda 750 Perkin Elmer spectrophotometer equipped with a diode array detector. A calibration curve was constructed by analyzing four lysozyme concentration levels at 280

nm, with the assumption that the unmodified and biotinylated protein had the same molar extinction coefficient.

The degree of biotinylation was estimated through Flow Injection Analysis (FIA)-MS, using an HPLC Dionex Ultimate 3000 system coupled with a linear ion trap (LTQ) mass spectrometer from Thermo Fisher Scientific. The mass spectrometer was equipped with an electrospray (ESI) source, operating in full scan acquisition mode (positive ion mode). FIA-MS analysis involved the injection of 10 µL of solution containing biotinylated lysozyme, with three replicates. A mobile phase consisting of water with 0.1% formic acid (v/v) at a flow rate of 200 µL/min was employed. The operating conditions were as follows: electrospray voltage, 3.5 kV, capillary temperature, 200 °C, capillary voltage, 20 V. Mass spectra were acquired over a 5-minute period in full scan mode in the *m/z* 110-2000 range.

**Immobilization of aptamers on magnetic beads.** A 4 µL volume of a stock suspension ($2 \times 10^9$ beads/mL, approximately equivalent to 30 mg/mL) of Dynabeads™ M-270 Carboxylic Acid (Life Technologies Italia, Thermo Fisher Scientific) was diluted in 100 µL of MES buffer. The magnetic beads (MBs) underwent two washing steps with MES buffer. Subsequently, MBs were resuspended in a 200 µL solution containing EDC and NHS, both at a concentration of 25 mg/mL. The suspension was shaken at 1500 rpm using a shaking heater block for 30 minutes at room temperature (Thermomixer®C, Eppendorf). Then, the beads were washed with MES buffer and suspended in a 2 µM aptamer solution. The immobilization process was allowed to proceed for 2 hours, carried out at 26 °C, 1500 rpm. After washing the MBs with 100 µL of MES and 100 µL of TRIS buffer, the functionalized MBs were incubated with 100 µL of EA (50 mM in TRIS buffer) to deactivate the previously activated sites (1 hour, 1500 rpm). MBs were subsequently washed with 100 µL of TRIS-T buffer and 100 µL of binding buffer for two cycles. Then, they were incubated with 200 µL of BSA (0.5% w/w) as a blocking agent for 1 hour at 26 °C, 1500 rpm. Finally, the MBs were washed twice with 100 µL of binding buffer.

The effectiveness of the functionalization on MBs was evaluated by employing the A40 aptamer modified at the 3'-end with Cy3 group. Fluorescence measurements were conducted on an Edinburgh FLS1000 fluorimeter (λexc=555 nm; λem= 565 nm) using a Xenon 450 W lamp as source, PMT-900 detector. Different concentrations of A40-Cy3 (200 nM, 500 nM, 1 µM, 2 µM) were examined for immobilization, and the fluorescence signal from A40-Cy3 was recorded both before and after aptamer immobilization on the MBs. The quantity of immobilized aptamer was determined by calculating the difference between the two solutions. Upon this calculation, signals from the first two

washing phases after immobilization on the modified MBs were also measured and considered in calculation of quantity of aptamers immobilized on MBs.

**Electrochemical apta-assay.** Single Walled Carbon Nanotubes Screen-Printed Electrodes (SWCNT-SPEs) and magnetic supports for Screen-Printed Electrodes (DRP-magnet) were acquired from Metrohm Italiana Srl (Origgio, Varese, Italy). The aptamer-modified MBs were incubated with 200 µL of lysozyme solution for 1 hour with agitation at 1500 rpm, at a temperature of 26 °C. Subsequently, the MBs were washed with 100 µL of binding buffer. Then, MBs were re-suspended in 200 µL of a solution containing 10 µg/mL Strep-ALP conjugate in TRIS buffer containing 5 mg/mL BSA, incubated for 15 minutes (26 °C, 1500 rpm). MBs were then washed with 100 µL of TRIS-T buffer and two times with 100 µL of TRIS buffer.

MBs were separated from the buffer and suspended in 50 µL of HQDP solution (1 mg/mL in TRIS buffer at pH 9.8). After a 6-minute incubation period, the entire solution was deposited onto the surface of a SWCNT-SPEs, which was mounted on the magnetic support for SPE to confine the magnetic particles on the working electrode surface. Differential Pulse Voltammetry (DPV) measurements were conducted using a PGSTAT204 potentiostat (Metrohm Autolab), with the following parameters: potential range, -0.5 to 0.2 V, scan rate, 12.6 mV/s, step size, 5 mV, modulation amplitude, 50 mV, modulation time, 0.1 s, and interval time, 0.4 s. Data acquisition and processing were performed using NOVA 2.0 software.

A DNA reference probe uniquely composed of 40 thymine bases (PolyT40) was utilized as a blank reference.

**Circular dichroism spectroscopy.** Circular dichroism (CD) experiments were conducted using a JASCO J-715 spectropolarimeter thermostated by a Peltier unit set at 26 °C using a 1 mm pathlength Suprasil™ quartz cuvette (volume 150 µL). Stock solutions of aptamer and lysozyme (10 µM) were prepared. Aptamer-protein mixtures were obtained by combining aptamer and protein solutions in a 1:1 ratio, resulting in a final concentration of 5 µM for each species. Spectra were acquired in the 200-320 nm range for sample in PBS-$Mg^{2+}$ buffer, and in the 210-300 nm range for TGK buffer. All the spectra were recorded through a continuous scan performed at 50 nm/min rate (data pitch of 0.2 nm, data integration time 8 s). Depending on signal intensity, spectra accumulation was set from 1 to 5 times.

The buffer contribution was subtracted from the spectra of the samples. Then CD spectra of the experimental mixtures were compared with the algebraic sum of the spectra of the single components.

This comparison allowed for the identification of spectral changes on the aptamer, the protein, or both induced by the interaction.

Aptamer thermal melting was performed by heating the aptamer solution up to 90 °C, using the Peltier unit. The solution was maintained at 90 °C for 1 min, and then cooled to room temperature to assess the reversibility of the process.

**Fluorescence titration.** An Edinburgh FLS1000 fluorimeter was used for emission spectra acquisition, using a 1 cm pathlength Suprasil™ quartz cuvette (volume 100 µL). Excitation and emission bandwidth were set at 3.00 and 2.00 nm, respectively (data pitch 1 nm, 1 repeat, dwell time 0.5 s).

Two distinct experiments were conducted for the study of aptamer-lysozyme interaction in two different buffer solutions (PBS-$Mg^{2+}$ and TGK). The objective was (i): to monitor the variation of fluorescence signal after every addition of titrant solution (lysozyme or aptamer according to the different strategy); (ii) to possibly build a binding curve by titration lysozyme with aptamer, that did not involve the presence of tags, permitting to derive the aptamer-lysozyme dissociation constant (Kd). Each titration was repeated three times to obtain an estimate of the experimental error. It was also ensured that the absorbance always remained below 0.1, so that the inner filter effect could be ruled out. Concentration of the specie being titrated was set at 1 µM.

For each approach, the experiments followed this order: the blank spectrum was initially recorded filling the cuvette with 99 µL of buffer. Next, 1 µL of the solution of analyte was added to achieve a final concentration of 1 µM. Subsequently, incremental additions of titrant solution (100 µM) were as 1 µL, 1 µL, 3 µL, and 8 µL. After each addition, the corresponding spectrum was acquired. The excitation wavelength and emission range were strategy-dependent. Strategies were planned as follows:

- First strategy: titration of A40-Dansyl and C42-Dansyl with lysozyme. After each addition, the spectrum within the emission range of 410-700 nm is acquired, with an excitation wavelength (λexc) of 330 nm;
- Second strategy: titration of lysozyme with A40 and C42, acquiring spectra within 310-550 nm range emission (λexc 298 nm).

The same procedures were carried out in absence of the titled; subsequently, each spectrum was subtracted from its corresponding blank signal and divided by the dilution factor. Data analysis and titration fitting to a binding isotherm function were carried out using MATLAB R2020b.

**Asymmetrical flow field-flow fractionation (AF4)-UV analysis.** For the AF4-UV analysis, a 1100 Series HPLC System (Agilent Technologies, Palo Alto, CA) was exploited, in connection with an Eclipse 3 module (Wyatt Technology Europe, Dernbach, Germany) to constantly control flow rate and operations. The AF4 channel was constituted by a Mini Channel (Wyatt Technology Europe), a membrane of regenerated cellulose (Nadir) of 5 kDa molecular cutoff, and a channel spacer (thickness 350 μm). An Agilent 1100 DAD UV/Vis spectrophotometer was exploited for online detection of the eluted species.

Analyses were performed on aptamer sequences A40, C42 and PolyT40, as well as on their respective mixtures with lysozyme. PBS-$Mg^{2+}$ binding buffer was used as elution medium.

## 2.4. Results and discussion

### 2.4.1. Anti-lysozyme aptamer selection

As previously mentioned, the final aim of the research project was the development of novel analytical strategies in which aptamers are exploited as biorecognition elements for sample treatment or aptasensing platforms for lysozyme analysis in food samples.

The first step consisted in the choice of the most exploited anti-lysozyme sequences in literature. As reported in **Table 2.1**, A80 and C80 sequences were taken into consideration, as well as the corresponding truncated versions A40, C42 and C30 [15,16,19,22,24]. The use of DNA aptamers is usually preferred for the development of analytical devices, due to the intrinsic higher stability of DNA molecule compared to RNA [27].

The selection of the sequences to be used as negative controls took into consideration the principle of SELEX process, that starts from an oligonucleotide library, in which every molecule presents the same flanking regions and a different randomized central portion: the latter is expected to play an important role in determining tridimensional conformation of the aptamer, responsible for its affinity to the target [28]. In view of these considerations, central portion of A80 and C80 aptamers were randomly scrambled, while maintaining unaltered the flanking regions, resulting in sequences A80R and C80R, respectively; these could permit to understand the sequence-specificity of binding [2]. PolyT40 was used as reference blank and as a negative control.

In the case of anti-lysozyme aptamers, the choice of the sequence and of the optimal binding conditions to be used for the development of an analytical approach for lysozyme determination is not trivial. For this reason, in the first part of investigation, we devised a strategy based on aptamer immobilization on magnetic micro-beads to investigate binding performances of different sequences in distinct buffers for lysozyme recognition. To do that, it was necessary to chemically biotinylate lysozyme (the biotinylated lysozyme was characterized in terms of concentration and degree of biotinylation). Biotinylation was necessary for exploiting the biotin-streptavidin high-affinity binding during subsequent steps of magnetic bead-based electrochemical assay, while biotinylated lysozyme simulated the behavior of the native protein. This strategy could also support the evaluation of the effect of different experimental conditions, such as binding buffer, pH, ionic strength and the assessment of sequence selectivity for the interaction.

### 2.4.2. Electrochemical assay set-up

The electrochemical assay was devised to record a signal that could directly be ascribable to the binding event, unlike assays reliant on conformational changes or competition events, where the signal indirectly correlates with the aptamer-target interaction. The assay involves a 5'-aminolink C6 aptamer as receptor immobilized on carboxyl magnetic beads, and biotinylated lysozyme as the target protein (**Figure 2.3**). As mentioned, the presence of biotin labels on the lysozyme was essential for enabling electrochemical detection. This process included utilizing a conjugated streptavidin-phosphatase alkaline (Strep-ALP) for the electrochemical reading: Strep-ALP binds to the biotinylated protein interacting with the aptamer. Subsequently, ALP catalyzes the dephosphorylation of the non-electroactive enzyme substrate HQDP into electroactive HQ, allowing its oxidation to quinone (Q) via DPV scan. This oxidation process generates a signal proportional to the quantity of the interacting target species.

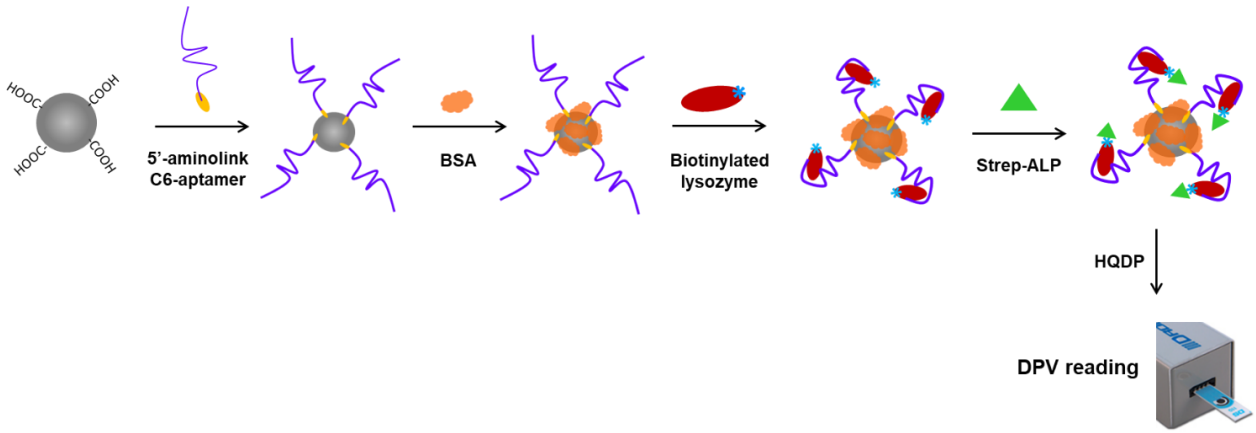


**Figure 2.3.** Steps of MB-based electrochemical assay

### 2.4.3. Evaluation of aptamer immobilization on magnetic beads

The MBs-based electrochemical assay required the aptamer immobilization on MBs, that was properly investigated. Immobilization involved covalently attachment of the aptamer to MBs through an EDC/NHS crosslinking reaction (**Figure 2.4**) exploiting the C6 amino group at 5' end of the aptamer and the carboxylic acid functional groups on MBs surface. A40 was employed as a model for this procedure, to assess the quantity of aptamers loaded onto the magnetic beads.

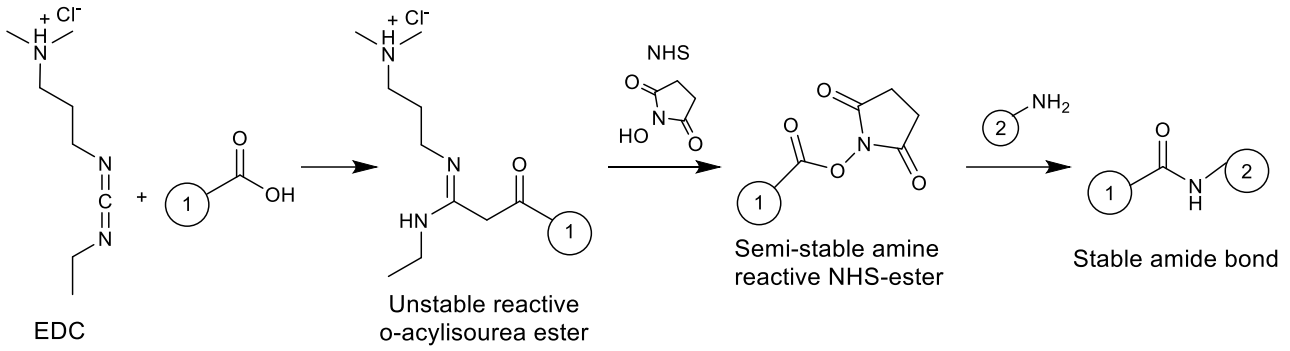


**Figure 2.4.** EDC/NHS crosslinking reaction

Initially, the immobilization of aptamers on the MBs was studied using sequences functionalized at 3'-end with biotin. In this way, the biotinylated aptamer, once immobilized, can be detected by DPV measurement, thanks to the use of the Strep-ALP conjugate, which will bind to biotin via streptavidin. However, it was observed a saturation of the DPV signal that led to the necessity of diluting beads suspensions to investigate immobilization with aptamers at higher concentration levels. Unfortunately, dilutions resulted in high signal dispersion, probably due to the handling errors associated to the high dilution factors that had to be applied to beads suspensions.

As a consequence, another approach was used for assessing the optimal initial concentration of aptamer to achieve effective bead functionalization: it was based on the estimate, through spectrophotometric measurements, of the quantity of immobilized aptamer from the difference between the aptamer concentration in the initial solution, prior to its interaction with the beads, and the concentration of the solution after functionalization. In this case, the intrinsic absorption of oligonucleotides at 260 nm could not be exploited for this purpose, since the NHS leaving group in the crosslinking reaction exhibits high absorption within the same UV light range, so it would have interfered for the measured signal. Consequently, in order to acquire a signal attributable only to the aptamer present in solution, it was decided to perform fluorescence spectroscopy analyses, using a 5'-aminolink C6 A40 labeled with Cyanine 3 at its 3'-end, able to give a specific fluorescent signal. The sulfoindocyanine Cy3 is a fluorescent dye that is widely used for exploring the structure and dynamics of nucleic acids using fluorescence-based methods. It exhibits a maximum excitation wavelength at 555 nm and a maximum emission wavelength at 565 nm [29].

In this way, fluorescence measurements permitted to establish the initial aptamer concentration capable of saturating the available sites on the beads and to estimate the number of moles of aptamer anchored to the beads, that is a useful information for MBs-based assay.

For this aim, fluorescence signal were acquired for (i) A40-Cy3 aptamer standard solutions (reference solutions) at different concentrations (200 nM, 500 nM, 1 µM, 2µM) (**Figure 2.5**), (ii) the corresponding surnatants, i.e the solution in contact with the magnetic beads after the immobilization phase, and (iii) the subsequent washing solution, that are essential to evaluate the portion of aptamer aspecifically absorbed on the surface of the beads. **Figure 2.5** illustrates a proportional signal variation dependent on Apt40-Cy3 concentrations, from which a calibration curve was constructed. This curve served to calculate the nanomoles of aptamer in the supernatant and washing solutions.

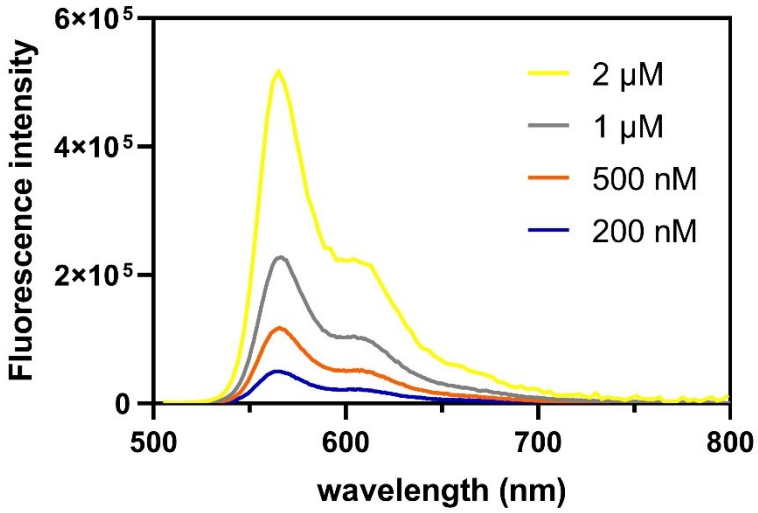


**Figure 2.5.** Fluorescence emission spectra of A40-Cy3 standard solutions at different concentrations

Then, aptamer immobilization on MBs at different concentrations was performed. In **Figure 2.6**, overlapping spectra of the A40-Cy3 reference solution, supernatant, and washing solutions are presented for the different concentration levels investigated. As expected, it is evident that as the initial aptamer concentration increased, a decrease in the percentage of the initial aptamer immobilized on the beads was observed, passing in terms of pmol from 98% for 200nM to 32% in the case of the solution at 2 µM.

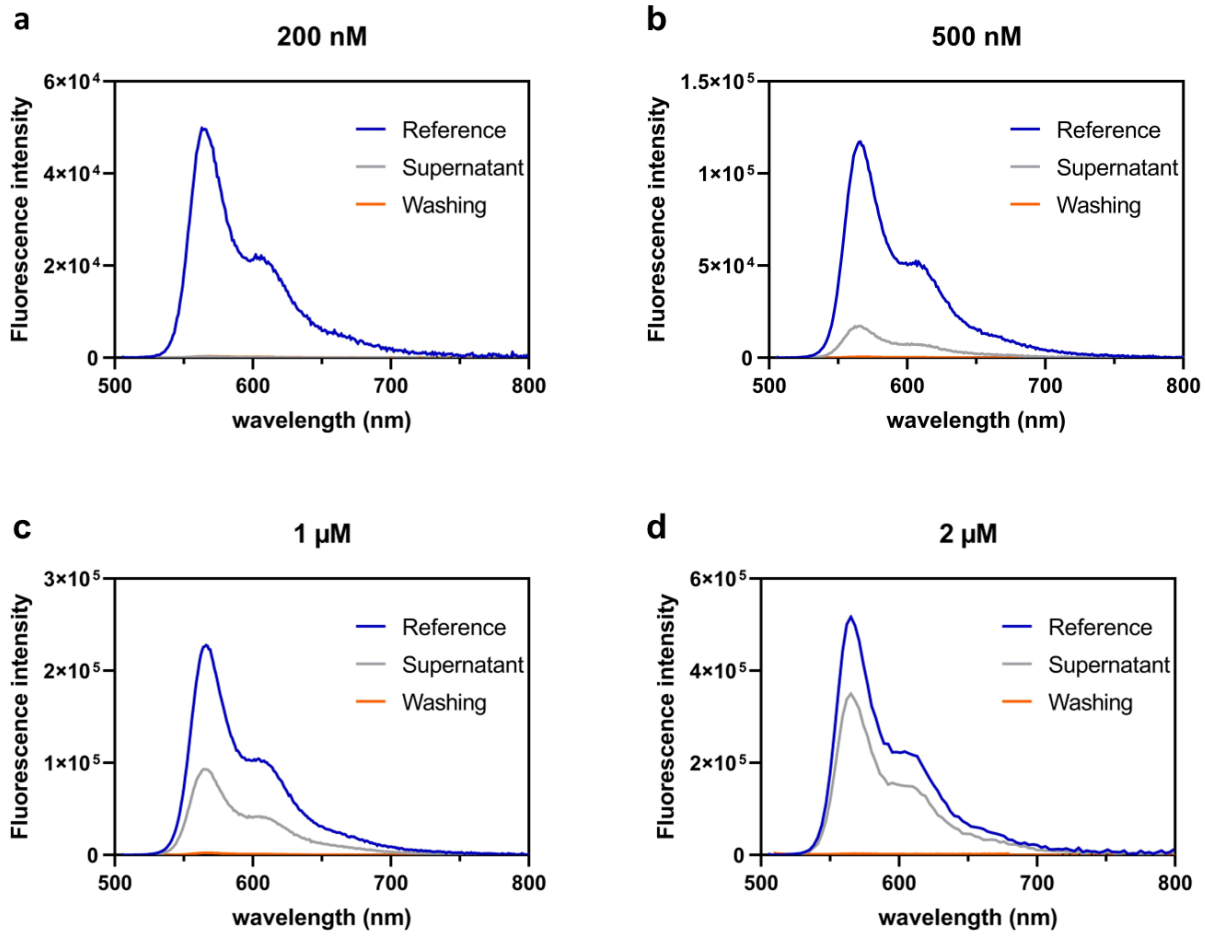


**Figure 2.6.** Fluorescence emission spectra of the reference solution (initial solution), supernatant, and first washing solution at different concentrations of A40-Cy3 during the functionalization of 4 µL of beads. **(a)** 200 nM; **(b)** 500 nM; **(c)** 1 µM; **(d)** 2 µM.

After calculating the picomoles of aptamer present in the supernatant and washing solutions, it was possible to infer the quantity immobilized on magnetic beads by difference respect to the reference solutions. When plotting the immobilized picomoles (pmol) at various aptamer concentrations, it becomes evident that an increase in the initial aptamer concentration corresponds to a higher amount of bound aptamer. A plateau is observed around 2 µM, stabilizing at a value of approximately 65 ± 3 pmol of aptamer, corresponding to 542 ± 25 pmol/mg beads of immobilized aptamer, as can be observed in **Figure 2.7**. To evaluate the reproducibility of the functionalization, experiments were carried out on three different days, obtaining a CV% in terms of immobilized pmol less than 6%.

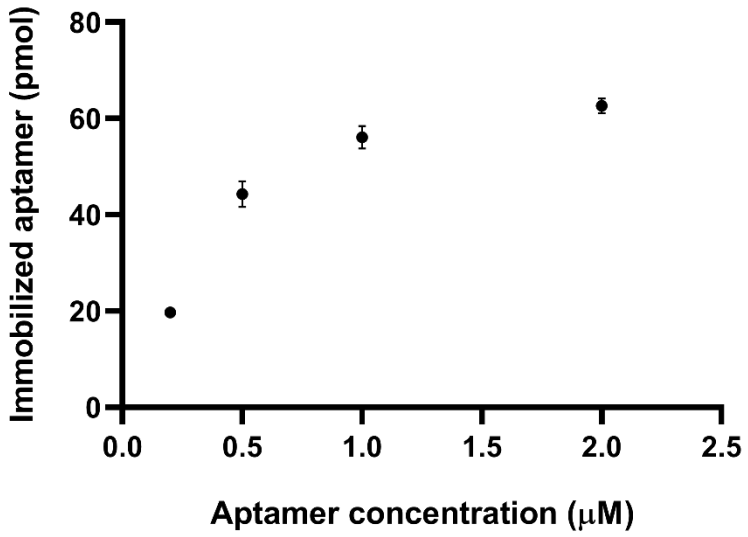


**Figure 2.7.** Trend of the quantity of immobilized aptamer (pmol) on 0.12 mg (4 μL) of beads while varying the concentration of the initial aptamer solution.

Subsequently, conformational flexibility of the immobilized aptamer was investigated by immobilizing an A40 sequence (2 μM) onto MBs and incubating it with a 2 μM single strand 20-mer DNA complementary to a section of the A40 aptamer and biotin-labeled at the 3' end. The subsequent incubation with Strep-ALP conjugate and electrochemical signal readout in presence of HQDP substrate proved the efficacy of complementary pairings (**Figure 2.8**). The figure compares DPV signals obtained from functionalized and non-functionalized magnetic beads: in presence of A40 a high voltammetric signal was obtained thus proving the successful immobilization of the aptamer on the magnetic support. Conversely, the flat signal observed with the non-functionalized magnetic beads ensured the absence of non-specific adsorption of the Strep-ALP conjugate on the micromagnetic substrate.

To verify the effectiveness of magnetic beads functionalization with longer sequences, similar pairing experiments were conducted with A80, yielding results comparable to those obtained with A40.

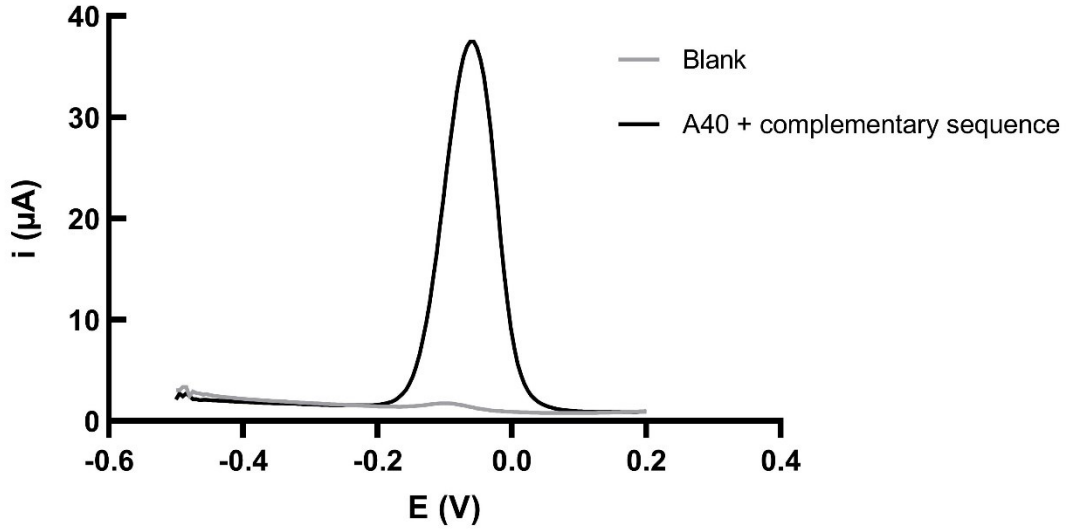


**Figure 2.8.** DPV voltammograms showing an effective immobilization of the A40 on MBs surface: overlay of the signal obtained with A40-modified MBs in presence of the 20-mer sequence complementary to A40 with the signal deriving from non-functionalized MBs.

### 2.4.4. Biotinylation of lysozyme

As previously explained, for performing electrochemical assay, it was necessary to use biotinylated lysozyme in order to subsequently exploit high-affinity binding between biotin and streptavidin conjugated to ALP enzyme for electrochemical readout.

Biotinylating lysozyme involved the use of a commercial kit with NHS-PEG4-biotin as the biotinylating agent, maintaining a lysozyme:biotin molar ratio of 1:5, exploiting carboxyl group of biotin to attach to amino groups of protein (amino terminal or side chain amines) (**Figure 2.9**).

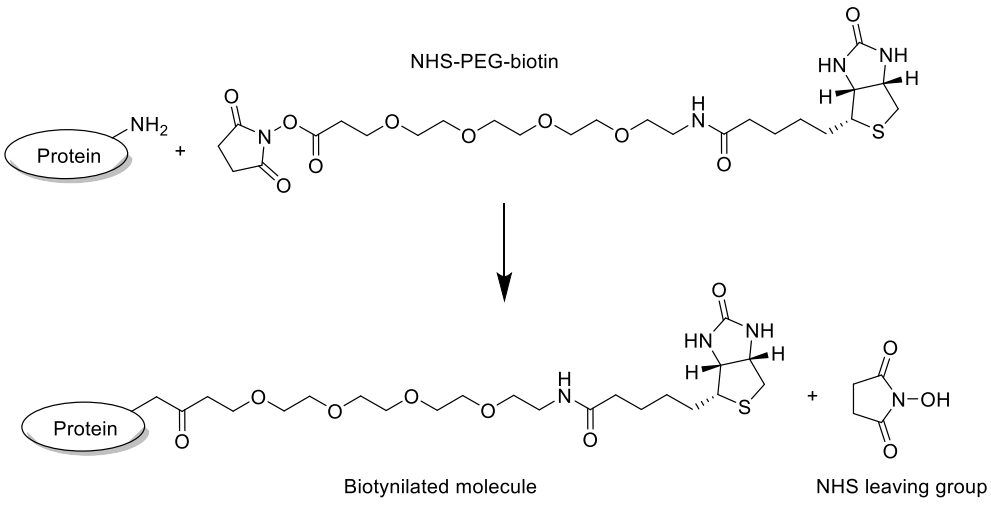


**Figure 2.9.** Biotinylating reaction scheme by using NHS-PEG-biotin group

Following dialysis to eliminate unreacted biotinylating reagents and NHS leaving groups, spectrophotometric measurements allowed to determine the concentration of biotinylated lysozyme (206 ± 6 µM). FIA-MS analysis permitted to characterize the biotinylated lysozyme and the acquired mass spectrum revealed various multi-charge distributions (prevalent charges: +9, +10, +11), each corresponding to different lysozyme species with distinct levels of biotinylation (**Figure 2.10**). Notably, there were no peaks associated with unmodified lysozyme, free biotinylating agents, or NHS, indicating successful biotinylation and effective dialysis.

In order to assess the average number of biotins per lysozyme molecule, the sum of the most abundant multicharged states for each lysozyme species was taken into account; the calculated value was 3.4 ± 0.1 biotin molecules per lysozyme molecule.

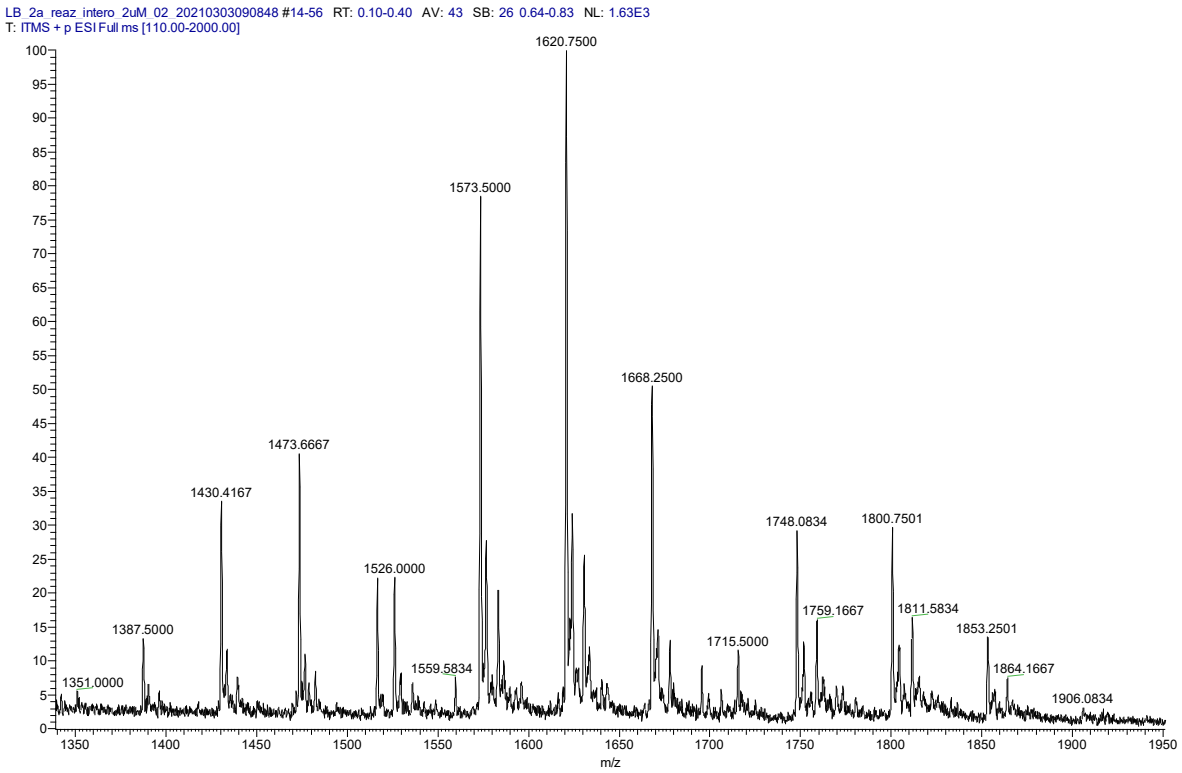


**Figure 2.10**. FIA-ESI-MS spectrum of biotinylated lysozyme

Additionally, CD spectra were acquired for both native and biotinylated lysozyme: spectra overlay shown in **Figure 2.11** confirmed that the biotinylation process did not alter lysozyme conformation.

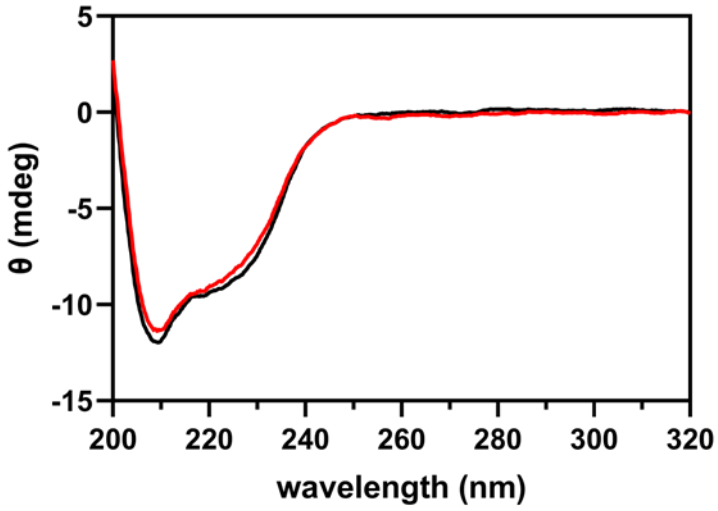


**Figure 2.11.** Comparison of CD spectra of native (black) and biotinylated lysozyme (red)

### 2.4.5. Study of the aptamer/lysozyme interaction by magnetic beads-based electrochemical assay

After aptamer immobilization on MBs and lysozyme biotinylation, MBs-based electrochemical assays were conducted to investigate the interaction between different aptamers and target lysozyme. Concentration of biotinylated lysozyme was set at 500 nM and MBs were functionalized with different sequences (refer to Table 2.1). PolyT40 was chosen as putative non-interacting sequence, thus MBs modified with PolyT40 may represent a blank reference. Since TRIS saline and PBS-$Mg^{2+}$ buffers are the most exploited for anti-lysozyme aptamers, they were used for electrochemical assay experiments.

In **Figure 2.12**, the signals obtained from all investigated aptamers are compared, including the averaged signal for PolyT40.

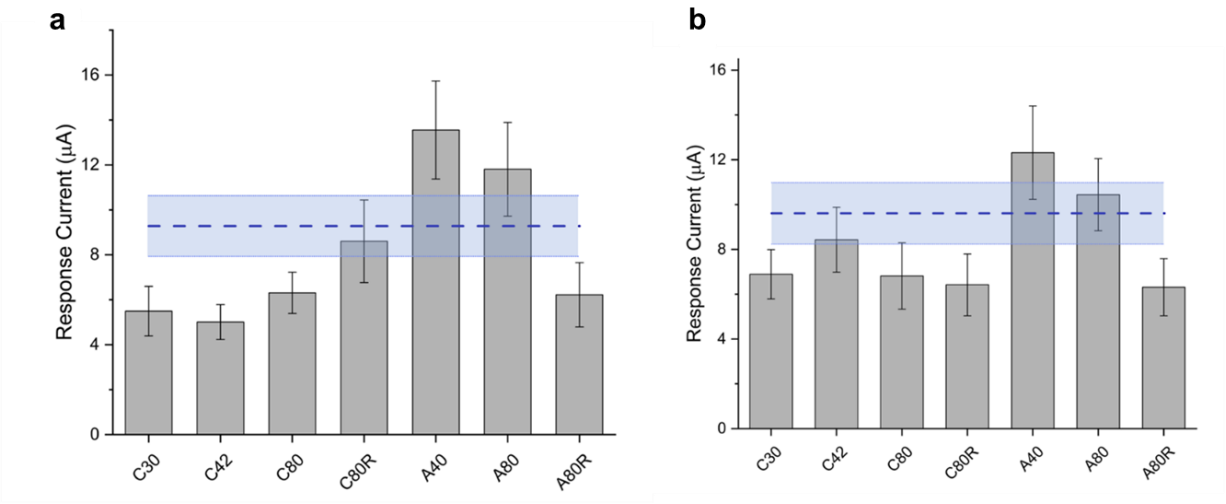


**Figure 2.12.** Comparison of DPV signals between the aptamers studied in **(a)** PBS-$Mg^{2+}$ and **(b)** TRIS saline buffers (n=3) from MBs-based electrochemical assays. Mean signal resulting from the immobilization of PolyT40 blank reference is reported as dashed blue line, with standard deviation reported as light-blue boxes

A40 and A80 aptamers showed a stronger interaction with the target; however, the relatively high signals obtained even with random sequences (C80R and A80R) and PolyT40 suggested an interaction unrelated to the specific sequence. Moreover, the high dispersion of the signals could be attributed to the nonspecific nature of the interactions.

Based on these observations, additional investigations were conducted on a limited set of sequences, with a specific focus on the aptamers that are most employed in literature for lysozyme determination, namely C42 and A40. These aptamers derive from truncation of C80 and A80 full-length sequences selected with SELEX experiments (C80 and A80, respectively), as discussed in the introduction section. PolyT40 was maintained as a reference blank and negative control.

At first, for C42, A40, and PolyT40 sequences the electrochemical assay was carried out in TGK, the buffer utilized for the selection of the A80 aptamer (**Figure 2.13**). The buffer composition had an effect on absolute and relative signals.

The signals in TGK were approximately three times higher than those recorded in PBS-$Mg^{2+}$ and TRIS saline buffers. This difference may be attributed to the absence of salts that typically act as DNA counterions, thereby levelling the signal intensity.

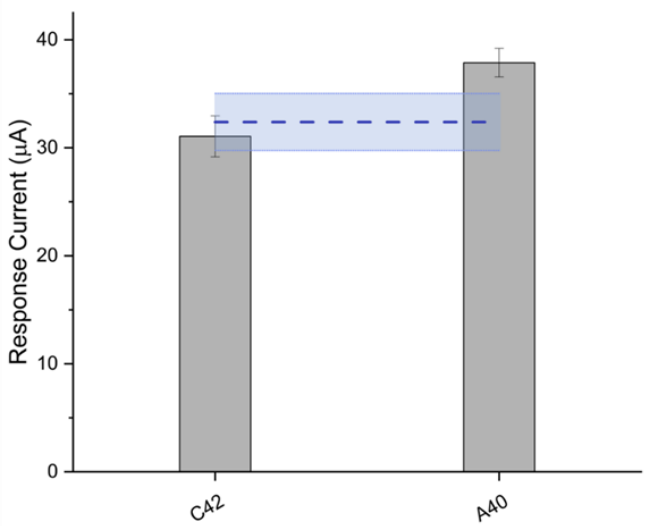


**Figure 2.13**. Comparison of DPV signals from MBs-based electrochemical assays of C42 and A40 aptamers in TGK buffer (n=3). Mean signal resulting from the immobilization of PolyT40 blank reference is reported as dashed blue line, with standard deviation reported as light-blue boxes

### 2.4.6. Conformational characterization through circular dichroism analysis

Results from electrochemical assay highlighted a different behavior of the aptamers depending on the buffer. For this reason, CD measurements were conducted, in collaboration with Prof. Luca Ronda, a biochemistat the University of Parma, to assess how the buffer might affect the secondary structure of the aptamers and, consequently, their affinity for the target.

CD technique is particularly useful to examine the structure of proteins and bioreceptors, among which aptamers, as well as to investigate conformational changes induced by bioreceptor-target interaction, especially when the target is a protein [30,31]. In the study by Mihai et al., aimed at the development of a label-free aptasensor based on SPR transduction for lysozyme in wines, CD measurements demonstrated a change in lysozyme conformation in the presence of the wine matrix, which had a negative impact on lysozyme-aptamer recognition event [18].

CD spectra were acquired in PBS-$Mg^{2+}$ and TGK buffers, since they have been shown to provide the greatest signal differences between the aptamers and the highest intensities, respectively. CD spectra are presented in **Figure 2.14**, where it can be noted a distinct conformation of C42 and A40 in the two buffers. In particular, A40 was observed to have shift of the peak (**Figure 2.14a**), while an inflection point shift is present for C42 (**Figure 2.14b**). Furthermore, PolyT40 was observed to be unaffected by buffer composition **(Figure 2.14c**). These findings confirmed the role of buffer in influencing aptamer structure, emphasizing the necessity of rationalization in the choice of binding buffer for subsequent development of aptamer-based analytical methods.

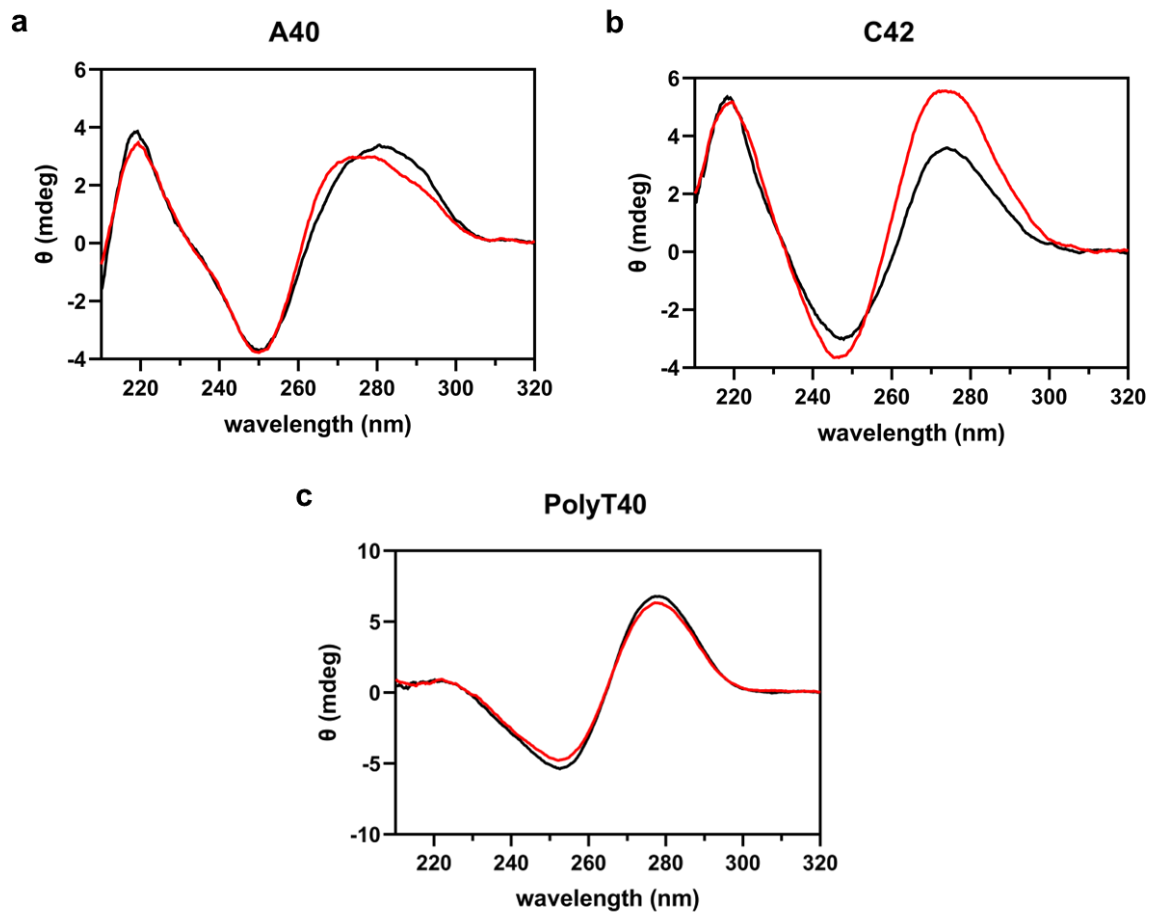


**Figure 2.14.** Overlay of CD spectra of **(a)** A40, **(b)** C42, **(c)** PolyT40 in buffers PBS-$Mg^{2+}$ (red) and TGK (black)

CD measurements were also conducted to examine the effect of denaturation on the conformation of the studied aptamers. Due to the wide range of different conformations that aptamers can adopt in solution, some studies in literature recommend performing a thermal melting followed by gradual cooling aimed at standardizing aptamer folding pathways and reducing batch-to-batch variations [6–8,10,23]. To investigate this, CD spectra of A40 and C42 were recorded before and after denaturation at 90°C. Upon comparison of the CD spectra, it was observed that denaturation and subsequent refolding did not induce any noticeable conformational changes in either aptamer (**Figure 2.15**).

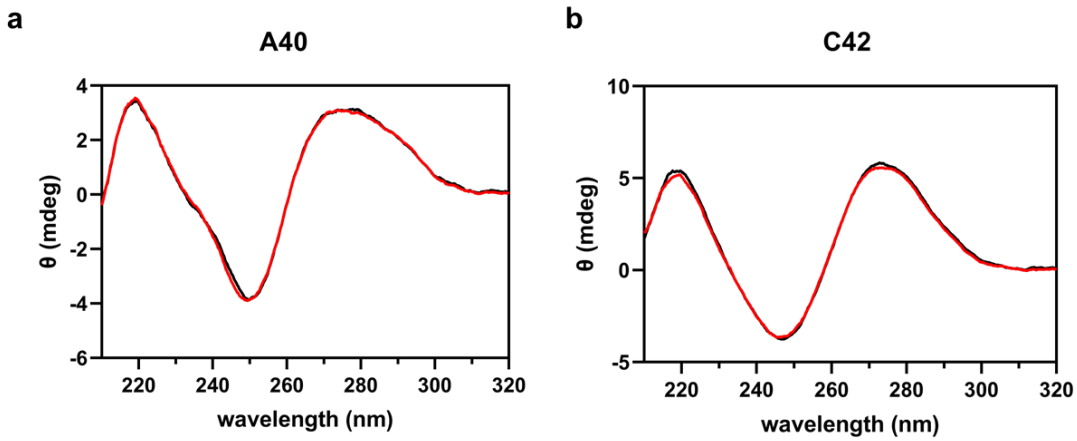


**Figure 2.15.** CD spectra of **(a)** A40 and **(b)** C42, recorded at 26 °C, before (red) and after (black) thermal denaturation at 90 °C

Study of lysozyme/aptamer interaction by CD was performed by comparing the experimental spectrum of an equimolar mixture of aptamer and lysozyme with the sum of the spectra of individual components, as detailed in the experimental section. In the presence of an interaction, a difference between the experimental spectrum and the algebraic sum of the CD spectra would be expected if the interaction caused conformational changes in the lysozyme, the aptamer, or both. The results presented in **Figure 2.16** indicated that no differences were observed in the PBS-$Mg^{2+}$ buffer, and minimal differences were noted in the TGK buffer, which, however, were not significant.

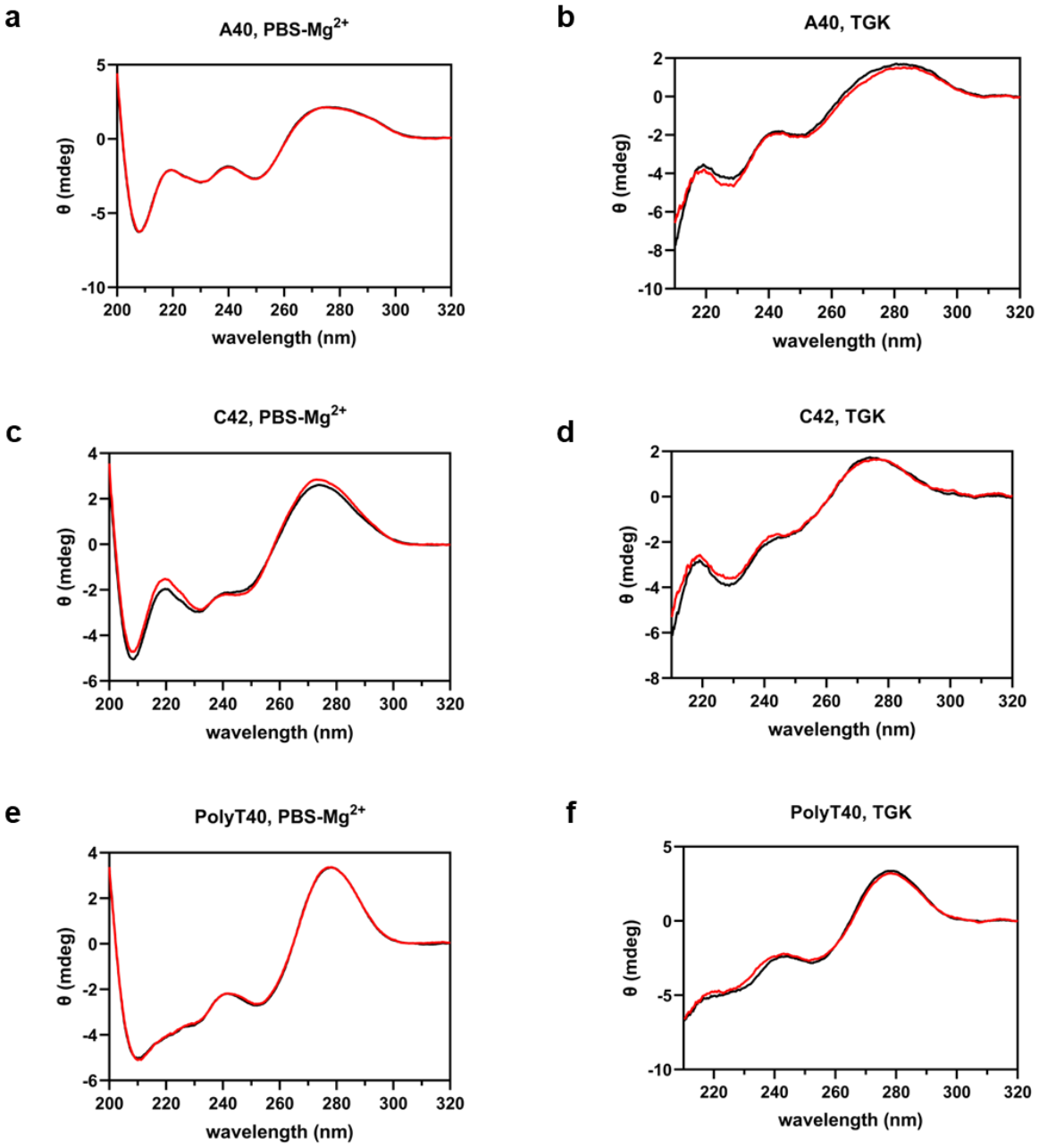


**Figure 2.16.** CD spectra of the equimolar mixture (red) and the algebraic sum (black) of lysozyme with A40 aptamer in **(a)** PBS-$Mg^{2+}$ and **(b)** TGK buffers; with C42 aptamer in **(c)** PBS-$Mg^{2+}$ and **(d)** TGK buffers; with PolyT40 in **(e)** PBS-$Mg^{2+}$ and **(f)** TGK buffers

In conclusion, the CD analysis did not allow to prove a lysozyme/aptamer interaction. However, these results did not rule out the existence of an interaction, since binding could not induce a conformational change in either the protein or the aptamer. Furthermore, these findings suggest that aptasensors relying on aptamer conformational changes could benefit from preliminary circular dichroism investigations to validate the detection principle of the sensor.

### 2.4.7. Study of aptamer-lysozyme interaction by fluorescence measurements

The aptamer-lysozyme interaction has been investigated using the fluorescence spectroscopy as well. These experiments were conducted with A40 and C42 in both PBS-$Mg^{2+}$ and TGK buffers. Two different titration approaches were carried out: titrating 1 µM of aptamer with increasing concentration of lysozyme or titrating 1 µM of protein with increasing concentrations of aptamer. The objectives of these experiments were to investigate aptamer-protein binding, and to finally construct a binding curve to calculate the dissociation constant (Kd).

Each titration was repeated three times for estimating the experimental error. It was also ensured that the absorbance always remained below 0.1, so that the inner filter effect could be ruled out.

***First strategy – Titration of the aptamer with lysozyme***

The first strategy consisted in aptamer titration with the protein. For this purpose, A40 and C42 functionalized at the 3' end with the Dansyl group (**Figure 2.17**) were used.

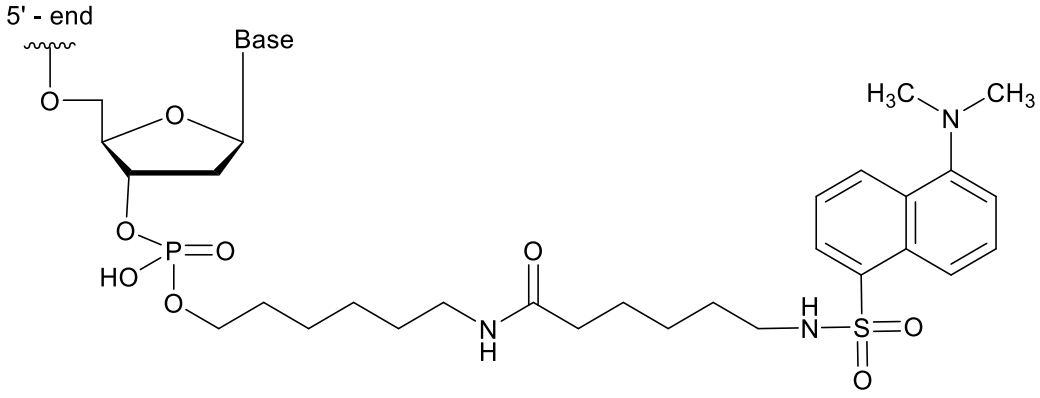


**Figure 2.17.** Molecular structure of an oligonucleotide sequence modified with Dansyl-X group at 3' end

The Dansyl fluorophore exhibits maximum absorption around 335 nm and maximum emission around 518 nm. These spectral characteristics are influenced by the chemical environment in which Dansyl is situated. Our analyses were based on the sensitivity of Dansyl emission spectrum to its chemical surroundings. In the presence of an interacting molecule that alters the chemical environment, Dansyl can exhibit significant changes in both intensity and a shift of the peak maximum.

As previously mentioned, the titration was conducted by maintaining a constant concentration of dansylated aptamer and sequentially adding lysozyme. This experiment involved A40-dansyl and C42-dansyl, in PBS-$Mg^{2+}$ and TGK buffers. The excitation was performed at a wavelength of 330

nm to directly excite the Dansyl group, while emission spectra were recorded in the 410-700 nm range. Results are shown in **Figures 2.18** and **2.19**.

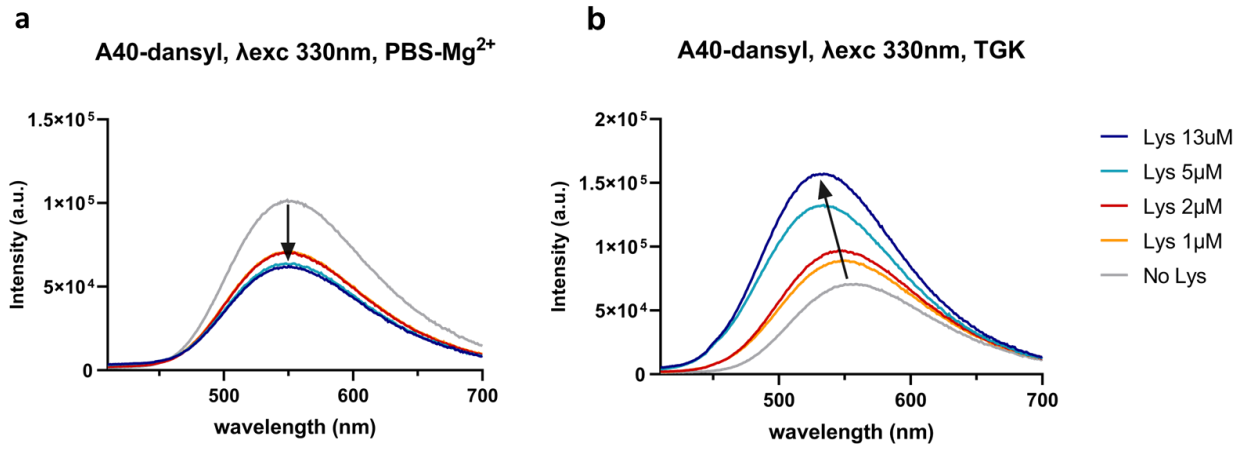


**Figure 2.18.** Emission spectra acquired during titration of A40-dansyl with lysozyme (Lys) (λexc 335 nm) in **(a)** PBS-$Mg^{2+}$ and **(b)** TGK buffer

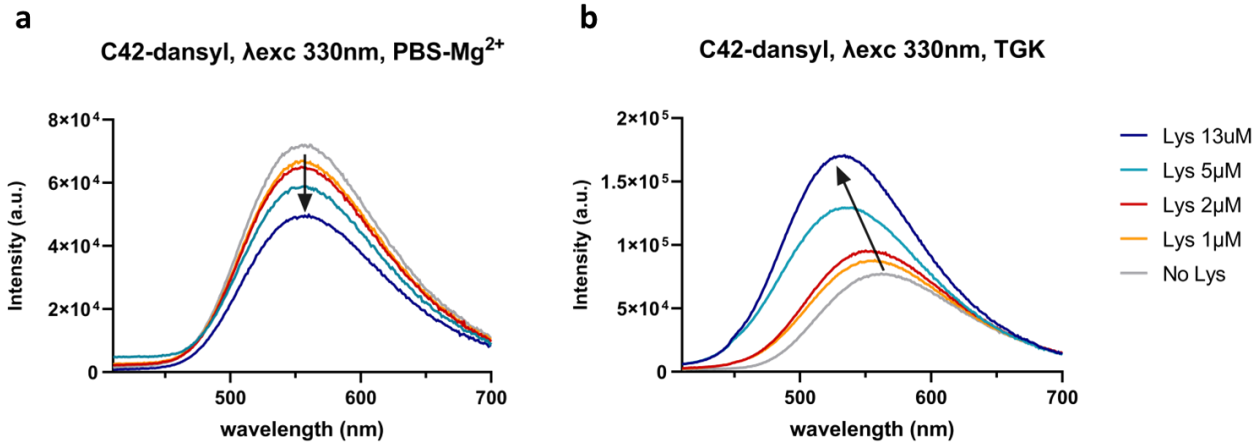


**Figure 2.19.** Emission spectra acquired during titration of C42-dansyl with lysozyme (Lys) (λexc 335 nm) in **(a)** PBS-$Mg^{2+}$ and **(b)** TGK buffer

In all cases, we observed variations in the emission spectrum upon the addition of lysozyme, with the signal changing depending on the buffer used while using the same aptamer. The change in intensity can be attributed to water, having a static quenching effect on dansyl fluorescence. Therefore, depending on whether the dansyl group is more or less exposed to the solvent, its fluorescence

intensity may vary. Specifically, in the PBS-$Mg^{2+}$ buffer, we observed a decreasing signal, likely due to solvent quenching. In contrast, in the TGK buffer, we observed a double effect for both aptamers: the intensity of the peak increased, while its maximum shifted to lower wavelengths. This shift may be caused by the movement of the dansyl molecule toward a more hydrophobic environment.
In both cases, it seems that the buffer influenced the aptamer's conformation differently. The visible differences induced by the buffers demonstrate that aptamers can adopt different binding modes depending on the buffer used, and, more importantly, buffer has a major impact on aptamer-protein interaction with respect to aptamer sequence.
Another observation regards the strength of binding. If the interaction were stronger (i.e., with a Kd in the nanomolar range), we would not observe a progressive variation, but rather signal saturation with the first addition of protein. The variation in the emission spectrum, observed up to a final lysozyme concentration of 13 µM, suggests that the Kd is in the µM range.
Considering that the binding efficiency could be influenced by the presence of the tag, a second titration strategy involved the use of untagged aptamers, and the native protein for Kd determination.

***Second strategy – Titration of lysozyme with the aptamer***

In this case, the investigation involved consecutive additions of the aptamer to lysozyme. To construct the binding curves, we exploited the intrinsic fluorescence of lysozyme, eliminating the need for tags on the aptamer.
The intrinsic fluorescence of the protein comes from the presence of aromatic amino acid residues. Specifically, we chose to selectively excite tryptophan (Trp) at 298 nm, which is more influenced by the chemical environment compared to tyrosine and phenylalanine. Upon each addition, we acquired the emission spectrum in the 310-550 nm range.
The aptamer-lysozyme interaction was studied for both A40 and C42 in PBS-$Mg^{2+}$ and TGK buffers to measure molecular binding and calculate the Kd constant. As a negative control, we used PolyT40.
For all the aptamers analyzed, we observed a similar behavior: the lysozyme fluorescence emission exhibited a maximum at 337 nm and decreased in intensity with increasing aptamer concentration (see **Figures 2.20** and **2.21**). This decrease may be attributed to static fluorescence quenching or a chemical environmental change in Trp due to the interaction with the aptamer.
**Figure 2.22** shows the binding curves for A40, C42 and PolyT40 aptamers in PBS-$Mg^{2+}$ and TGK buffers, obtained by collecting signals at 337 nm maximum; the calculated Kd values are reported in **Table 2.2**.

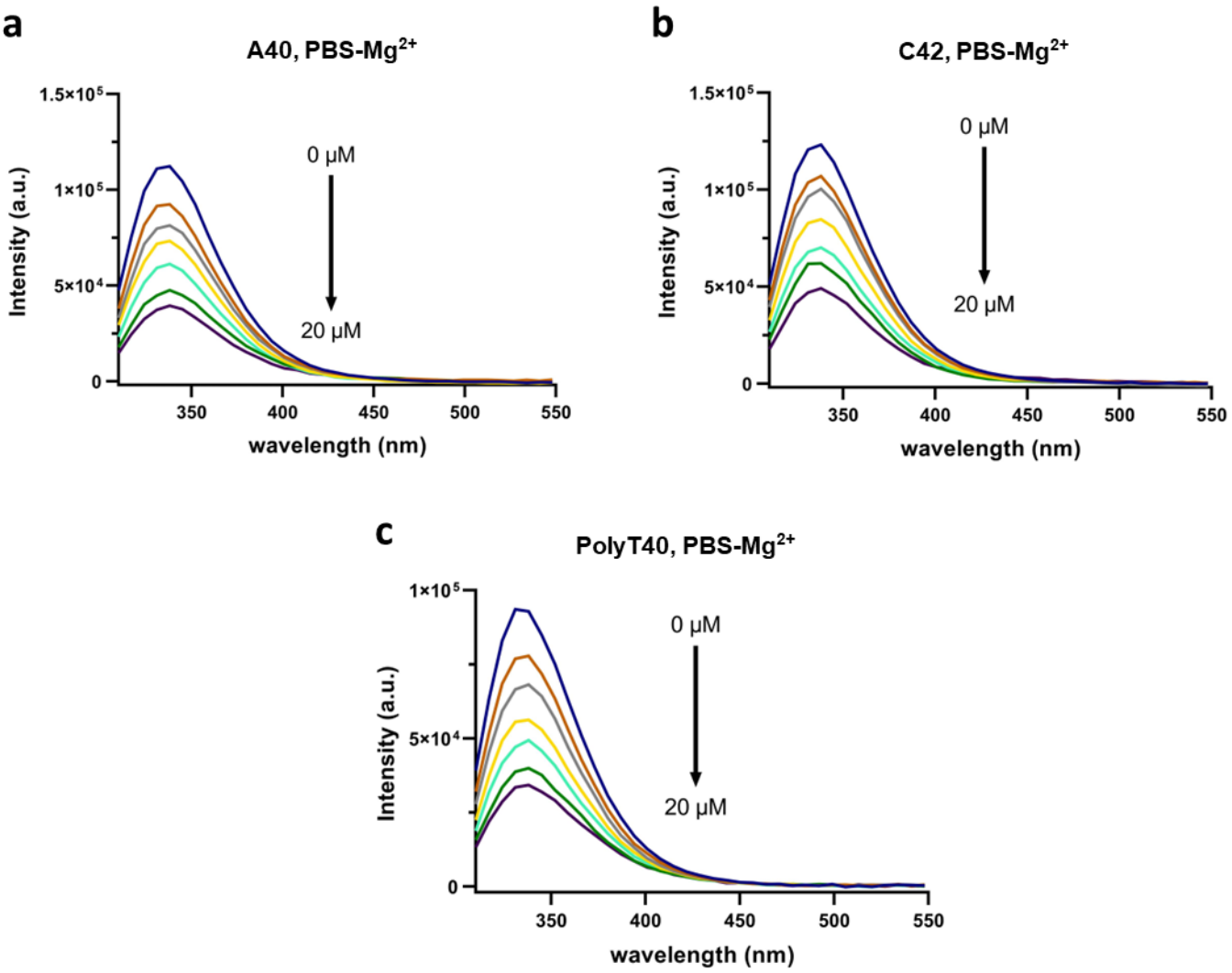


**Figure 2.20.** Emission spectra (λexc 298 nm) acquired during the titration of lysozyme in PBS-$Mg^{2+}$ with **(a)** A40, **(b)** C42 and **(c)** PolyT40

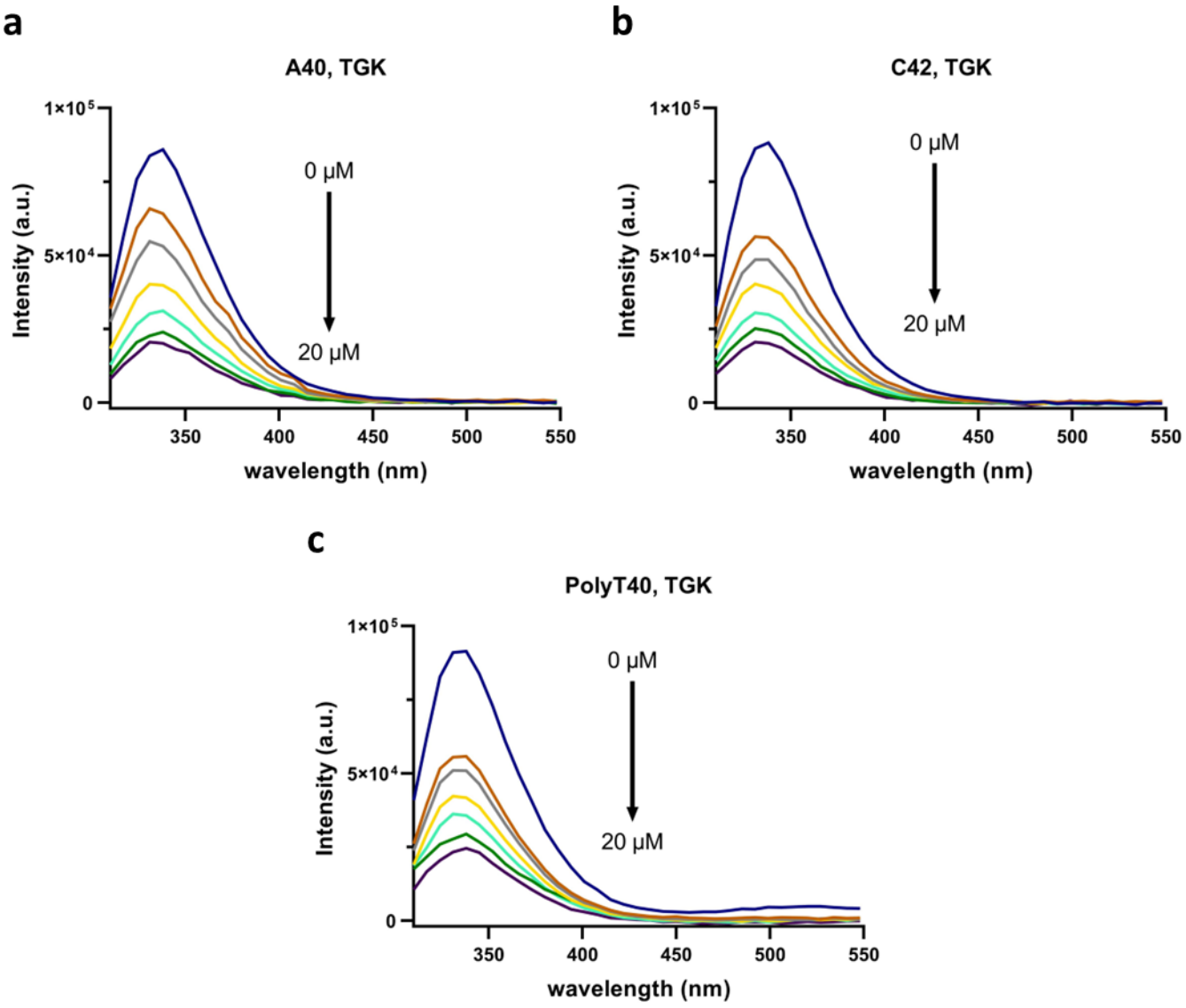


**Figure 2.21.** Emission spectra (λexc 298 nm) acquired during the titration of lysozyme in TGK with **(a)** A40, **(b)** C42 and **(c)** PolyT40

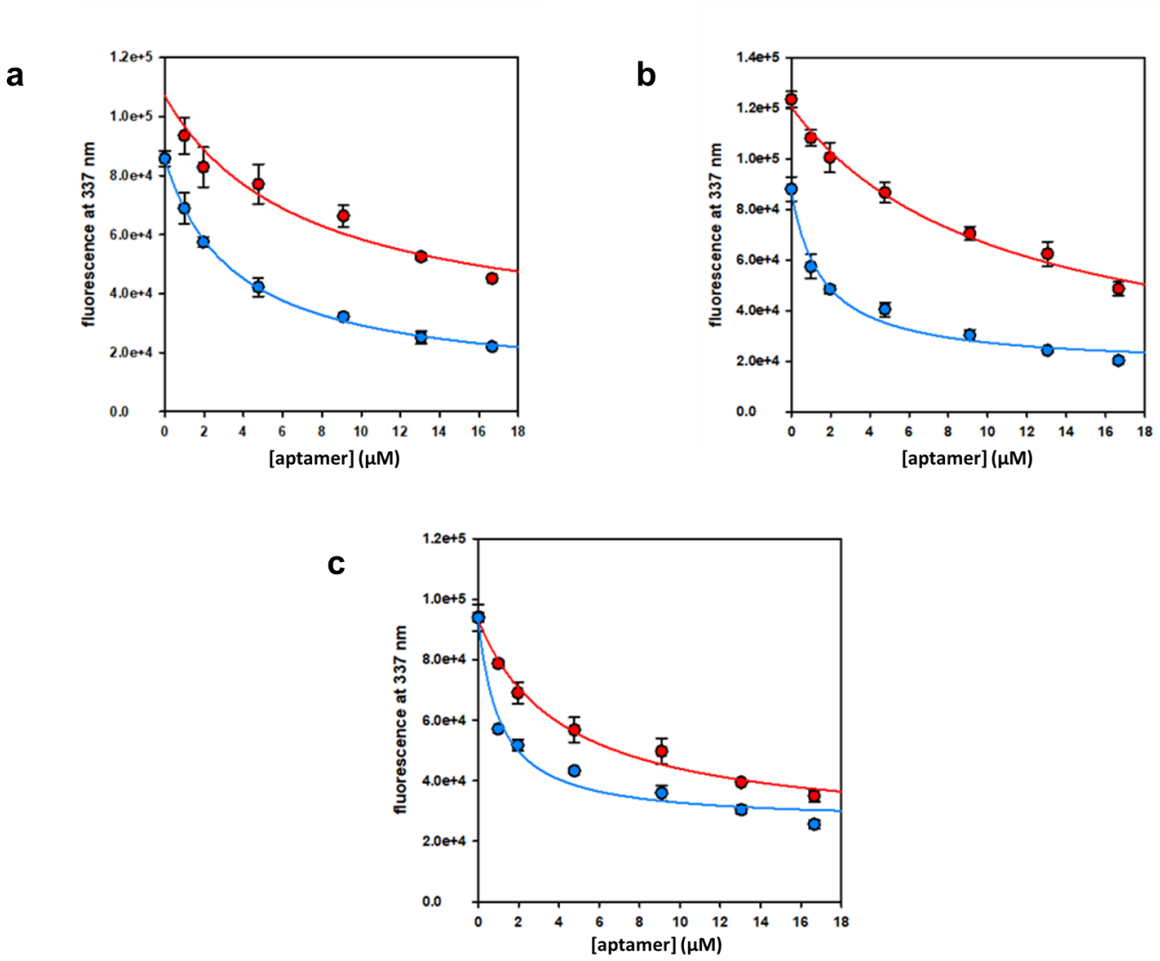


**Figure 2.22.** Binding curves form fluorescence titration for **(a)** A40, **(b)** C42, and **(c)** PolyT40 in both PBS-$Mg^{2+}$ (in red) and TGK buffers (in blue). Data collected from three independent experiments (n=3)

**Table 2.2.** Dissociation constant (Kd) for A40, C42 and PolyT40 in PBS-$Mg^{2+}$ and TGK buffers

| | **Kd (μM)** | |
|---|---|---|
| | PBS-$Mg^{2+}$ | TGK |
| A40 | 7.0 ± 4.0 | 3.5 ± 0.3 |
| C42 | 10.5 ± 3.9 | 1.6 ± 0.4 |
| PolyT40 | 4.3 ± 1.1 | 1.1 ± 0.3 |

On the basis of these findings, the interaction does not seem to be strictly sequence-specific; furthermore, the Kd values are at μM levels. The Kd observed in PBS-$Mg^{2+}$ closely align with those reported by Potty et al. in a 20 mM TRIS buffer when the NaCl concentration is raised to 100 mM [32]. In that particular study, when compared to scrambled sequences, the authors demonstrated that the binding affinity of C42 and other DNA analogs of RNA aptamers selected by Kirby et al. [33] is not strictly dictated by the sequence itself but rather is facilitated by non-specific ionic interactions between the negatively charged DNA sequence and the positively charged lysozyme. These interactions are primarily mediated by polyelectrolytes [34].

### 2.4.8. Asymmetrical flow field-flow fractionation analysis

Asymmetrical flow field-flow fractionation (AF4) is a versatile separation technique, performing separation inside a narrow channel, thus not having any stationary phase, but only a bulk phase [35–37]. A liquid carrier is pumped along the channel, establishing a parabolic flow profile, resulting in moving analytes towards the outlet. The application of a cross-flow field, i.e. a secondary flow of liquid, perpendicular to the main flow promotes the separation of components based on their hydrodynamic radius. Thus, the retention time depends on diffusive flux, and diffusion coefficient of particles is responsible for separation. The system and the principle of separation of the technique are reported in **Figure 2.23**.

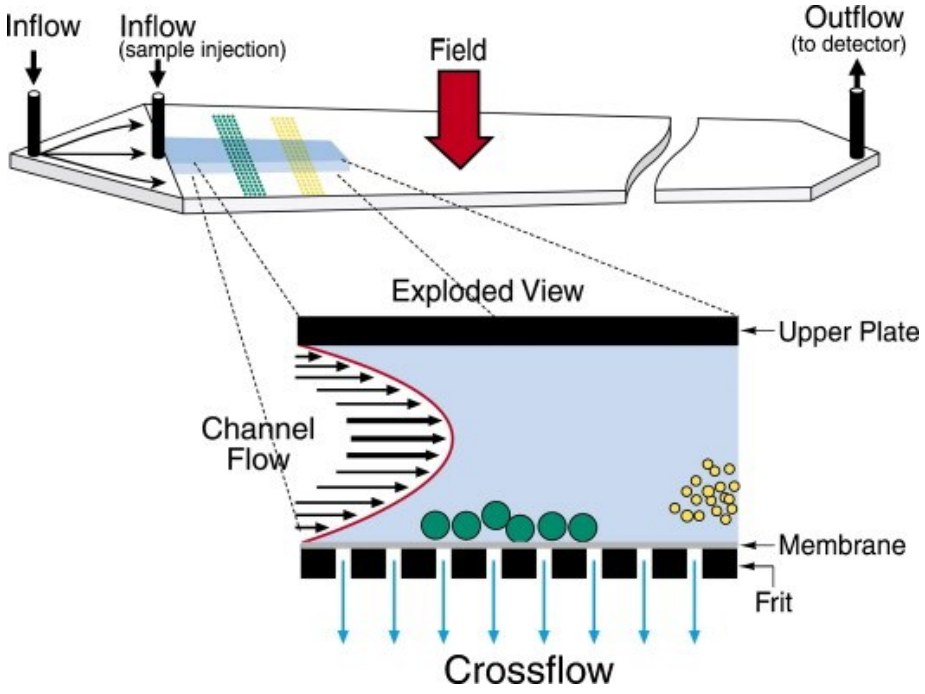


**Figure 2.23.** Illustration of AF4 system and separation principle of macromolecules**.** Reprinted from Ref. [35]. Copyright © 2023, with permission from Elsevier

The absence of stationary phase in AF4 makes it a *soft* technique, in which there is no possibility of having unwanted interactions with it. Another important advantage is the possibility to study the formation of complexes between macromolecules, performing separation in native conditions, simulating pH and ionic strength conditions desired, and in presence of interferents; this could permit to preserve structural integrity of complexes, detecting formation of complexes and conformational changes, and to obtain information on affinity and selectivity of binding.

In collaboration with the group of Prof. P. Reschiglian (University of Bologna) the potentialities of of (AF4)-UV were investigated for the development of a screening method aimed at shortlisting the most promising anti-lysozyme aptamers for analytical applications. The approach was studied on anti-lysozyme aptamers in PBS-$Mg^{2+}$ buffer. During the development of the method, lysozyme and aptamer sequences were observed to have similar retention times, due to a comparable molar mass. For this reason, it was decided to investigate the interaction between the two species by following the signal of the unbound aptamer, that decreases at higher concentration of lysozyme. As reported in the UV spectra of **Figure 2.24a**, protein and aptamers present maximum absorbance at two distinct wavelengths (280 and 260 nm, respectively), and this permitted to monitor aptamer signal exclusively, by working at 260 nm (**Figure 2.24b**).

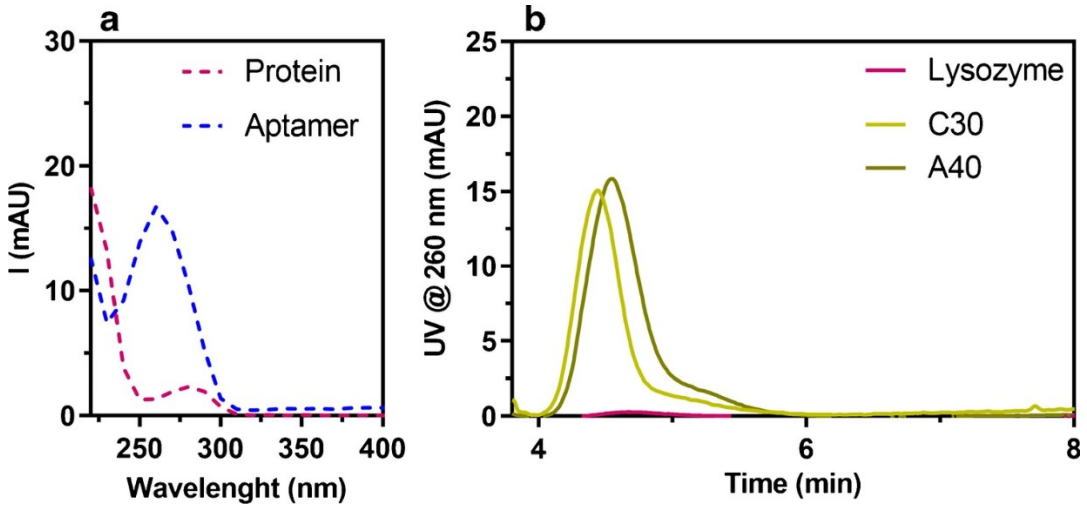


**Figure 2.24. (a)** UV spectra of lysozyme (pink dashed lines) and A40 sequence (blue dashed lines), representing protein and aptamer, respectively. **(b)** AF4-UV overlay fractograms of lysozyme, C30 and A40 aptamers (wavelength 260 nm). Reprinted from Ref. [26]. Licensed under a Creative Commons Attribution 4.0 International License

Calculated Limits of Quantification (LOQ) resulted in low pmol range of mass for all the aptamers investigated, and linearity was confirmed between LOQ and the maximum amount injected. The choice of monitoring aptamer signal permitted to easily apply the developed method to any aptamer sequence, independently from the nature of the target. Moreover, it is worth to highlight the ability to get valuable information about aptamer-target interactions not requiring the presence of labels on the involved species.

The binding of anti-lysozyme aptamers to the target was investigated by mixing the oligonucleotide sequence (5 μM) with increasing concentration of protein (5, 10, 25, 50 μM), analyzing each mix by AF4-UV. In **Figure 2.25** are present the fractograms for A40 and A80R sequences, which showed different behavior in presence of lysozyme. As can be seen, increasing lysozyme concentration led to a decrease in aptamer signal (in correspondence to the retention time indicated by the dashed line); at the same time, a peak corresponding to the bound specie is visible at higher retention time, as protein concentration increases. From **Figure 2.25a** it is possible to observe that A40 have better binding performances than A80R: the first presents a decrease in signal of free aptamer specie as lysozyme concentration grows, whereas the signal of the complex appears only at the higher protein concentration for A80R.

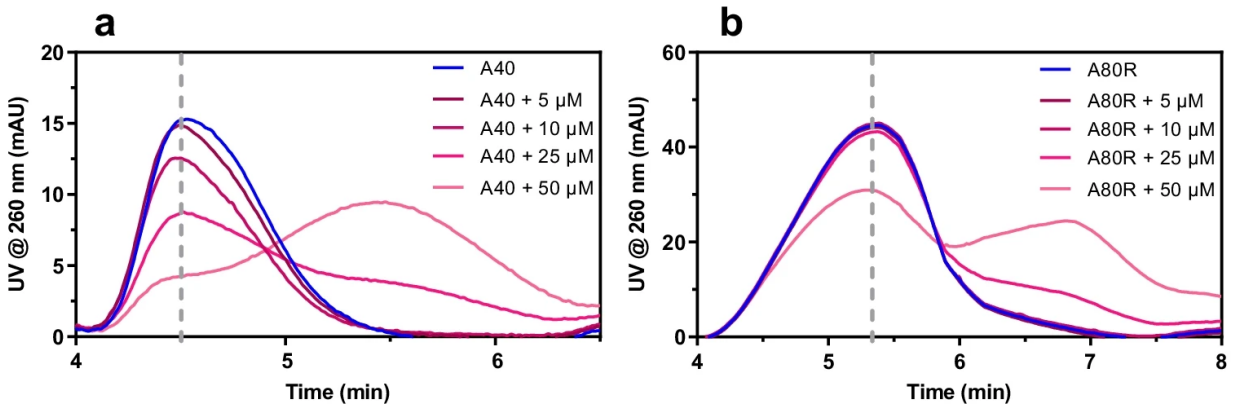


**Figure 2.25.** AF4-UV (260 nm) fractograms of **(a)** A40 and **(b)** A80R, and aptamer-lysozyme mixtures. Free aptamer and aptamer-lysozyme complex present distinct retention times. Signal intensity is recorded at retention time corresponding to the maximum of free aptamer, indicated by vertical grey dashed line. Reprinted from Ref. [26]. Licensed under a Creative Commons Attribution 4.0 International License

On the basis of the recorded fractograms, the binding affinity for each sequence was calculated as a percentage of bound aptamer, by comparing the signal reference in absence of protein with the signal of the mix, expressed as:

$$\% \ (I_{\text{apt alone}} - I_{\text{apt mix}})/I_{\text{apt alone}}$$

The percentage values of bound aptamer for the sequences investigated in function of lysozyme concentration level are presented in **Figure 2.26**, allowing an easy comparison of binding performances of distinct aptamers towards lysozyme. A80 sequence presents the higher affinity, reaching 80% of bound fraction at the higher lysozyme concentration level (50 µM), while randomly scrambled sequence A80R reached 20% in the same conditions. Best performances were obtained by A80 and A40 in terms of affinity to lysozyme, but, even in this case, investigated concentrations were in µM range, with results in line with those obtained by florescence spectroscopy titration and MBs electrochemical assay.

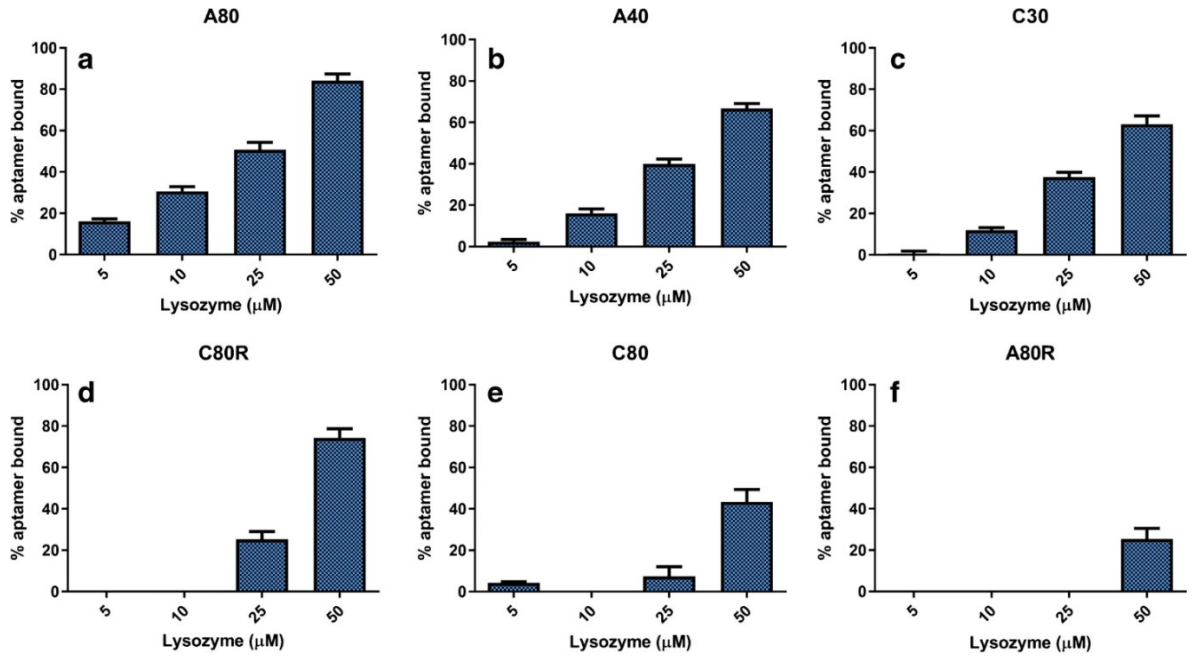


**Figure 2.26.** Percentage of bound aptamer with lysozyme target (n=3) for sequences: **a.** A80; **b.** A40; **c.** C30; **d.** C80R; **e.** C80; **f.** A80R. Reprinted from Ref. [26]. Licensed under a Creative Commons Attribution 4.0 International License

To complement the information provided by AF4-UV techniques reported by Marassi et al. [26], C42 and PolyT40 sequences were investigated following the same procedure. For better visualization and comparison with sequences analyzed in the previously reported approaches, results on A40 sequences, presented above in **Figure 2.26**, were reported also in **Figure 2.27**. In this case, C42 is shown to have a similar behavior compared to PolyT40 negative control sequence.

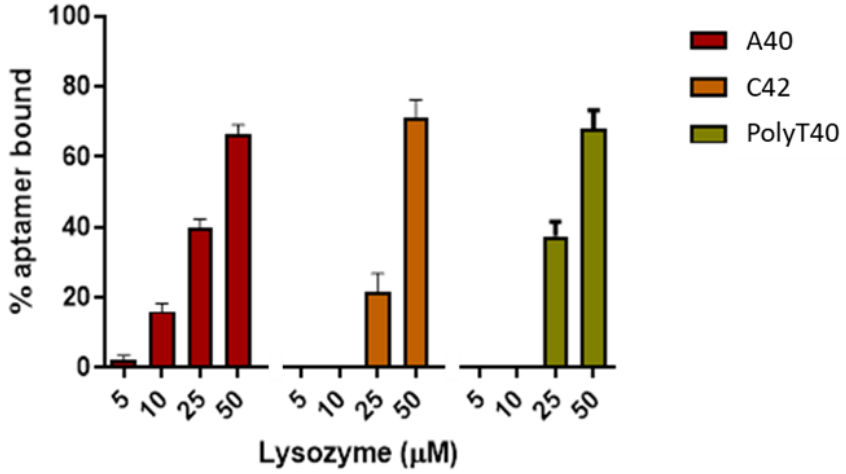


**Figure 2.27.** Percentage of bound aptamer for A40, C42 and PolyT40 (n = 3) with lysozyme

Looking at the results overall and considering affinities of sequences reported in **Figures 2.26** and **2.27**, it can be observed that DNA sequences from the "Clone" group originating from Cox and Ellington's publication [21] (C80, truncated sequences C30 and C42, and randomly scrambled C80R) all present poor binding performance, especially compared to A80 and A40 sequences. Moreover, C80R presents a slightly higher percentage of bound aptamer than C80, that indicates scarce sequence-specificity of binding. The inconsistency of these results with the high affinity observed by Cox and Ellington [21] (Kd ranging in nM concentration level) is probably ascribable to a misinterpretation of the original table listing the template DNA sequences that that has spread throughout the scientific community over the years, as claimed by the same Cox and Ellington some years later. [10,21,33]. Several works report that RNA and DNA versions of the same aptamer can have different behavior, resulting in large differences in affinity towards a target [6,8,32,38].

In order to further demonstrate the reliability of the developed multi-technique approach experiments on a presumed positive control (the SELEX-selected RNA C80) are currently underway.

## 2.5. Conclusions

The role of aptamers as bioreceptors capable of binding target analytes for different applications in analytical chemistry has been debated within the scientific community in recent years. In particular, there is a call for greater rigor in evaluating effective analytical potentialities of aptamers and assessing selectivity of binding, also in presence of interferent compounds, in view of application of analytical methods in real matrix. Lysozyme from chicken egg due to its allergenicity represents a common target for many analytical methods, especially aptasensors, and was selected as target case study. In this work, the binding properties of DNA aptamers targeting lysozyme and widely employed in literature were investigated by means of a multi-technique approach. The affinity between anti-lysozyme aptamers and lysozyme resulted lower than expected, since Kd in the range of μM were obtained. In addition, a  a similar binding behavior was observed for negative control sequences, such as randomly scrambled sequences and PolyT40, highlighting a poor sequence-selectivity of binding. The obtained results are in line with those of a growing group of articles that question the real potentialities of aptamers. To do that, for the development of reliable aptamer-based analytical methods it is encouraged a more rigorous evaluation of binding capabilities of aptamers, through the investigation of the binding in different conditions (buffer, pH, ionic strength), and taking into consideration the investigation of negative controls as well.

## Bibliography


(1) Ni, S.; Zhuo, Z.; Pan, Y.; Yu, Y.; Li, F.; Liu, J.; Wang, L.; Wu, X.; Li, D.; Wan, Y.; Zhang, L.; Yang, Z.; Zhang, B. T.; Lu, A.; Zhang, G. Recent Progress in Aptamer Discoveries and Modifications for Therapeutic Applications. *ACS Appl Mater Interfaces* **2021**, *13* (8), 9500–9519. https://doi.org/10.1021/acsami.0c05750.

(2) Mattarozzi, M.; Toma, L.; Bertucci, A.; Giannetto, M.; Careri, M. Aptamer-Based Assays: Strategies in the Use of Aptamers Conjugated to Magnetic Micro- and Nanobeads as Recognition Elements in Food Control. *Anal Bioanal Chem* **2022**, *414* (1), 63-74. https://doi.org/10.1007/s00216-021-03501-6.

(3) Wu, Y.; Belmonte, I.; Sykes, K. S.; Xiao, Y.; White, R. J. Perspective on the Future Role of Aptamers in Analytical Chemistry. *Anal Chem* **2019**, *91* (24), 15335–15344. https://doi.org/10.1021/acs.analchem.9b03853.

(4) Baird, G. S. Where Are All the Aptamers? *Am J Clin Pathol* **2010**, *134* (4), 529–531. https://doi.org/10.1309/AJCPFU4CG2WGJJKS.

(5) Bottari, F.; Daems, E.; De Vries, A. M.; Van Wielendaele, P.; Trashin, S.; Blust, R.; Sobott, F.; Madder, A.; Martins, J. C.; De Wael, K. Do Aptamers Always Bind? The Need for a Multifaceted Analytical Approach When Demonstrating Binding Affinity between Aptamer and Low Molecular Weight Compounds. *J Am Chem Soc* **2020**, *142* (46), 19622–19630. https://doi.org/10.1021/jacs.0c08691.

(6) Cho, E. J.; Lee, J. W.; Ellington, A. D. Applications of Aptamers as Sensors. *Annual Review of Analytical Chemistry* **2009**, *2*, 241–264. https://doi.org/10.1146/annurev.anchem.1.031207.112851.

(7) Zong, C.; Liu, J. The Arsenic-Binding Aptamer Cannot Bind Arsenic: Critical Evaluation of Aptamer Selection and Binding. *Anal Chem* **2019**, *91* (16), 10887–10893. https://doi.org/10.1021/acs.analchem.9b02789.

(8) Zhao, Y.; Yavari, K.; Liu, J. Critical Evaluation of Aptamer Binding for Biosensor Designs. *TrAC - Trends in Analytical Chemistry* **2022**, *146*. https://doi.org/10.1016/j.trac.2021.116480.

(9) McKeague, M.; De Girolamo, A.; Valenzano, S.; Pascale, M.; Ruscito, A.; Velu, R.; Frost, N. R.; Hill, K.; Smith, M.; McConnell, E. M.; DeRosa, M. C. Comprehensive Analytical Comparison of Strategies Used for Small Molecule Aptamer Evaluation. *Anal Chem* **2015**, *87* (17), 8608–8612. https://doi.org/10.1021/acs.analchem.5b02102.

(10) Miller, A. A.; Rao, A. S.; Nelakanti, S. R.; Kujalowicz, C.; Shi, T.; Rodriguez, T.; Ellington, A. D.; Stovall, G. M. Systematic Review of Aptamer Sequence Reporting in the Literature Reveals Widespread Unexplained Sequence Alterations. *Anal Chem* **2022**, *94* (22), 7731–7737. https://doi.org/10.1021/acs.analchem.1c04407.

(11) Dhanapala, P.; De Silva, C.; Doran, T.; Suphioglu, C. Cracking the Egg: An Insight into Egg Hypersensitivity. *Mol Immunol* **2015**, *66* (2), 375–383. https://doi.org/10.1016/j.molimm.2015.04.016.

(12) Urisu, A.; Kondo, Y.; Tsuge, I. Hen's Egg Allergy. *Chem Immunol Allergy* **2015**, *101*, 124–130. https://doi.org/10.1159/000375416.

(13) Banciu, R. M.; Numan, N.; Vasilescu, A. Optical Biosensing of Lysozyme. *J Mol Struct* **2022**, *1250*. https://doi.org/10.1016/j.molstruc.2021.131639.

(14) Artesani, M. C.; Donnanno, S.; Cavagni, G.; Calzone, L.; D'Urbano, L. Egg Sensitization Caused by Immediate Hypersensitivity Reaction to Drug-Containing Lysozyme. *Annals of Allergy, Asthma and Immunology* **2008**, *101* (1), 105. https://doi.org/10.1016/S1081-1206(10)60843-5.

(15) Lin, Y.; Sun, Y.; Dai, Y.; Zhu, X.; Liu, H.; Han, R.; Gao, D.; Luo, C.; Wang, X. A Chemiluminescence Assay for Determination of Lysozyme Based on the Use of Magnetic Alginate-Aptamer Composition and Hemin@HKUST-1. *Microchimica Acta* **2020**, *187* (5). https://doi.org/10.1007/s00604-020-04254-2.

(16) Rezaei, B.; Jamei, H. R.; Ensafi, A. A. An Ultrasensitive and Selective Electrochemical Aptasensor Based on RGO-MWCNTs/Chitosan/Carbon Quantum Dot for the Detection of Lysozyme. *Biosens Bioelectron* **2018**, *115*, 37–44. https://doi.org/10.1016/j.bios.2018.05.012.

(17) Han, B.; Zhao, C.; Yin, J.; Wang, H. High Performance Aptamer Affinity Chromatography for Single-Step Selective Extraction and Screening of Basic Protein Lysozyme. *Journal of Chromatography B* **2012**, *903*, 112–117. https://doi.org/10.1016/J.JCHROMB.2012.07.003.

(18) Mihai, I.; Vezeanu, A.; Polonschii, C.; Albu, C.; Radu, G. L.; Vasilescu, A. Label-Free Detection of Lysozyme in Wines Using an Aptamer Based Biosensor and SPR Detection. *Sens Actuators B Chem* **2015**, *206*, 198–204. https://doi.org/10.1016/j.snb.2014.09.050.

(19) Melinte, G.; Selvolini, G.; Cristea, C.; Marrazza, G. Aptasensors for Lysozyme Detection: Recent Advances. *Talanta* **2021**, *226*. https://doi.org/10.1016/j.talanta.2021.122169.

(20) Luo, R.; Zhou, X.; Chen, Y.; Tuo, S.; Jiang, F.; Niu, X.; Pan, F.; Wang, H. Lysozyme Aptamer-Functionalized Magnetic Nanoparticles for the Purification of Lysozyme from Chicken Egg White. *Foods* **2019**, *8* (2). https://doi.org/10.3390/foods8020067.

(21) Cox, J. C.; Ellington, A. D. Automated Selection of Anti-Protein Aptamers. *Bioorg Med Chem* **2001**, *9* (10), 2525–2531. https://doi.org/10.1016/S0968-0896(01)00028-1.

(22) Tran, D. T.; Janssen, K. P. F.; Pollet, J.; Lammertyn, E.; Anné, J.; Van Schepdael, A.; Lammertyn, J. Selection and Characterization of DNA Aptamers for Egg White Lysozyme. *Molecules* **2010**, *15* (3), 1127–1140. https://doi.org/10.3390/molecules15031127.

(23) Zhao, L.; Li, L.; Zhu, C.; Ghulam, M.; Qu, F. PH-Responsive Polymer Assisted Aptamer Functionalized Magnetic Nanoparticles for Specific Recognition and Adsorption of Proteins. *Anal Chim Acta* **2020**, *1097*, 161–168. https://doi.org/10.1016/j.aca.2019.11.001.

(24) Ocaña, C.; Hayat, A.; Mishra, R. K.; Vasilescu, A.; del Valle, M.; Marty, J. L. Label Free Aptasensor for Lysozyme Detection: A Comparison of the Analytical Performance of Two Aptamers. *Bioelectrochemistry* **2015**, *105*, 72–77. https://doi.org/10.1016/j.bioelechem.2015.05.009.

(25) Toma, L.; Mattarozzi, M.; Ronda, L.; Marassi, V.; Fortunati, S.; Giannetto, M.; Zattoni, A.; Careri, M. Are Aptamers Really Promising as Receptors for Analytical Purposes? Insights into Anti-Lysozyme DNA Aptamers through a Multi-Technique Study. *Anal Chem*, *in press* (accepted on 17 January **2024**).

(26) Marassi, V.; Mattarozzi, M.; Toma, L.; Giordani, S.; Ronda, L.; Roda, B.; Zattoni, A.; Reschiglian, P.; Careri, M. FFF-Based High-Throughput Sequence Shortlisting to Support the Development of Aptamer-Based Analytical Strategies. *Anal Bioanal Chem* **2022**, *414* (18), 5519-5527. https://doi.org/10.1007/s00216-022-03971-2.

(27) Amero, P.; Lokesh, G. L. R.; Chaudhari, R. R.; Cardenas-Zuniga, R.; Schubert, T.; Attia, Y. M.; Montalvo-Gonzalez, E.; Elsayed, A. M.; Ivan, C.; Wang, Z.; Cristini, V.; Franciscis, V. De; Zhang, S.; Volk, D. E.; Mitra, R.; Rodriguez-Aguayo, C.; Sood, A. K.; Lopez-Berestein, G. Conversion of RNA Aptamer into Modified DNA Aptamers Provides for Prolonged Stability and Enhanced Antitumor Activity. *J Am Chem Soc* **2021**, *143* (20), 7655–7670. https://doi.org/10.1021/jacs.9b10460.

(28) Gelinas, A. D.; Davies, D. R.; Janjic, N. Embracing Proteins: Structural Themes in Aptamer-Protein Complexes. *Curr Opin Struct Biol* **2016**, *36*, 122–132. https://doi.org/10.1016/j.sbi.2016.01.009.

(29) Sanborn, M. E.; Connolly, B. K.; Gurunathan, K.; Levitus, M. Fluorescence Properties and Photophysics of the Sulfoindocyanine Cy3 Linked Covalently to DNA. *Journal of Physical Chemistry B* **2007**, *111* (37), 11064–11074. https://doi.org/10.1021/jp072912u.

(30) Kelly, S. M.; Jess, T. J.; Price, N. C. How to Study Proteins by Circular Dichroism. *Biochim Biophys Acta Proteins Proteom* **2005**, *1751* (2), 119–139. https://doi.org/10.1016/j.bbapap.2005.06.005.

(31) Thevendran, R.; Citartan, M. Assays to Estimate the Binding Affinity of Aptamers. *Talanta* **2022**, *238*. https://doi.org/10.1016/j.talanta.2021.122971.

(32) Potty, A. S. R.; Kourentzi, K.; Fang, H.; Schuck, P.; Willson, R. C. Biophysical Characterization of DNA and RNA Aptamer Interactions with Hen Egg Lysozyme. *Int J Biol Macromol* **2011**, *48* (3), 392–397. https://doi.org/10.1016/j.ijbiomac.2010.12.007.

(33) Kirby, R.; Cho, E. J.; Gehrke, B.; Bayer, T.; Park, Y. S.; Neikirk, D. P.; McDevitt, J. T.; Ellington, A. D. Aptamer-Based Sensor Arrays for the Detection and Quantitation of Proteins. *Anal Chem* **2004**, *76* (14), 4066–4075. https://doi.org/10.1021/ac049858n.

(34) Kohlberger, M.; Gadermaier, G. SELEX: Critical Factors and Optimization Strategies for Successful Aptamer Selection. *Biotechnol Appl Biochem* **2022**, *69* (5), 1771–1792. https://doi.org/10.1002/bab.2244.

(35) Yohannes, G.; Jussila, M.; Hartonen, K.; Riekkola, M. L. Asymmetrical Flow Field-Flow Fractionation Technique for Separation and Characterization of Biopolymers and Bioparticles. *J Chromatogr A* **2011**, *1218* (27), 4104–4116. https://doi.org/10.1016/j.chroma.2010.12.110.

(36) Giddings, J. C.; Yang, F. J. F.; Myers, M. N. Flow Field-Flow Fractionation: A Versatile New Separation Method. *Science (1979)* **1976**, *193*, 1244–1245. https://doi.org/10.1126/science.959835.

(37) Wahlund, K. G. Flow Field-Flow Fractionation: Critical Overview. *J Chromatogr A* **2013**, *1287*, 97–112. https://doi.org/10.1016/j.chroma.2013.02.028.

(38) Ellington, A.; Szostak, J. Selection in Vitro of Single-Stranded DNA Molecules That Fold into Specific Ligand-Binding Structures. *Nature* **1992**, *355*, 850–852. https://doi.org/10.1038/355850a0.

# 3. Ambient Mass Spectrometry techniques for the detection of allergenic proteins from working surfaces: egg white lysozyme as case study

## 3.1. Introduction

As described in Chapter 1, food allergies involve immune responses to food proteins, triggering allergic reactions in sensitized people varying from mild to extremely severe. Since there are no specific cures for food allergy, avoidance of allergenic foods becomes crucial for affected individuals. To protect consumers, the European Union regulates 14 food ingredients with allergenic properties, requiring their mention on food labels (EU Regulation n. 1169/2011). A risk element associated with exposure to allergens in food is represented by the unwanted presence of an allergenic component in a food product caused by labeling errors or cross-contaminations during the production process [1–7].

In this context, the effectiveness of cleaning procedures of working surfaces in food facilities represents a known issue due to the risk of cross-contamination by food allergens [8]. In fact, incomplete or ineffective cleaning procedures may lead to the presence of allergenic components on the surfaces where food is prepared, resulting in contaminated final products [9]. Food industry, restaurants and refectories require reliable, fast, and easy methods to verify the absence of allergens, involving the use of a swab for surface sampling. Consequently, there has been an increasing focus on various strategies for the analysis of food contact surface to ensure efficacious cleaning procedure, prevent cross-contamination, and ultimately guarantee the safety of food products throughout the entire workflow/product chain [10].

At the moment, commercially available swabbing tests include colorimetric and immunochemical assays. Surface tests based on colorimetric measurements are widely used to check the presence of any protein on a surface: they are based on visual detection of color change when the swab is mixed with a proper reagent; they do not differentiate between proteins and are less sensitive than allergen-specific tests. Protein-specific immunochemical tests, such as enzyme-linked immunosorbent assay (ELISA), are based on recognition of allergenic protein by an antibody; these assays are selective for a specific target, but may present cross-reactivity, and lack the ability to perform multiplexing analysis [10–12].

Methods based on chromatography coupled with mass spectrometry are the most powerful approaches for detecting contaminants in food matrices, exploiting the separation capability of chromatography and the sensitivity, accuracy, and selectivity of MS, especially High Resolution MS

(HRMS) [12]. However, these methods involve high costs, time-consuming procedures, and complex sample preparation.

In this context, a valid methodological alternative can be Ambient Mass Spectrometry (AMS) that actually has not yet been investigated for the analysis of proteins on food contact surfaces. As discussed in the Introduction section of the present Thesis, the potentialities of AMS can be exploited for the development of high-throughput analytical strategies giving protein-specific signals and avoiding cross-reactivity risk. In particular, AMS techniques involve minimal or no sample treatment, in absence of chromatographic separation: the sample is desorbed and ionized in native conditions, at atmospheric pressure, thus performing a direct analysis of the sample. AMS currently counts more than 50 different techniques, both commercialized and custom, suited for liquid or solid sample [13–15]. The evolution of several distinct configurations is a result of the straightforward design of most of these techniques, for which the configuration is often home-made.

In the context of the analysis of allergenic protein residues on food contact surfaces, the most strategic AMS technique is Swab Touch Spray-Mass Spectrometry (Swab TS-MS) [9,16]. In its simple design, the swab used to sample the contaminated surface is then used directly as support for desorption and electrospray-like ionization: the metallic body of the swab permits the application of the potential to produce electrosprayed charged droplets from a rayon-cellulose tip where the sample has been previously collected by swabbing. Up to now, Swab TS-MS technique has been uniquely exploited for determination of small molecules, including drugs of abuse, oncometabolites, organic gunshot residues, and pesticides [16–22]; to the best of our knowledge this technique has not yet been investigated for the analysis of proteins and peptides.

## 3.2. Aim of the work

The aim of the research activities was the expansion of the framework of Swab TS-MS towards the analysis of allergenic proteins sampled from food contact surfaces by using properly developed swabbing strategies. These activities have been in part carried out during a visiting period of 6 months at the University of Barcelona under the supervision of Prof. Encarnación Moyano Morcillo. At first, the activities focused on the development of the Swab TS-MS method for the analysis of lysozyme from chicken egg, the allergenic protein selected as case study, followed by the assessment of the analytical quality parameters.

Then, swabbing strategies on contaminated surfaces are developed in view of establishing a suitable coupling with Swab TS-MS technique. For this purpose, the analyses were performed using a conventional LC-MS/MS method monitoring the target unique tryptic peptides of lysozyme. The LC-MS/MS method could serve also as confirmation technique.

Ultimately, potentialities of Paper Spray–MS (PS–MS) are also investigated for this application, as a possible alternative to the more straightforward Swab TS–MS technique.

## 3.3. Materials and methods

**Materials**. Acetonitrile (LC-MS grade, ≥ 99.9% purity), methanol (MeOH, ≥ 99.9% purity), absolute ethanol (EtOH, 99.8% purity), formic acid (FA, >98% purity), ammonium bicarbonate (>99% purity), DL-dithiothreitol (DTT, > 99% purity), iodoacetamide (IAA, > 99% purity), trypsin from bovine pancreas (> 99% purity), and lysozyme from chicken egg-white (LYS, > 99% purity) were purchased from Sigma-Aldrich (St. Louis, Missouri, USA). Egg-white powder (>80% protein content) was obtained from Farmalabor (Assago, Italy). Deionized water was prepared with a Milli-Q element A10 system (San Francisco, CA, USA). Rayon-tipped aluminum swabs were purchased from Copan Italia (Brescia, Italy).

**Sample preparation.** Stock solutions were prepared in 50 mM $NH_4HCO_3$ buffer at pH 8 at a concentration of 1000 mg/L for lysozyme and 36800 mg/L for egg-white powder (corresponding to a lysozyme concentration of 1000 mg/L).

***In-solution digestion*.** Tryptic digestion was performed on standard solutions of lysozyme, or egg-white powder, after protein reduction and alkylation. Reduction was carried out by addition of DTT to a final concentration of 10 mM and incubating the mixture for 40 min at room temperature. For alkylation reaction, IAA was added to a final concentration of 40 mM and the mixture was left reacting in the dark for 40 min. Then, enzymatic digestion was performed by adding a trypsin solution (1 mg/mL, in 50 mM $NH_4HCO_3$ at pH 8) to the sample, in order to obtain a trypsin:protein ratio of 1:20 (w/w), and incubating overnight at 37 °C. Ultimately, the digestion reaction was quenched by addition of 1% formic acid (v/v), prior to the analysis. Experiments with reduced enzymatic digestion time were carried out by incubating the trypsin (trypsin:protein ratio of 1:20 (w/w)) at 37 °C for 2 h and quenching the reaction with 1% (v/v) formic acid immediately after.

***Swabbing/swab digestion*.** A steel surface was divided into 10x10 cm that were sprayed with 500 µL of standard solutions of lysozyme (100 mg/L). Immediately after surface contamination, swab was used for surface sampling, following a predefined scheme, i.e. moving the swab in a zig zag pattern horizontally, vertically and diagonally, while rotating the swab's tip, in order to cover the entire area. Swab digestion was performed by incubating swab's tip into solutions containing reactives for 2-hours digestion. Peptides were analyzed by LC–ESI–MS/MS.

***In situ digestion/swabbing*.** A steel surface was divided into 10x10 cm that were sprayed with 500 µL of standard solutions of either lysozyme or egg-white at different concentration levels (1000 and 100 mg/L of target protein). The contaminated surfaces were then left to dry out completely. *In situ* digestion was carried out by spraying each reagent on the 10x10 cm contaminated surfaces as follows: 1 mL of 5 mM DTT was uniformly sprayed and left reacting at room temperature for 40 min, covering

the surface with aluminum foil to prevent solvent evaporation. Alkylation reaction was obtained by spraying 500 µL of 40 mM IAA and keeping the wetted surface in the dark for 40 min. Enzymatic digestion was then carried out by spraying on the surface a volume of 500 µL of a trypsin solution (trypsin:protein ratio of 1:20 (w/w)) that was left reacting for 2 h. During this time, 0.5-1 mL of bicarbonate buffer was sprayed on the surface once every 20-30 min, to keep the surface wetted due to solvent evaporation. Ultimately, sampling was performed by swabbing the surface, as reported above in "*Swabbing/swab digestion*" protocol. Tryptic digestion was quenched with 1% (v/v) formic acid. In case of LC-MS/MS analysis, sampled solution was recovered by centrifuging the tip of the swab inside a reaction tube, whereas in case of Swab TS-MS the swab is directly mounted in front of the MS interface.

**LC–ESI–MS/MS analysis.** High-performance liquid chromatography-tandem mass spectrometry analyses were performed on an UltiMate™ 3000 Basic Automated LC System (Thermo Fisher Scientific, San Jose, CA) coupled to an LTQ instrument (Thermo Fisher Scientific) equipped with a linear ion trap mass analyzer and an electrospray ionization source. The system was controlled by the X-calibur software (Thermo Fisher Scientific). For LC separation, a Kinetex C18 column (100 mm x 2.1 mm, i.d. 2.6 µm) (Phenomenex, CA, USA) was used. Tryptic digests were analyzed using a binary solvent gradient of 0.1% (v/v) formic acid aqueous solution (solvent A) and 0.08% (v/v) formic acid in acetonitrile (solvent B). After column equilibration, samples were injected (20 µL) and eluted at a constant flow of 0.2 mL/min. The optimized gradient started with 2% B for 1 min, then increased to 45% B in 21 min and to 85% B in 2 min, and it was maintained for 2 min. At 28 min the gradient returned to 2% B and equilibrated for 7 min before the next sample injection. The ESI tuning conditions were set as follows: spray voltage, 3.5 kV; sheath gas, auxiliary gas and sweep gas, 50, 20 and 5 arbitrary units, respectively; capillary temperature, 200 °C; capillary voltage, 20 V; tube lens, 100 V. In MS/MS, the mass spectrometer operated in scheduled product ion scan acquisition mode, monitoring the product ions of the unique target peptides reported in **Table 3.1,** where also the extracted transitions for each peptide are detailed**,** with the optimized collision energies. Peptide uniqueness for lysozyme sequence only was verified by BLAST search (blastp algorithm).

**Table 3.1.** Extracted MS/MS transitions, acquisition segment time and normalized collision energies (CE) for the target peptides from lysozyme.

| **Precursor ion sequence; abbreviation (*m/z*; charge state)** | **Segment time (min)** | **CE** | **Product ion sequence (*m/z*; product ion type)** |
|---|---|---|---|
| HGLDNYR; *HGL* (*m/z* 437.7; +2;) | 0 – 12.5 | 25 | GLDNYR (*m/z* 737.5; $y_6^+$) HGLDNYR (*m/z* 428.7; $[M+H]^+ - H_2O$) NYR (*m/z* 452.2; $y_3^+$) |
| FESNFNTQATNR; *FES* (*m/z* 714.8; +2) | | 35 | FESNFNTQATNR (*m/z* 697.3; $[M+2H]^{2+} – H_20 – NH_3$]) SNFNTQATNR (*m/z* 1152.5382; $y_{10}^+$) NTQATNR (*m/z* 804.3959; $y_7^+$) |
| GTDVQAWIR; *GTD* (*m/z* 523.3; +2) | 12.5 – 16.1 | 20 | GTDVQAWIR (*m/z* 514.4; $[M+2H]^{2+}$-$H_2O$) QAWIR (*m/z* 673.3: $y_5^+$) AWIR (*m/z* 545.3 ;$y_4^+$) |
| GYSLGNWVCAAK; *GYS* (*m/z* 663.3; +2) | | 35 | GNWVCAAK (*m/z* 905.4; $y_8^+$) CAAK (*m/z* 449.2177; $y_4^+$) SLGNWVCAAK (*m/z* 553.2766; $y_{10}^{2+}$) |
| NTDGSTDYGILQINSR; *NTD* (*m/z* 877.4; +2) | | 35 | LQINSR (*m/z* 730.4; $y_6^+$) QINSR (*m/z* 617.3365; $y_5^+$) INSR (*m/z* 489.2780; $y_4^+$) |

**Swab Touch Spray–Mass Spectrometry analysis.** Home-made Swab TS-MS set-up used is shown in **Figure 3.1**. The swabs came in a sterile, ready-to-use form, individually packaged in tubes to facilitate transportation and storage. The swab has a plastic cap on the opposite end, serving as a convenient holder, eliminating the need for direct handling.

Initially, Swab TS-MS experiments were conducted by dispensing 30 µL volume of standard solution using a pipette; subsequently, Swab TS-MS analysis were performed from swabs after sampling from contaminated steel surfaces, as described in the paragraph "Surface contamination and *in situ* digestion" above. The swab was then vertically positioned above a 90°-bent modified transfer line to enhance the stability of the swab's electrospray. The distance between the swab and the line was fixed at 8 mm. To apply high voltage to the swab handle, we utilized a custom-made high voltage cable, connected to the instrument's high voltage supply, and secured it with a copper clamp. A separate external syringe pump was employed to continuously deliver ethanol to the swab at 6 µL/min through a silica capillary. The swab tip was wetted by activating the syringe pump, and once the solvent formed a hemisphere at the tip because the gravity, the high voltage was applied to initiate the electrospray event.

Mass spectra were acquired by a Quadrupole-Orbitrap mass spectrometer (Q-Exactive, Thermo Fisher Scientific, San Jose, CA, USA) equipped with an atmospheric pressure interface. High-resolution mass spectra were acquired in positive ion mode in full scan (HRMS) or product ion scan acquisition modes (MS/HRMS), by isolating through the quadrupole the precursor ion, then inducing fragmentation in the HCD cell at the optimized collision energy for each precursor ion. Nitrogen gas (99.95% pure, Air Liquide, Madrid, Spain) was exploited as collision gas. Mass resolution was set at 70,000 FWHM (*m/z* 200). All ions were assigned with mass errors less than 5 ppm. Automatic gain control (AGC) was set at $5*10^6$ for all the experiments. Maximum injection time was set at 200 ms. S-lens radiofrequency and capillary temperature were set at 80% and 250° C, respectively. Xcalibur™ software (Thermo Fisher Scientific, San José, CA, USA) was used for data acquisition and processing. Accurate mass calibration was performed every 72 hours using the calibration solution Pierce™ LTQ Velos ESI Positive Ion Calibration Solution. Before each analysis, a buffer solution that had undergone the digestion procedure was used to record blank spectrum, to be subtracted from the sample spectrum for data analysis.


**Figure 3.1.** Home-made configuration of Swab Touch Spray–Mass Spectrometry source

As for signal acquisition, centered mass (centroid mode) was selected in order to acquire the whole isotopic distribution of peptide precursor ion, with a proper isolation width; collision energies (CE) were optimized for every transition, by direct infusion of digested standard lysozyme solution, selecting the value giving the most intense transition but still permitting detection of precursor ion. Precursor ion of lysozyme target tryptic peptides in MS/HRMS mode are represented in **Table 3.2**, as well as most intense fragment mass and collision energy for each peptide. Uniqueness of selected peptide for lysozyme sequence was verified through BLAST software (blastp algorithm).

**Table 3.2.** Peptide sequence, monoisotopic *m/z* values for precursor and product ions, and normalized collision energies (CE) for MS/HRMS experiments. The first product ion for every peptide is the most intense.

| **Peptide sequence (abbreviation)** | **Precursor ion (*m/z*; charge)** | **CE** | **Product ions (*m/z*; type)** |
|---|---|---|---|
| NLCNIPCSAL LSSDITASVNCAK (*NLC*) | 1254.5982; +2 | 48 | *m/z* 1893.9045; $y_{18}^+$<br>*m/z* 678.3239; $y_6^+$<br>*m/z* 850.4087; $y_8^+$ |
| NTDGSTDYGI LQINSR (*NTD*) | 877.4212; +2 | 34 | *m/z* 730.4206; $y_6^+$<br>*m/z* 617.3365; $y_5^+$<br>*m/z* 489.2780; $y_4^+$ |
| FESNFNTQATNR (*FES*) | 714.8288; +3 | 28 | *m/z* 1152.5382; $y_{10}^+$<br>*m/z* 697.3102; $[M+2H]^{2+}$-$NH_3$-$H_2O$<br>*m/z* 804.3959; $y_7^+$ |
| GYSLGNWVCAAK (*GYS*) | 663.319; +2 | 21 | *m/z* 905.4298; $y_8^+$<br>*m/z* 449.2177; $y_4^+$<br>*m/z* 553.2766; $y_{10}^{2+}$ |

MRFA peptide was investigated as internal standard. MRFA at 20 mg/L concentration was added to ethanol solvent used to wet the swab tip during the analysis. **Table 3.3** describes MS/HRMS product ions of MRFA peptide.

**Table 3.3.** MS/HRMS product ions of MRFA peptide; CE set to 35

| **Precursor ion** | **Product ions (*m/z*; type)** |
|---|---|
| MRFA<br>*m/z* 524.26496<br>$[M+H]^+$ | *m/z* 271.1223; $(b_2\text{-}NH_3)^+$ |
| | *m/z* 288.1489; $(b_2^+)$ |
| | *m/z* 453.2279; $(b_3+H_20)^+$ |

**Bioinformatic processing** Mass spectrometric isotopic distribution of peptides and their fragments were obtained by MMass Mass Spectrometry tool software, loading FASTA sequence of Lysozyme from chicken egg white. Since digestion protocol involved the use of IAA as alkylating agent, a carbamidomethylation was considered as fixed modification on every cysteine residue, as well as methionine oxidation as variable modification.

**Analytical quality parameters of Swab TS-MS method.** For signal-to-noise ratio (S/N) calculation, the noise was determined based on the background signal intensity over a region close to the area in which the diagnostic ions of the analyte appear. LODs were estimated considering in the averaged mass spectrum a signal of the analyte three times higher than the background noise.
Precision of the method is described by intra- and inter- swab coefficient variation percentages (CV %) at two concentration levels (1000 and 28.5 μg/L). Intra-swab precision was calculated as the CV% of signals acquired at different times of analysis within 5 minutes, from the same swab. Inter-swab precision was calculated as the CV% of signals acquired by different swabs loaded with the same sample, on different days.
Calibration curves were established by spiking on tip's swab digested solution of standard lysozyme (30 μL) at concentrations of 5, 28.5, 50, 100, 500, 1000 mg/L.

**Paper spray–Mass Spectrometry (PS–MS) analysis.** Custom PS set-up used is shown in **Figure 3.2.** A triangular piece of paper, measuring 10 mm in height and 8 mm in base width, was held with a copper clip, aligning the apex with the mass spectrometer inlet at a distance of 4 ± 1 mm. Whatman® qualitative filter paper Grade 1 (Whatman plc, Maidstone, Kent, United Kingdom) and Nylon Filter membranes 0.45 and 0.22 μm pore size (Merck KGaA, Darmstadt, Germany) were investigated. For every analysis, 10 μL of sample was loaded onto the paper and let it dry for 2 min. After addition of 50 μL of extracting solvent onto the back of the paper, the high voltage was applied through the copper clip, that was connected to the copper clamp of a high voltage cable connected to MS instrument, generating the spray from the sharp corner of the paper.
Mass spectra were acquired by a Finnigan LTQ (Thermo Electron Corporation, San Jose, CA, USA) equipped with an atmospheric pressure interface. The spectra were acquired in Full scan acquisition mode (positive polarity) for the detection of entire lysozyme and digested lysozyme. Spray voltage was 3.5 kV, capillary temperature, 200° C, tube lens voltage, 100 V, capillary voltage, 20 V.

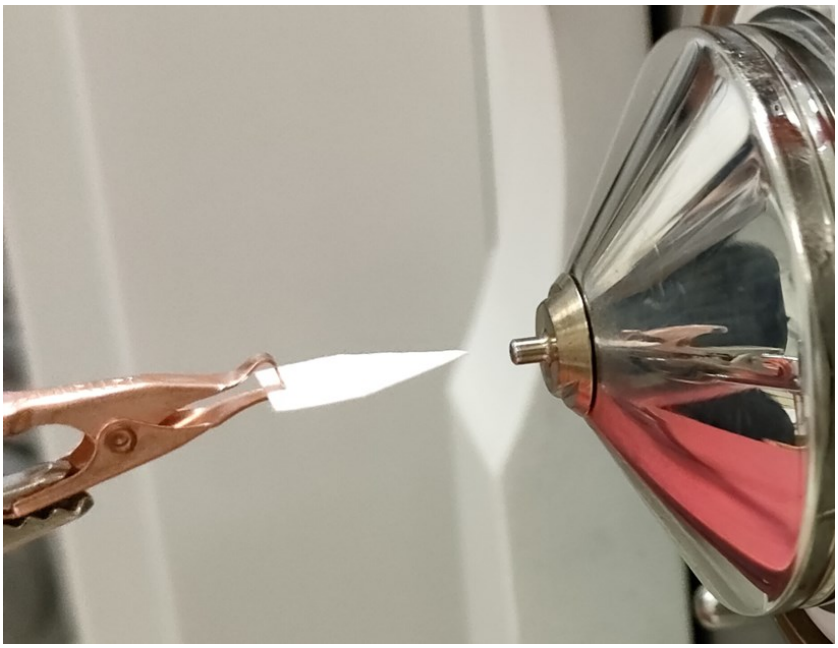

**Figure 3.2.** Snapshot on Paper Spray–Mass Spectrometry source

## 3.4. Investigation of Swab Touch Spray–Mass Spectrometry potentialities and development of the method

At first, the suitability of Swab TS–MS for the detection of proteins and peptides was investigated by analyzing the intact and digested lysozyme, respectively. These experiments represent the starting points for the subsequent development of a Swab TS-MS method for the detection of lysozyme residues on contaminated food preparation surfaces or kitchen utensils.

The Swab TS-MS analysis of intact lysozyme led to unsatisfactory results, probably due to difficulties in the desorption process ascribable to high affinity of soluble proteins with polar rayon cellulose covering the tip of the swab, or steric hindrance issues. Then, the suitability of the Swab TS-MS was verified for a mixture of peptides derived from tryptic digestion of lysozyme; in this case, satisfactory results were obtained, leading to the detection of the main unique lysozyme peptides, as showed in **Figure 3.3**.

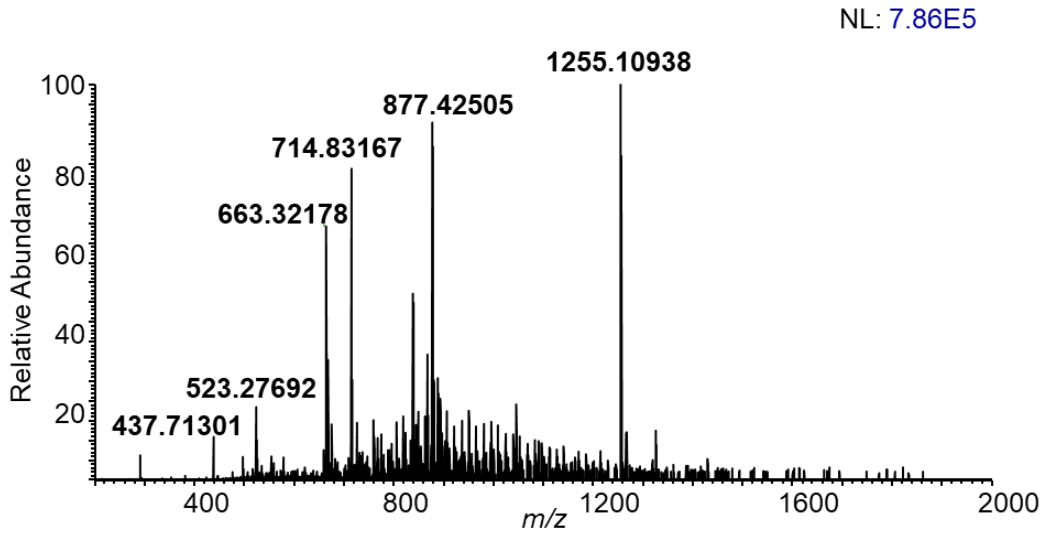


**Figure 3.3.** Swab TS-MS full scan spectrum of 500 mg/L digested lysozyme, acquired by Q-Orbitrap mass analyzer (Full scan mode)

### 3.4.1. Peptide selection

Peptides from tryptic digestion of lysozyme were selected according to the intensity of their signal. Product ions were selected in MS/HRMS mode for every peptide, as well as optimal collision energies, by direct infusion of digested lysozyme solutions.

**Figure 3.4** shows the MS/HRMS extracted ion chronograms for the peptides *NLC* (*m/z* 1255.1 → 1893.9045), *NTD* (*m/z* 877.4 → 730.4206) and *FES* (*m/z* 714.8 → 1152.5382), acquired consecutively within the same analysis. In the first part of the chronogram a blank sample was analyzed; this corresponds to an ammonium bicarbonate buffer that overtook digestion procedure (in absence of the protein). After blank sample acquisition, the swab containing the digested lysozyme was mounted. For subsequent data analyses, the mass spectrum of the blank was subtracted from that of the sample, in order to remove the contributions from rayon of the tip and reagents of digestion. The present procedure was repeated for all the analyses performed.

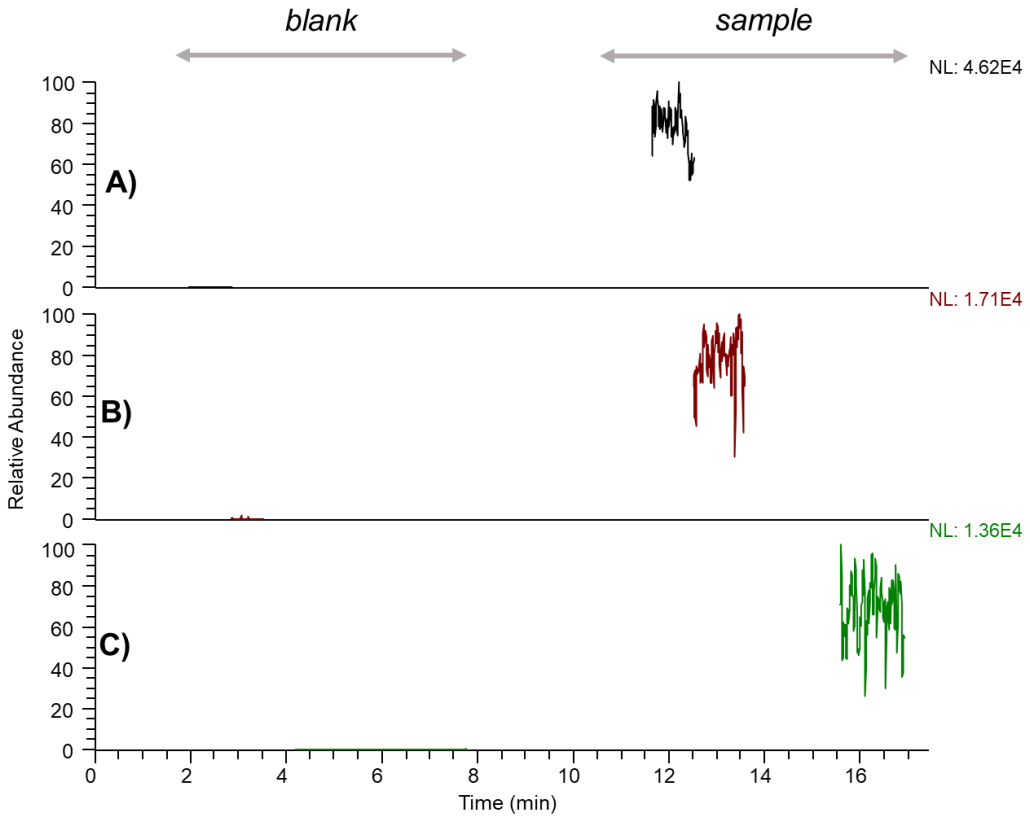


**Figure 3.4**. MS/HRMS extracted ion chronogram of blank and digested lysozyme. **A)** peptide *NLC*, *m/z* 1255.1 → 1893.9045; **B)** peptide *NTD*, *m/z* 877.4 → 730.4206 **C)** peptide *FES* 714.8 → 1152.5382. Mass accuracy ≤ 5 ppm.

### 3.4.2. Experimental conditions for Swab Touch Spray-Mass Spectrometry analysis

Geometrical parameters, swab orientation and solvent composition affect signal quality, especially in terms of absolute intensity and stability. It is important to point out that material constituting the body of the swab is fundamental to establish electrical connection with a high-potential source and generate a potential difference respect to the MS inlet. The coating material of the swab tip needed to be sufficiently polar to facilitate current conduction and promote the formation of electrospray at the tip's end. Consequently, swabs with an aluminum body and a cellulose rayon tip were employed, taking also advantage of rayon's ability to absorb significant sample volumes.

First, it was necessary to determine the optimal distance between swab tip and the MS transfer inlet. As mentioned earlier, Swab TS-MS requires a modified transfer line, with a L shape to adapt to the vertical position of the swab and to facilitate the formation of Taylor cone, thus properly oriented towards the MS to improve sampling efficiency. The distance between the transfer line and the swab tip plays a crucial role in the ionization process: a small distance may result in excessively high electric force, potentially causing ionization but also leading to electric discharges. Conversely, if the distance is too high, the electric force becomes too weak, leading to ionization failure. An empirically determined distance of 8 mm between the swab tip and the transfer inlet was selected to ensure a stable spray while preventing electric discharge. This value is in accordance with the distance used in the majority of the studies dealing with Swab TS-MS technique [23].

The solvent used for the analysis, also named extracting solvent, since it is fundamental for extraction of analytes from swab's tip material, is continuously supplied to wet the swab's tip, representing another critical parameter. In contrast to PS-MS, where a sharp corner facilitates Taylor's cone formation, in Swab TS-MS, a solvent hemisphere wets the swab's tip, instead of a corner. A typical emitter radius for ESI is on the order of micrometers, while cone radius of swab is millimeters. This aspect makes the formation of the Taylor cone in Swab TS-MS more challenging, particularly with solvents having high surface tension. The greater the surface tension, the more challenging it becomes to exceed the Rayleigh limit to induce ESI-like ionization. The selected solvent or solvent mixture must be enough polar to induce ionization. In the case of water, its use as pure solvent was early discarded due to its extremely high surface tension ($72.86 \pm 0.05$ $mNm^{-1}$ at 20°C [24]); nevertheless, various solvent mixtures of methanol (MeOH) and ethanol (EtOH) with water and with formic acid were tested. Acetonitrile is another solvent commonly employed in reversed-phase chromatographic separation and peptide separation methods. However, its surface tension, (29.25 $mNm^{-1}$), is slightly higher than that of EtOH and MeOH (22.39 and 22.50 $mNm^{-1}$ at 20°C, respectively [25]), hence was not investigated.

Each solvent or mixture has a unique surface tension, conductivity and volatility: these properties influence the spray voltage required to enable ionization, and flow rate value, that brings solvent to swab's tip to keep it wet. Conductivity of the mixture is crucial because it can influence ionization, but also cause electric discharges if it is too high. For this reason, a proper compromise between spray voltage and ion current has to be found. In fact, the greater is surface tension, the higher will be the spray voltage to apply to start ionization; when this happens, the conductivity and the ionic strength of the solvent influence the ion current, which must not exceed 2 μA because of the risk of electric discharges and tip overheating. In addition, since ionization process involves heat dissipation, the volatility of the extracting solvent influences the wetness of swab's tip, so that it has an effect on the signal as well.

For all the reasons discussed, MeOH and EtOH were selected to empirically assess spray voltage and solvent flow rate necessary to guarantee a stable and constant cone-jet electrospray plume. Mixtures of MeOH and EtOH with $H_2O$ (70:30 v/v) were also taken into consideration, due to its polarity (**Table 3.4**). Stability of electrospray cone-jet was visually assessed, using a camera to constantly follow variations in electrospray.

**Table 3.4.** Flow rate and spray voltage used for different solvents in Swab TS-MS experiments.

| **Solvent** | **Flow rate** | **Spray voltage** |
|---|---|---|
| MeOH: $H_2O$ 70:30 (v/v) | 3 μL/min | 5.7 kV |
| MeOH | 6 μL/min | 5.5 kV |
| EtOH: $H_2O$ 70:30 (v/v) | 4 μL/min | 6.2 kV |
| EtOH | 6 μL/min | 5.5 kV |

As can be seen from **Table 3.4**, pure solvents of MeOH and EtOH behave in the same way, in terms of minimal spray voltage to induce electrospray ionization, and solvent flow rate. Mixtures of MeOH and EtOH with $H_2O$ required a slightly higher potential to induce electrospray, and also resulted in a less stable cone formation. More importantly, presence of water frequently led to electric discharges and unstable electrospray. For these reasons, mixtures of MeOH and EtOH with water were no further investigated.

Hence, the following solvents were selected to assess which gives better extraction and ionization, resulting in higher signal of the peptides:

- MeOH
- EtOH
- MeOH + 0.1 % FA (v/v)
- EtOH + 0.1 % FA (v/v)

The addition of FA to the solvent was explored as it could favor protonation in positive ion mode. Results are represented in the following bar chart, which shows the extracted MS/HRMS peptide – fragment transitions for three selected peptides giving the highest signals (**Figure 3.5**).

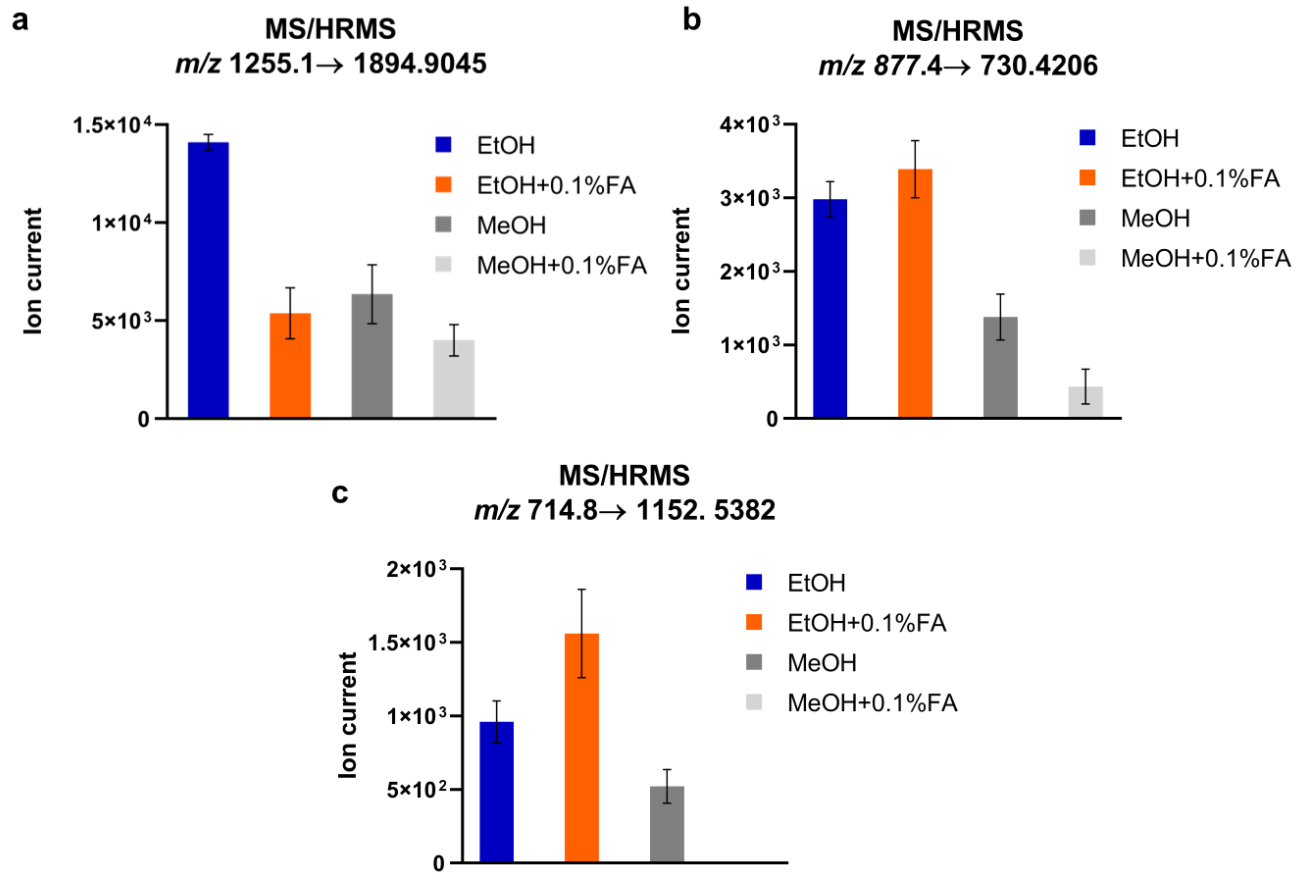


**Figure 3.5.** Bar charts reporting the extracted signal for the best peptide–fragment transition using different solvent mixtures. MS/HRMS signal from **a)** peptide *NLC*, *m/z* 1255.1 → 1893.9045; **b)** peptide *NTD*, *m/z* 877.4 → 730.4206; **c)** peptide *FES* 714.8 → 1152.5382

The obtained results permitted to select EtOH as solvent since it generally exhibited better extraction and ionization efficiency respect to MeOH. Adding of 0.1% FA to EtOH results in a slightly higher signal for *NTD* and *FES* peptides, with the notable difference for *NLC* peptide, for which the addition of FA resulted in a lower signal. For this reason, EtOH as pure solvent was selected as extracting solvent of the method.

As reported in Materials and Methods, digestion procedure usually involves quenching of trypsin digestion by the addition of formic acid to the protein solution. After selecting EtOH as extracting solvent of the method, the additions of FA to the analyzed peptide solution were investigated. In particular, we considered additions of 0.5% and 1% (v/v) of FA, that were compared with the results previously obtained without the addition of FA (**Figure 3.6**).

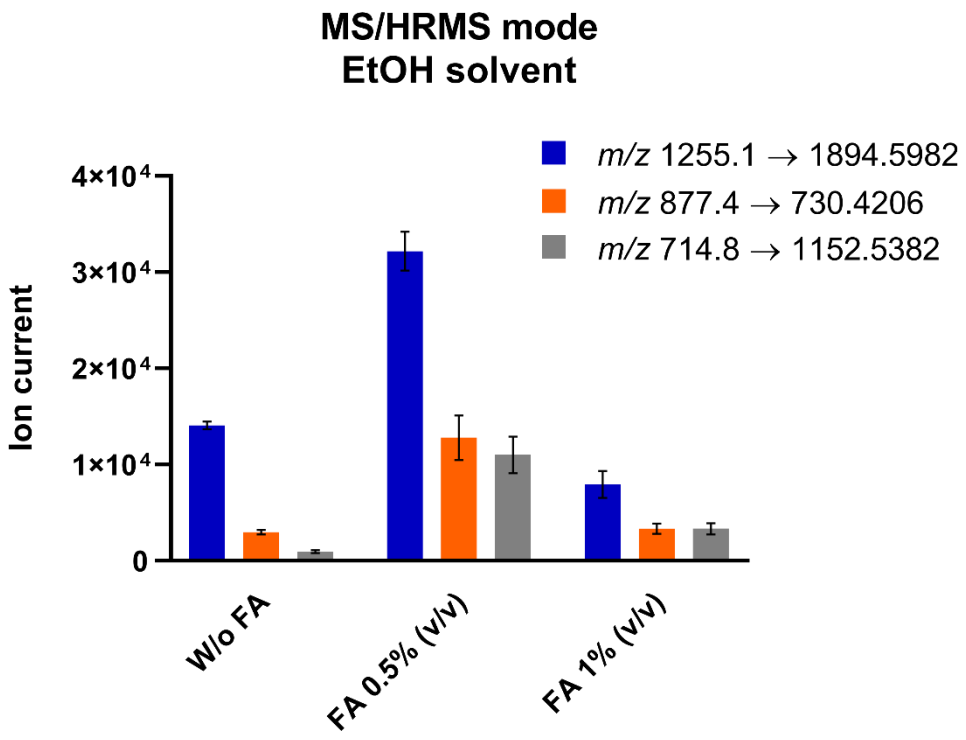


**Figure 3.6.** Swab TS-MS signal comparison for *NLC*, *NTD* and *FES* peptides in MS/HRMS mode obtained with the addition of 0.5%, 1% (v/v) or no Formic Acid (w/o) to digested solutions

As can be seen in **Figure 3.6**, adding 0.5% FA resulted in a better signal enhancement than 1% (v/v) for all the peptides of lysozyme taken into consideration.

For all these reasons, EtOH was selected for further analyses, as well as the addition of 0.5% FA to the sample. This choice is intended to obtain the best possible results, but still makes even more green the developed method. In fact, the present method uses a solvent flow rate of 6 µL/min, that is

extremely less expensive than a typical flow rate exploited for a conventional hyphenated method, where hundreds of µL are consumed per minute.

Signal duration over the time was also evaluated, showing good signal and detectability for at least 5 minutes, as shown in **Figure 3.7** for the *NTD* peptide, *m/z* 1255.1 → 1894.9045 transition.

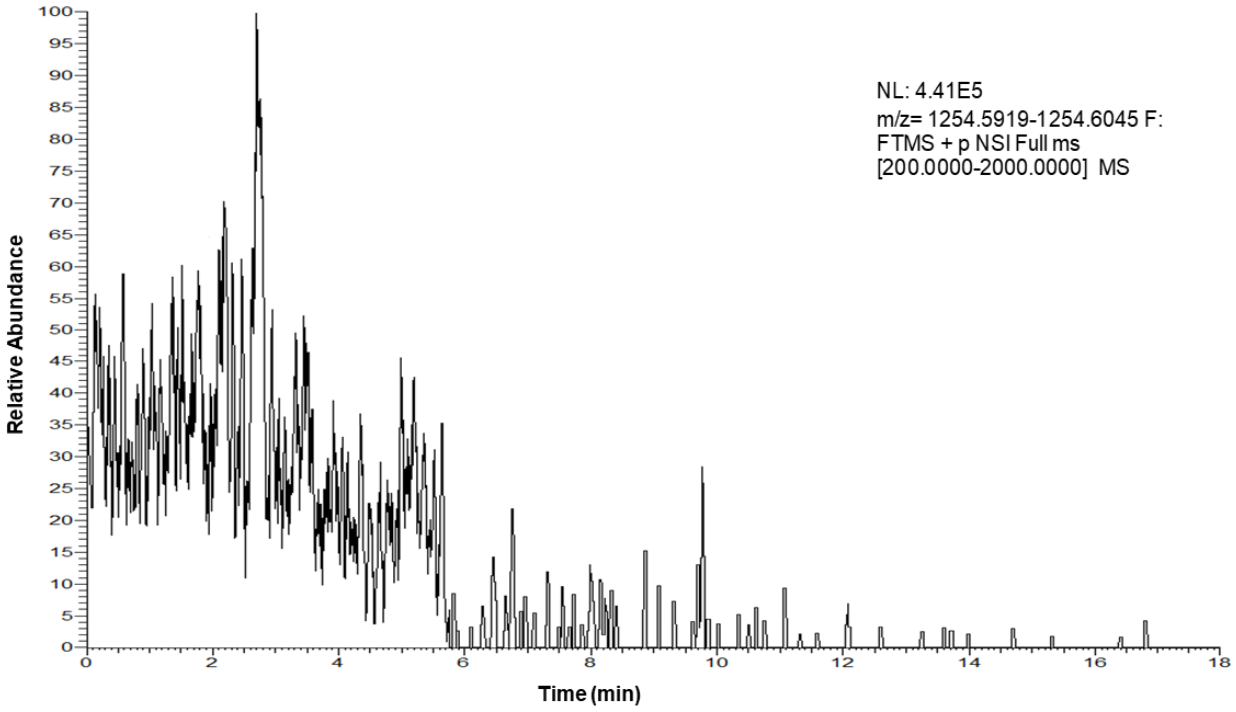


**Figure 3.7.** Chronogram showing the extracted MS/HRMS signal for the peptide *NLC*, *m/z* 1255.1 → 1893.9045, from the analysis of digested standard lysozyme (100 µg/L)

### 3.4.3. Analytical quality parameters on lysozyme standard

Precision of the method was assessed by intra- and inter-swab CV%. The intra-swab CV% was calculated <5% (n=3), whereas inter-swab CV% was <19% (n=3), indicating a very good precision of the method, taking into account the nature of AMS techniques and the qualitative purpose of the method.

Peptides *NLC* and *NTD* were selected for the method validation thanks to the stability and intensity of their signal. LODs for the two peptides were calculated in both HRMS and MS/HRMS acquisition modes, obtaining values at low mg/L levels of concentration, being MS/HRMS the mode giving the best values (**Table 3.5**).

**Table 3.5.** LODs values for *NLC* and *NTD* peptides referred to the concentration of digested lysozyme in ammonium bicarbonate buffer loaded on the swab.

| **Peptide** | **Acquisition mode** | **Target *m/z* or MS/HRMS transition** | **LOD (mg/L)** |
|---|---|---|---|
| *NLC* | HRMS mode | 1254.5982 | 3.4 |
| | MS/HRMS mode | 1255.1 → 1893.9045 | 1.2 |
| *NTD* | HRMS mode | 877.4212 | 7.8 |
| | MS/HRMS mode | 877.4 → 730.4206 | 3.1 |

Taking into consideration the volume of digested lysozyme loaded on the swab (30 µL), LODs can be expressed as absolute amount of digested lysozyme on the swab. In particular, LOD corresponds to 51 ng of digested Lys solution for *NTD* peptide, and 93 ng for *NLC* peptide loaded on the swab. Even if the purpose of the analysis was qualitative, for both peptides it was investigated the dynamicity of the response in MS/HRMS mode over a predefined concentration range, as reported in **Figure 3.8**.

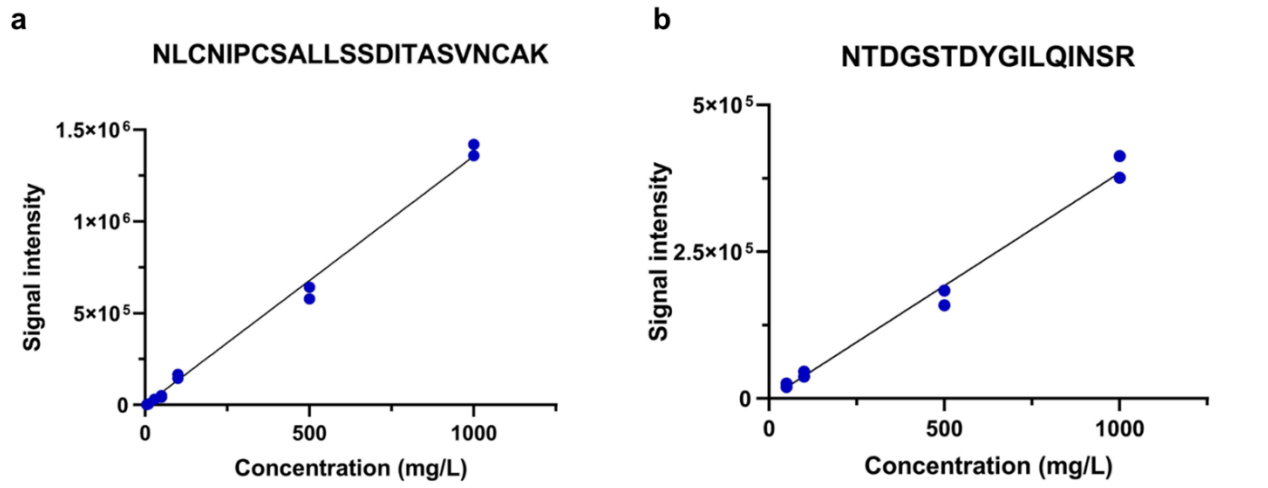


**Figure 3.8.** Calibration curves for digested standard lysozyme. **a)** peptide *NLC*, concentration 5,10, 28.5, 100, 500 and 1000 mg/L; equation y=1357(±23)x; $R^2$=0.9963. **b)** peptide *NTD*, concentration 28.5, 100, 500, 1000 mg/L; Equation 384(±11)x; $R^2$= 0.9943. In both cases, the intercept resulted not significant (*t* test, $p>0.05$)

### 3.4.4. Swab Touch Spray-Mass Spectrometry performance - egg white powder

A further step of the study was the application of the developed Swab TS-MS method to egg white powder. In particular, egg white powder was digested following the same procedure as for standard lysozyme, and then loaded on the swab tip. In **Figure 3.9** are shown portions of the MS/HRMS mass spectrum evidencing the isotopic pattern, in which the relative abundances are in accordance with the theoretical ones; the mass accuracy is always lower than 5 ppm and 1 ppm for *NLC* and *NTD* peptides, respectively (error referred to monoisotopic ion).

In order to assess the different response of lysozyme in the buffer and in the matrix, digested solutions of lysozyme (100 mg/L) in ammonium bicarbonate and egg white were analyzed. In particular, in the case of egg white, calculations were made considering the endogenous quantity of lysozyme. A signal 10 times lower was obtained in matrix respect to standard solution. This result can be ascribable to different factors: (i) signal suppression due to the ESI-matrix effect, (ii) decrease in digestion efficiency of lysozyme in the matrix compared to the buffer (iii) possible interactions of the native lysozyme with other matrix components.

LOD was reported at 1.2 µg digested lysozyme in egg powder referring to the peptide *NLC*, that has the best response.

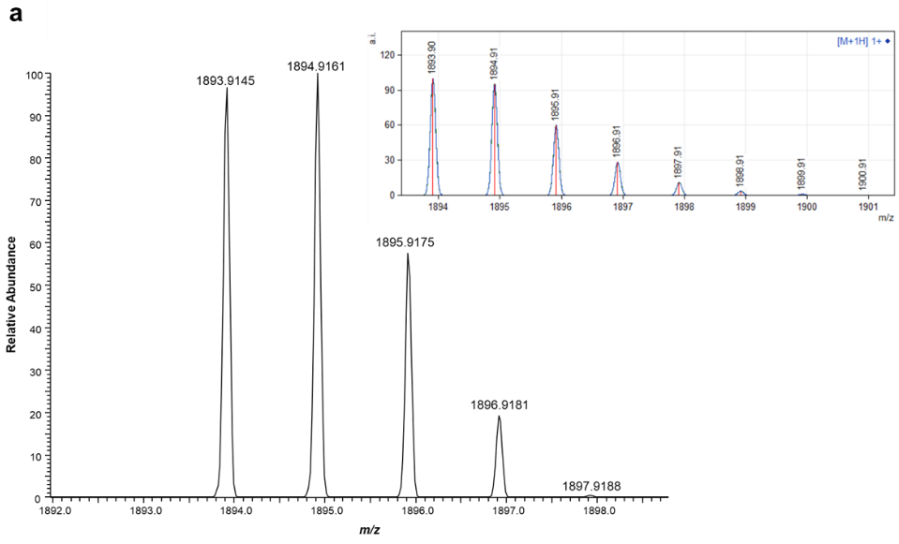

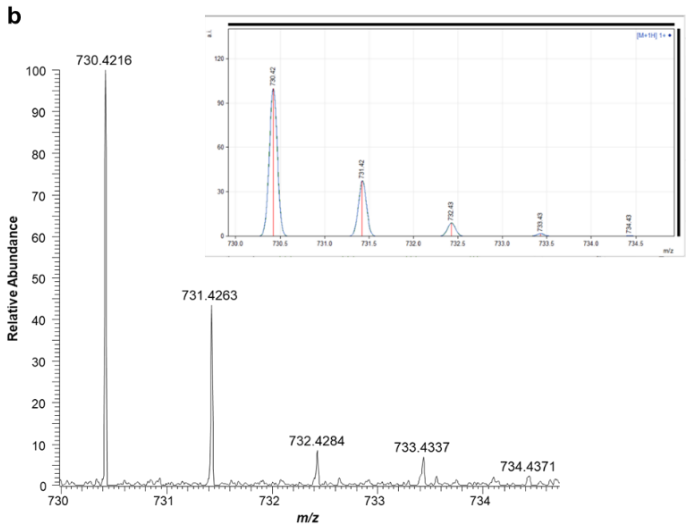


**Figure 3.9.** Swab TS-MS analysis of 36800 mg/L of egg white powder, corresponding to 1000 mg/L of lysozyme, MS/HRMS acquisition mode. Mass spectra evidencing the isotopic pattern of the most intense product ion for **a)** *NLC* peptide, mass accuracy < 5ppm; **b)** *NTD*, mass accuracy < 1ppm. Simulated isotopic distribution from MMass software for the peptide fragment is reported top right

### 3.4.5. Internal standard for Swab Touch Spray–Mass Spectrometry analysis

The precision of the method was satisfactory, especially for a qualitative application. Anyway, taking into account the novelty of the approach, it was investigated the possibility to use an internal standard (IS) to be added to the extracting solvent. Preliminary experiments were carried out with the MRFA peptide (**Figure 3.10**), frequently used for ESI-MS calibration.

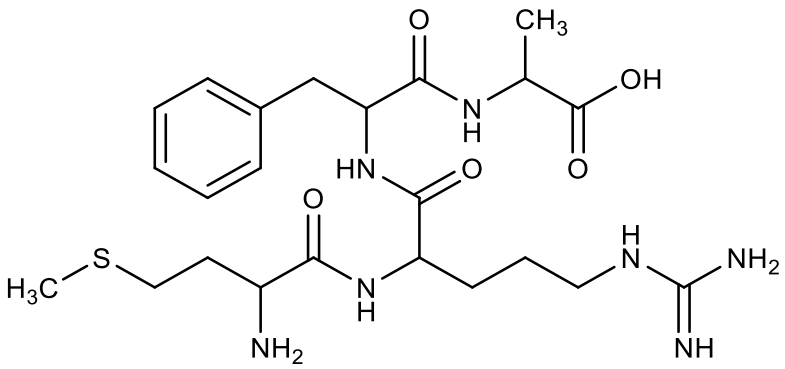

**Figure 3.10.** MRFA peptide structure

MRFA was introduced into the extracting solvent, yielding a good signal response even at low concentrations (20 µg/L). A mass spectrum of MRFA peptide is reported in **Figure 3.11**. The signal correction has not significantly improved the precision of the method, and in some cases resulted worse; this was probably due to the manual switching from a MS/HRMS event to another, not permitting simultaneous acquisition of the signals for both the analyte and IS. Consequently, utilization of MRFA as IS could be considered, starting from standardized conditions and taking advantage of an automated multiplexing acquisition mode. The latter would enable extremely rapid alternate MS/HRMS acquisition of the analyte and IS.

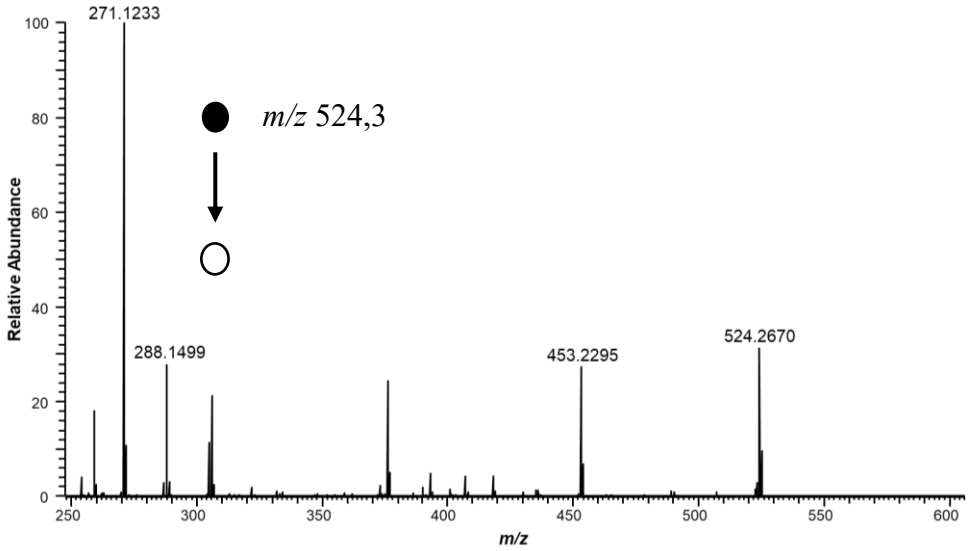


**Figure 3.11:** Swab TS-MS/HRMS product ion scan mass spectrum of MRFA peptide, positive acquisition mode. Mass error < 5 ppm

### 3.4.6. Preliminary results about Paper Spray–Mass Spectrometry analysis of lysozyme

PS–MS represents one of the most exploited AMS techniques in literature and a possible alternative to Swab TS–MS for performing a simple and rapid analysis. As reported in Introduction section, the detection of protein and peptides through PS–MS has been reported in literature, albeit in a limited number of publications [26–29]. For this reason, some preliminary experiments were carried out using this technique to analyze lysozyme as intact protein and after tryptic digestion.

Since the present study is intended to investigate surface contamination by allergenic ingredients, the exploitation of PS–MS would not be as straightforward as Swab TS–MS, but it would need the collection of sample from swab after surface swabbing, then the sample can be loaded on the paper substrate. The two mentioned techniques are similar in their simple design, but PS–MS involves an easier formation of the electrospray thanks to the sharp corner of the paper that allows generating a

more intense electric field, thus making easier the electrospray ionization from solvents with high surface tension. In addition, a lower value of potential is required, compared to that used in Swab TS–MS. Solvent represents another crucial parameter for the analysis, as it acts extracting/desorbing the analyte from the paper and eliciting the ionization. Mixtures of MeOH and ACN with $H_20$ (70:30 v/v) were investigated, since these solvents are commonly used for chromatographic separation of peptide mixtures. The addition of water to the mixture is aimed at improving ionization and reducing volatility of extracting solvent.

Two distinct substrates, chromatographic paper grade I and Nylon filter paper (pore size 0.45 and 0.22 µm, respectively), were investigated.

In contrast to Swab TS-MS, PS-MS permitted to detect non only the peptides, but also the intact lysozyme, as shown in **Figure 3.12**. Both MeOH:$H_2O$ 70:30 v/v and ACN:$H_2O$ 70:30 v/v mixtures, with chromatographic paper grade I, resulted suitable for lysozyme detection. Detection was not possible using Nylon filter paper as a substrate; in addition, this material exhibited low absorbency, causing the substrate to bend downward, causing difficulties in the electrospray formation.

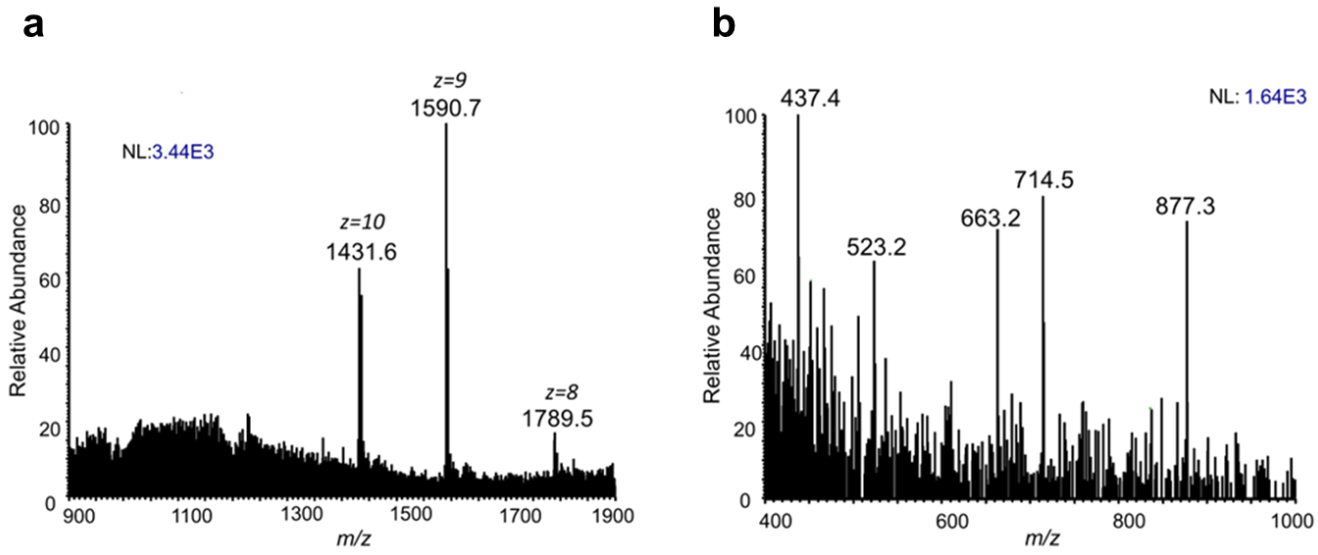


**Figure 3.12.** Full scan Paper Spray–MS spectra of **a**) multi-charge distribution of intact lysozyme; **b**) peptide mixture from tryptic digestion of lysozyme. Experimental conditions: chromatographic paper grade I, Solvent: MeOH:$H_2O$ 70:30 (v/v)

The possibility of protein detection by PS–MS is confirmed, as for entire protein and tryptic peptides, representing a feasible alternative to Swab TS–MS technique for investigation of allergen-contaminated surfaces. Steps required for the analysis of peptides or entire proteins from contaminated surfaces by PS–MS are represented in **Figure 3.13**. In particular, detection of peptides

would require performing a *swabbing/swab digestion* procedure, and then loading digested solution onto the substrate for PS-MS analysis (*swabbing/swab digestion* strategies is applicable also for Swab TS-MS analysis, and will be discussed later). On the other hand, detection of the intact protein would permit to skip the digestion procedure, however PS-MS requires to recover the analyte/analytes from the swab prior analysis by centrifugation.

Performances of the technique for detection of both types of analyte (peptides and entire protein) should be evaluated in the next future, after a proper optimization of experimental conditions, among which the type of paper substrates. In this regard, pore size of the exploited paper may represent a key point for analyte transport up to the tip of the substrate.

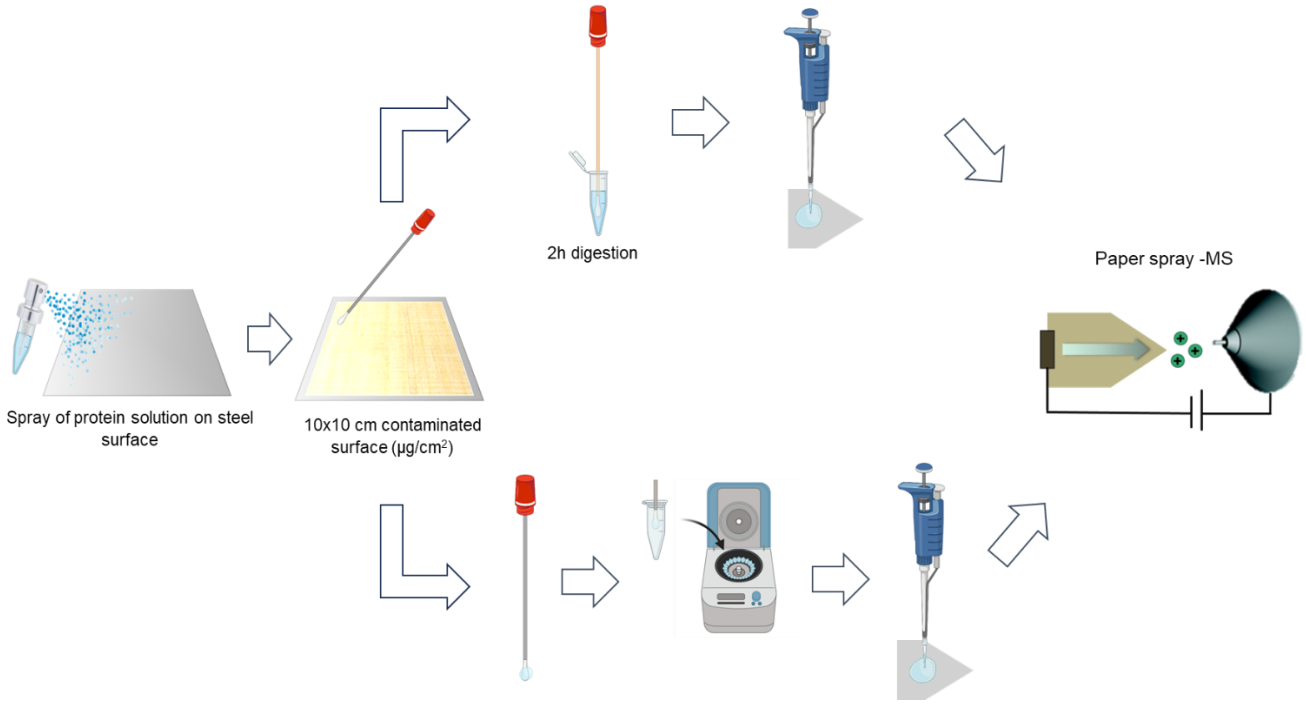


**Figure 3.13.** Graphical representation of possible ways to analyze proteins from surface swabbing by PS-MS

## 3.5. Development of swabbing strategies compatible with Swab Touch Spray-Mass Spectrometry method

It is worth to mention that the present is the first study aimed at analyzing residues of allergenic proteins from food preparation surfaces by an AMS technique, and in particular exploiting Swab TS-MS. Thus, after the development of a Swab TS-MS method for the detection of digested lysozyme, it was necessary to investigate possible swabbing strategies from surfaces contaminated with allergenic proteins, in order to directly couple the swab sampling with the MS-based analysis. Of course, it would have been more straightforward if the target for Swab TS-MS was the intact protein, because after sampling the swab could have been directly mounted for the analysis. Since the targets were lysozyme tryptic peptides, two possible approaches can be proposed.

The first (*swabbing/swab digestion*) is the swabbing of the contaminated surface, followed by the immersion of the swab in a reaction tube where reduction, alkylation and digestion are carried out; then, the digested samples can be loaded on a new swab for Swab TS-MS analysis.

Another approach (*in-situ digestion/swabbing*) involves the development of an on-surface (*in situ*) digestion of proteins in order to directly sample peptides by swabbing and immediately analyze them using Swab TS-MS. Of course, this second strategy better embraces the philosophy of AMS, and in particular of Swab TS-MS.

The investigation of the swabbing strategies was carried out using a conventional LC-ESI-MS/MS technique, which permitted to evaluate the feasibility of the approaches.

For this purpose, a bottom-up LC-ESI-MS/MS method was developed for the analysis of digested lysozyme. Identification of peptides from lysozyme was made by Data Dependent Acquisition (DDA) analysis of digested solutions of standard protein. Acquired data were analyzed by Bioworks software 3.3 (SEQUEST algorithm) to identify peptide sequences giving most intense signal. After verification of the uniqueness of these peptides respect to lysozyme sequence through BLAST software, chromatographic separation was devised, and the CID collision energy was optimized for each peptide. In particular, the MS/MS events were scheduled on the basis of the retention times. For the three most intense peptides, limits of detection were obtained in the 0.1-0.3 mg/L range.

### 3.5.1. Digestion from swab

In order to evaluate the feasibility of the *swabbing/swab digestion* approach, a preliminary comparison was made between the signals obtained with the conventional tryptic digestion of a lysozyme solution at a certain concentration (*in-solution digestion*) and the signals obtained when the same lysozyme solution was previously absorbed by the swab and then the swab immersed in DTT, IAA and trypsin solution into a reaction tube (*swab digestion*). To do this, we firstly evaluated the loading volume of the swab, in order to assess the maximum volume that the swab was able to absorb, resulting 30 µL. On the basis of this value, it was possible to proceed with proper dilutions in order to inject into the LC-MS/MS system the same (presumed) concentration of digested lysozyme. Signal comparison is reported in **Figure 3.14**, and it is possible to observe that no significant differences (n=3, t-test, $p>0.05$) in terms of MS/MS signal intensity of lysozyme tryptic peptides were observed (**Figure 3.14b**), indicating an effective recovery of the lysozyme from the swab.

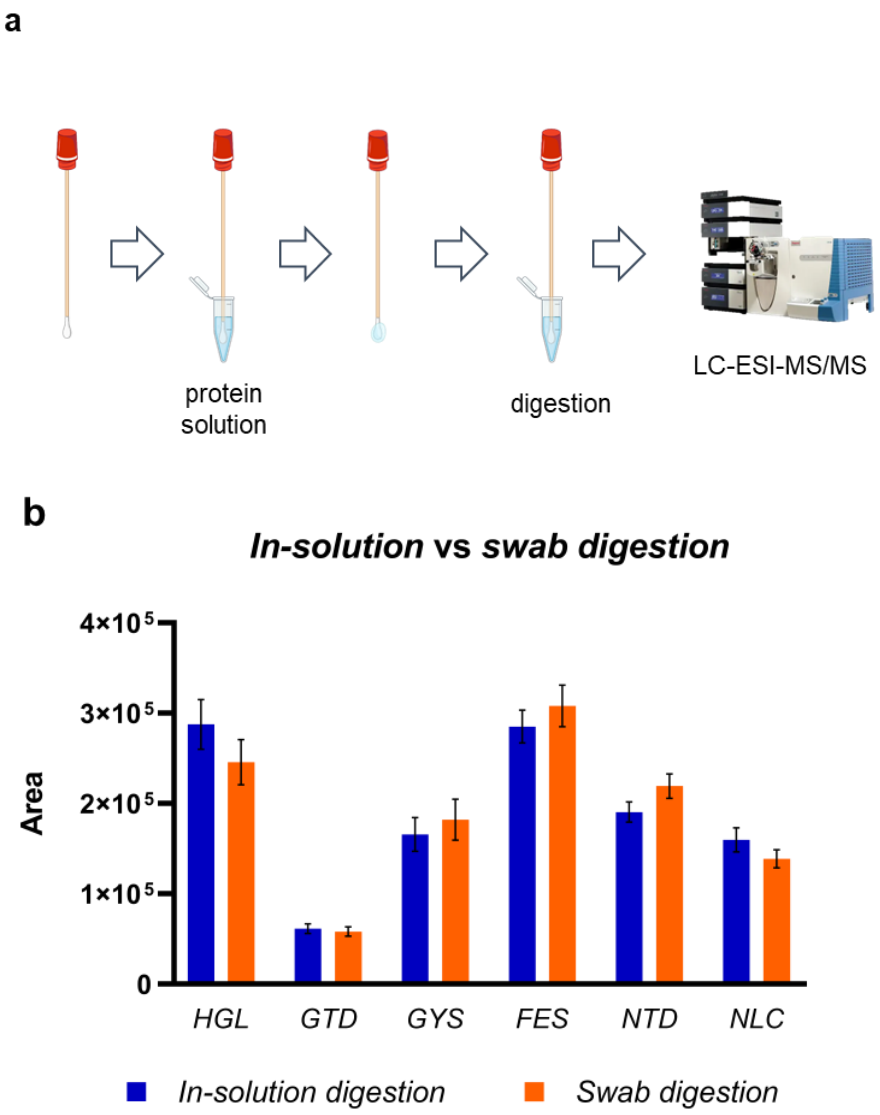


**Figure 3.14. a)** Graphical representation of swab digestion procedure; **b)** Comparison of LC-ESI-MS/MS areas for lysozyme tryptic peptides obtained from standard *in-solution digestion* (blue) and *swab digestion* (orange) protocols; standard lysozyme concentration 8 mg/L

An important requirement that swabbing methods must meet, as well as AMS techniques, is to minimize sample handling as much as possible, with respect to conventional methods. Since conventional digestion protocol is conducted overnight, for this application we investigated the possibility to reduce the digestion time to 2h in order to achieve shorter sample handling. The percentage decrease of peptide signals was in the range 5-25%, thus largely acceptable in the face of a significant reduction of digestion time (overnight vs 2h).

This finding was confirmed also in egg white powder matrix: the obtained results permitted to set 2 hours as time required by tryptic digestion for subsequent analyses.

### 3.5.2. *Swabbing/swab digestion*

After assuming 2 hours as default time for incubation with trypsin, *swabbing/swab digestion* was carried out, following the procedure as explained in the experimental section and schematized in **Figure 3.15**. A stainless steel 10x10 cm surface was sprayed with 500 µL of standard solution of lysozyme (100 mg/L) and then immediately sampled by swab. The lysozyme on the swab was submitted to digestion procedure and peptides were analyzed by LC-ESI–MS/MS.

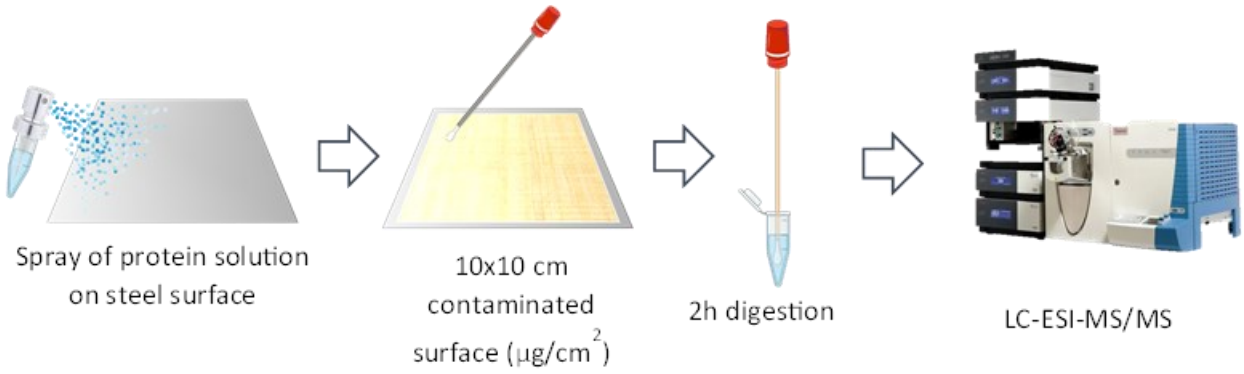


**Figure 3.15.** Graphical representation of *swabbing/swab digestion* procedure, involving swab sampling and swab digestion

In order to assess the amount of lysozyme sampled by the swab, a calibration curve was constructed by injection of lysozyme digested in solution at different concentrations in the 1.4 - 20 mg/L range. This permitted to assess that swab sampled 3.7 (± 0.9) µg of lysozyme (n=3). These quantities approximately correspond to one tenth of the quantity sprayed on surface, thus permitting to understand the efficiency of swab in protein sampling from a contaminated surface.

### 3.5.3. Development of *in situ digestion/swabbing* procedure

In view of implementation of Swab TS-MS analysis upon sampling peptides directly from the surface, it was investigated the feasibility of a protocol that performed digestion of proteins directly on surface. For this reason, focus was directed to the development of a *in situ digestion*/*swabbing* procedure, which implies surface contamination, *in situ* digestion (by sequential addition of sprayed DTT-IAA-trypsin reagents), and swab sampling. This strategy has taken inspiration from the study of Calvano et al.[31], where an approach based on *in situ* digestion was developed for the detection of proteinaceous binders of paint layer, performing a bottom-up proteomic approach and MALDI-TOF-MS analysis.

The graphical representation of the protocol is shown in **Figure 3.16**. After swab sampling, the sample present on the swab's tip is recovered by centrifugation prior the LC-ESI-MS/MS analysis, that is not required for the more straightforward Swab TS-MS analysis (**Figure 3.16**).

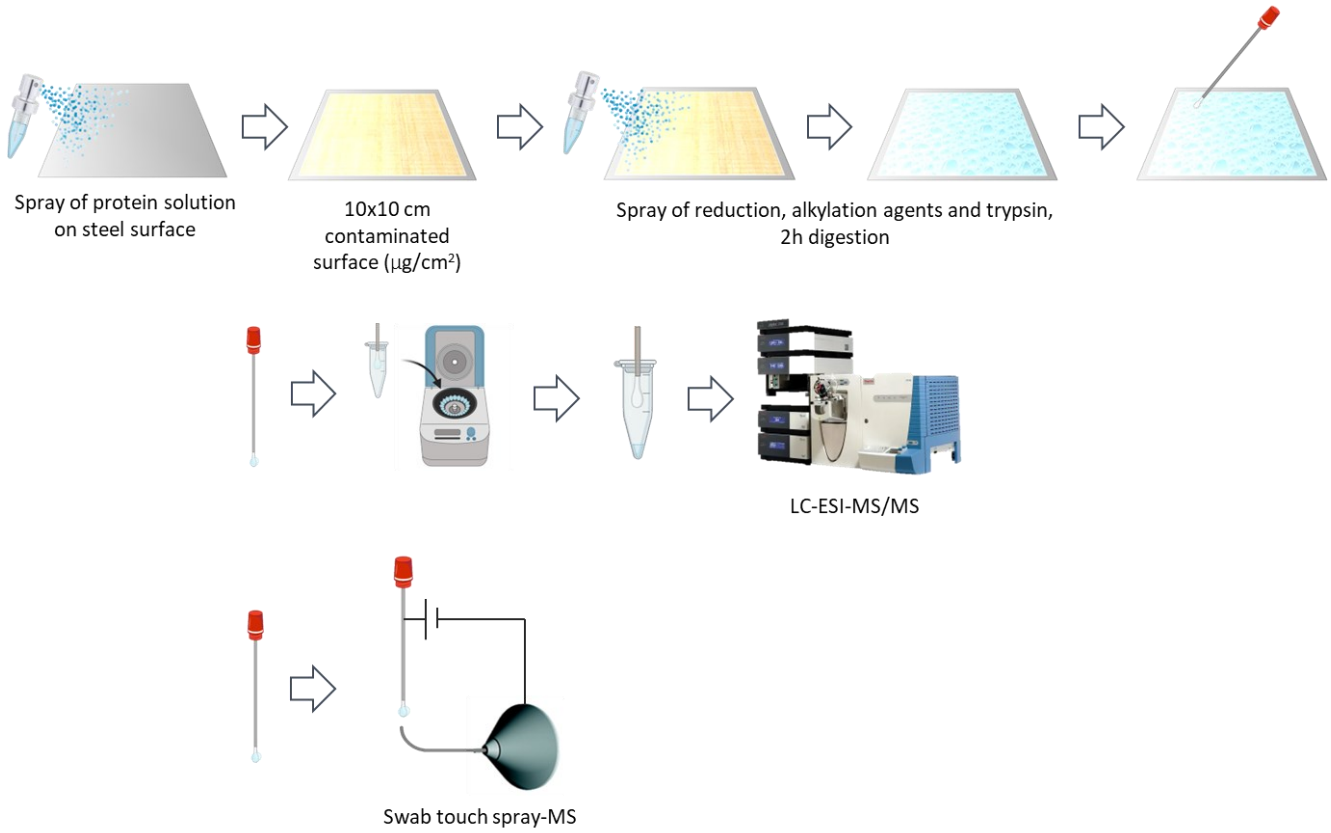


**Figure 3.16.** Graphical representation of *in situ digestion/swabbing* protocol, followed by two possible types of analysis (LC-ESI-MS/MS and Swab TS-MS). After spraying a protein-containing solution onto a surface, reagents for digestion are added. Swab used for sampling peptides from the surface can be centrifuged in order to analyze the supernatant by HPLC-MS, or directly converted into a support for Swab TS-MS analysis

In this case, the assessment of recovery of the sampled proteins resulted difficult since it was observed a different efficiency of protein sampling on the basis of the peptide taken into account. This can be evidenced reporting, for each peptide, the ratio of the signal obtained by the two swabbing protocols (i.e *in situ digestion/swabbing* and *swabbing/swab digestion*) as in **Figure 3.17**. *In-situ digestion/swabbing* resulted less efficient respect to the *swabbing/swab digestion* protocol, with a signal decrease from about 150-fold to 4-fold depending on the peptide.

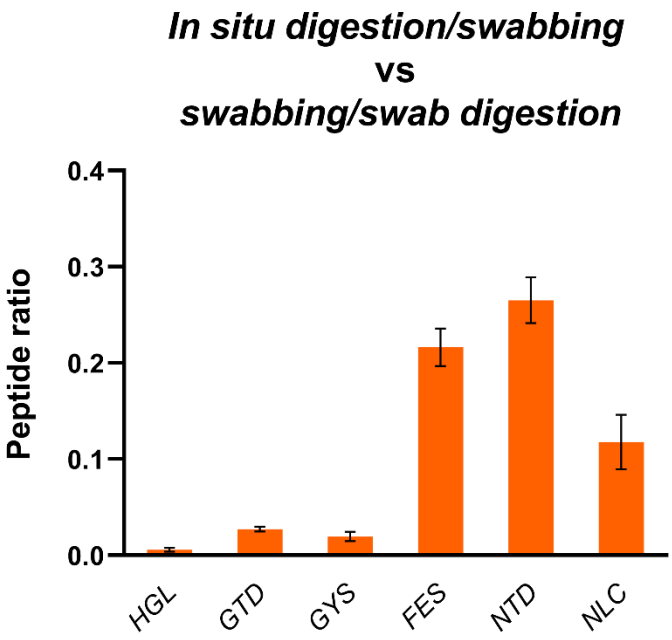


**Figure 3.17.** Comparison of *in situ digestion* to *swabbing/swab digestion* procedure, reported as signal ratio of different peptides between the two procedures. Both experiments were performed by spraying lysozyme on two distinct 10x10 cm squared surface (100 mg/L concentration)

Further investigations permitted to explain these findings in terms of a different peptide profile when digestion is carried out *in solution* respect to *in situ*, directly on the surface, as shown in **Figure 3.18,** where the signal of a peptide is normalized respect to *NTD* peptide chosen as reference. Interestingly, *in situ digestion* has a greater negative impact on certain peptides compared to others.

The *in situ digestion/swabbing* was applied also for lysozyme detection after the contamination of the surface with egg white powder at different µg/cm$^2$ contamination levels. The results confirmed the same peptide profile observed for standard lysozyme (**Figure 3.18**).

In **Figure 3.18**, a yellow rectangle highlights results on standard lysozyme digested in three distinct procedures (*in situ digestion/swabbing*, *swab digestion* and *in solution digestion*, respectively from left to right).

The results reported on the differential negative impact that *in situ digestion* has on distinct peptides are consistent with what is reported in **Figure 3.17**.

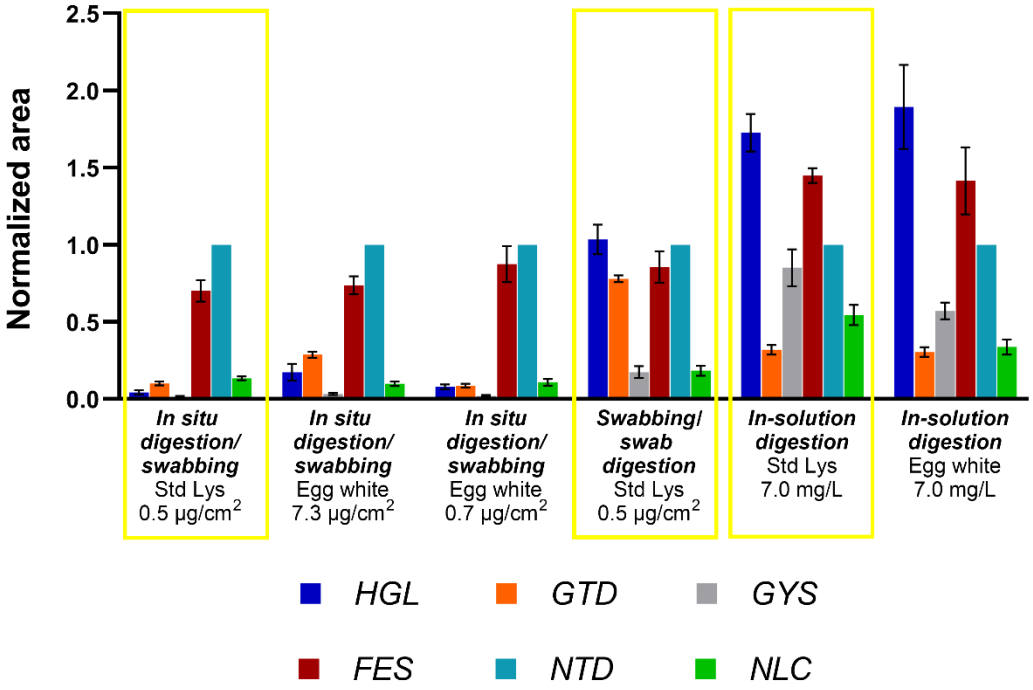


**Figure 3.18.** Normalized signals of peptides for lysozyme, both from standard solution (Std Lys) or in egg white powder, in case of *in-solution digestion*, *swabbing/swab digestion* and *in situ digestion/swabbing* procedures. A yellow rectangle highlights experiments from every procedure, performed on standard solution of lysozyme, permitting comparison between different peptide profiles while performing distinct digestion procedures. Comparison of the same digestion procedure between lysozyme digested from standard solution or in egg white powder permits to notice a similar digestion pattern. Signals are normalized respect to *m/z* 877.4 → 730.4 extracted transition (peptide *NTD*)

It is important to specify that *in situ* digestion implies contamination of a working surface by allergenic proteins but, more important, other chemicals like DTT, IAA and trypsin. Addition of other chemicals might be unwanted if carried out on a surface where food products are continuously made. For this reason, the *in situ digestion/swabbing* method is intended to be exploited for study development of new cleaning procedures, to be conducted on dedicated surfaces. Nevertheless, in-solution digestion after protein swab sampling is a viable method to avoid further contamination on the surface.

### 3.5.4. Surface contamination with egg white powder at different concentration levels

Analysis of contaminated surface with egg white at different concentrations was performed in order to establish the detection limit of the *in situ digestion/swabbing* strategy. As previously said, investigated swabbing strategies were functional to enable direct AMS screening, as well as LC-MS/MS confirmatory analysis (as presented in **Figure 3.16**). LODs for both LC-MS/MS and Swab TS-MS method were established, using *in situ digestion/swabbing* procedure.

It is important to notice that limits are reported as a quantity of lysozyme or egg white powder that contaminates a working surface ($\mu g/cm^2$). Moreover, it has to be taken into account that the percentage of lysozyme in the egg white powder was 2.7%.

### 3.5.5. *In situ digestion/swabbing* and Liquid Chromatography–Electrospray Ionization-Tandem Mass Spectrometry analysis of lysozyme from egg white

The stainless-steel surface was contaminated with egg white at different $\mu g/cm^2$ concentrations, and samples were analyzed by HPLC-ESI-MS/MS, in order to determine the minimal detectable residue on the surface. In **Figure 3.19**, extracted chromatograms of six MS/MS transition by HPLC-ESI-MS/MS analysis from surface contamination of egg white at 0.7 $\mu g/cm^2$ (corresponding to 0.023 $\mu g/cm^2$ lysozyme) are presented.

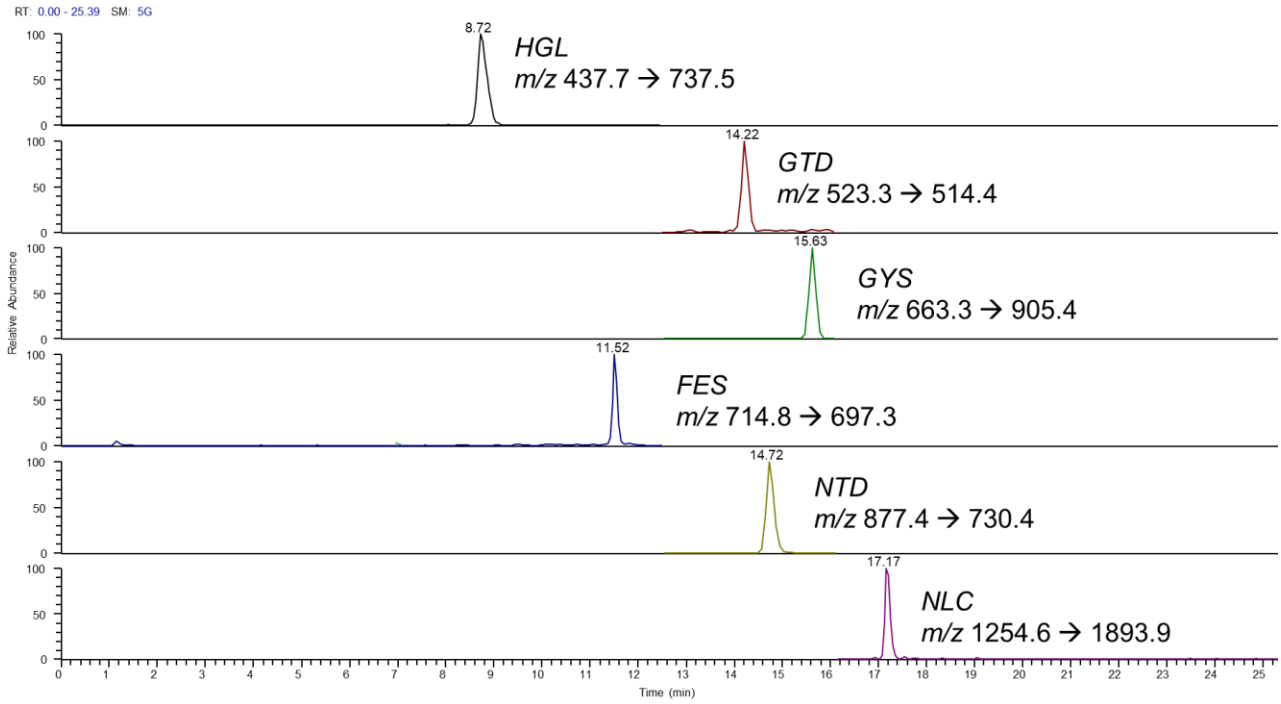


**Figure 3.19.** Extracted chromatogram of 6 peptide transitions of lysozyme from surface contamination at 0.7 µg/cm$^2$ of egg white (corresponding to 0.023 µg/cm$^2$ of lysozyme), LC-ESI-MS/MS analysis

The limit of detection (signal giving a S/N ratio of 3) was assessed as 0.003 µg/cm$^2$ of egg white, corresponding to a lysozyme contamination level of 82 pg/cm$^2$, calculated on the two most intense peptides (*FES* and *NTD*). Such limit is acceptable, especially considering the reduced efficiency of the *in situ* procedure compared to *swabbing/swab digestion*. Signal intensities of target peptides at three different surface contamination levels and performing *in situ digestion/swabbing* procedure are reported in **Figure 3.20**.

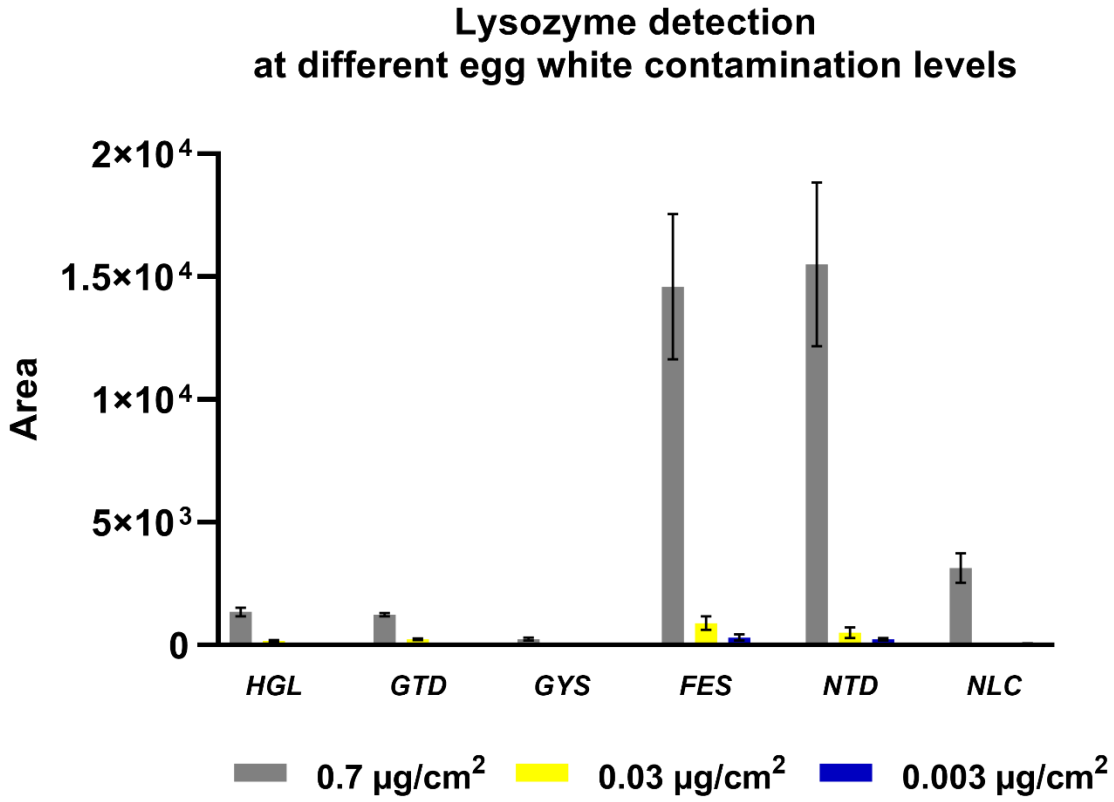


**Figure 3.20.** Signal from lysozyme peptides at different levels of surface contamination of egg white powder (n=3), performing *in situ digestion/swabbing* strategy and analysis by LC-ESI- MS/MS

### 3.5.6. *In situ digestion* – Swab Touch Spray-Mass Spectrometry/High Resolution Mass Spectrometry analysis of lysozyme from egg white

Finally, Swab TS-MS analysis was performed after *in situ digestion/swabbing* of a surface contaminated with chicken egg white powder. According to *in situ* procedure for contamination and protein digestion on steel surface, solutions of chicken egg white powder at different concentrations were sprayed, in order to assess the limits of detection of the entire procedure. LOD was estimated at a surface contamination level of 68 µg/cm$^2$ of egg white powder (1.84 µg/cm$^2$ of Lys). MS/HRMS spectra of two target peptides are reported in **Figure 3.21**. As expected, the present limit is notably higher that that one reported by HPLC-MS/MS detection. Advantage of the Swab TS-MS consists in the rapidity of the measure, since there is not required any chromatographic separation.

**a**

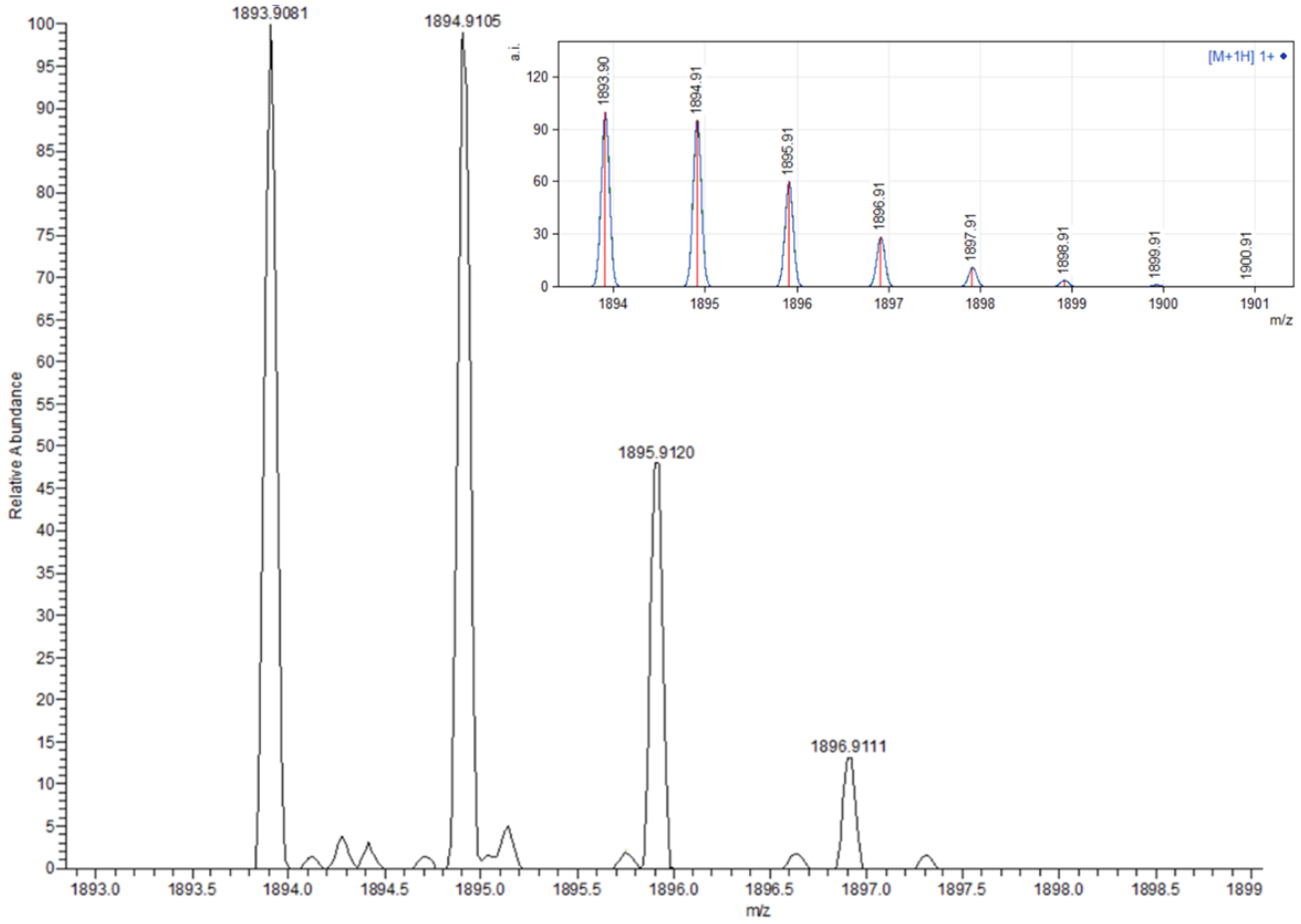
1893.9081
1894.9105
1895.9120
1896.9111
Relative Abundance
m/z
a.i.
[M+1H] 1+
1893.90
1894.91
1895.91
1896.91
1897.91
1898.91
1899.91
1900.91

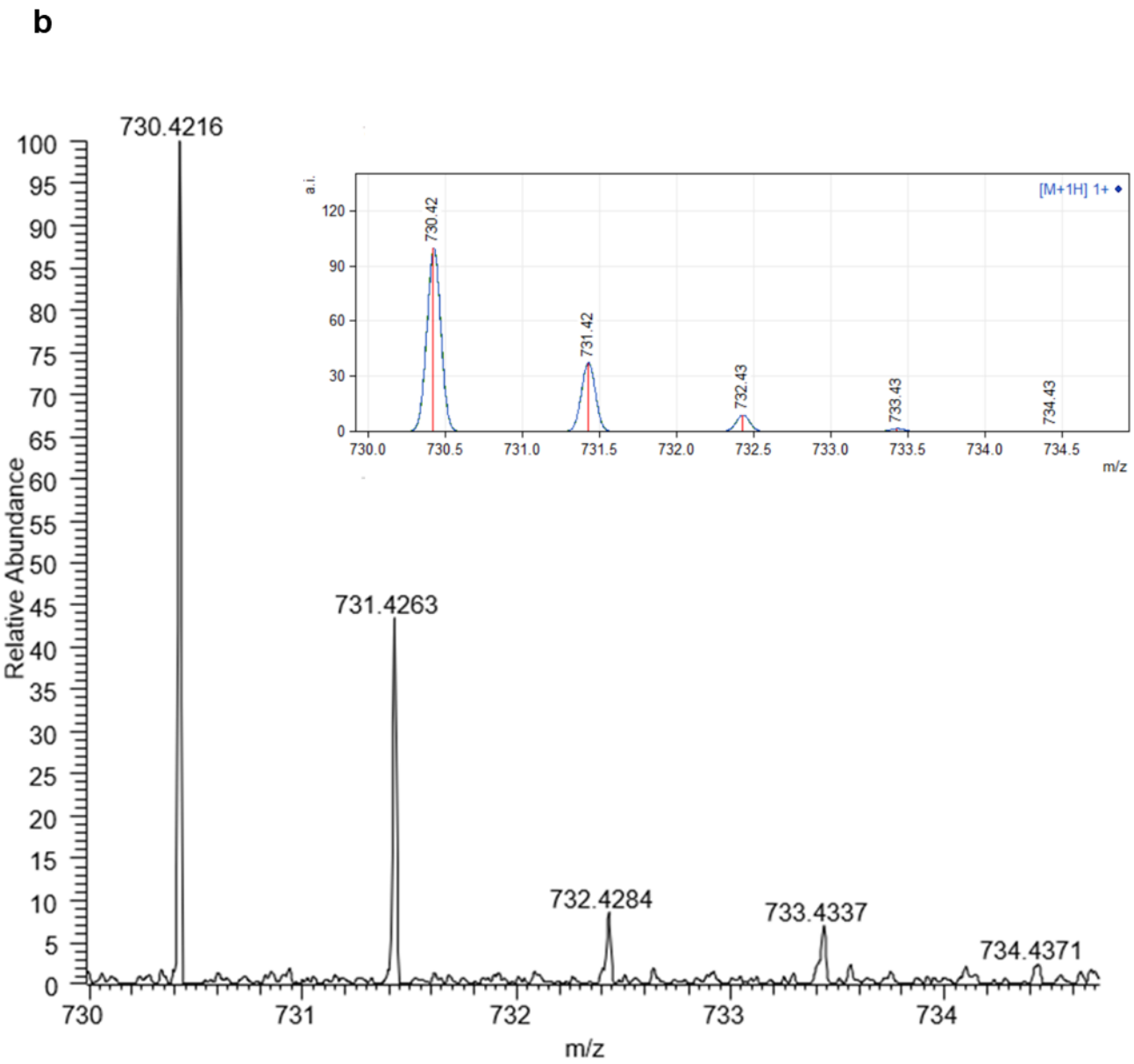


**Figure 3.21.** MS/HRMS spectra by Swab TS-MS analysis from surface contamination at 368 µg/cm$^2$ of egg white (corresponding to 10 µg/cm$^2$ of Lys) for **a)** *NLC* peptide (mass accuracy < 3 ppm) and **b)** NTD peptide (mass accuracy < 1 ppm). Simulated isotopic distribution of peptide fragments is reported top right of each figure. In both cases, experimental distribution follows the same pattern of simulated

When the *in-situ digestion/swabbing* with Swab TS-MS method was applied to real matrix, a physical contamination of L-shape modified transfer line was observed; for this reason the transfer line required frequent cleaning to prevent it from clogging. This is probably due to the powdery nature of the egg white used for contamination. In general, the application of AMS technique to real matrices has to face the complexity of the matrix while keeping to a minimum the sample treatment.

## 3.6. Conclusions

Swab TS-MS has born as a convenient technique for its rapidity and minimally invasive sampling, exploited in clinical field of application, moving through drug detection, investigation of tumor presence onto sampled tissues, or even organic gunshot residues after firearm discharge in forensic analysis. To the best of our knowledge, this work represents the first time Swab TS-MS technique is being used for protein detection, and in particular in the food allergen field. The aim of the present work consisted in developing Swab TS-MS method for the detection of food allergenic protein residues on food-contaminated working surfaces. On the basis of the working principles, Swab TS – MS technique could be particularly suitable for this purpose, since it exploits the swab, used for sampling, as a probe for desorption and ionization.

In this work, egg white lysozyme was used as case study, taking into account that egg is the second most important allergenic ingredient globally, following cow's milk. Egg allergy is primarily induced by four proteins of egg white, included lysozyme, ovotransferrin, ovoalbumin, and ovomucoid. The work can be divided into two parts: in the first, the suitability of Swab TS-MS for lysozyme detection was assessed, and a method for detection of digested lysozyme was developed. In the second part, study of swabbing strategies from contaminated surfaces was conducted, in view of the implementation of Swab TS-MS analysis. The study of swabbing strategies was conducted by HPLC-ESI-MS/MS techniques, that also represent a confirmatory method. Lysozyme from chicken egg white was selected as case study.

Swab TS-MS permitted the detection of digested lysozyme, and not of the intact protein. Different experimental conditions, such as geometric factors, solvent nature and composition, acquisition mode, were studied, in order to find a good compromise between signal intensity and stability over the analysis time.

It has to be pointed out that the selection of EtOH as extracting solvent has a great impact for its sustainability, and it contributes to increase the greenness of the developed method. In fact, all AMS are green by definition, since they require an extremely reduced consumption of time and solvents. The developed Swab TS-MS method involves 6 μL/min of solvent flow rate, and analysis lasts up to 5 minutes. This represents a minimal consumption, especially if compared with a conventional hyphenated MS method, consuming hundreds of microliters per minute for tens of minutes. Hence, the developed method is compliant with Green Analytical Chemistry (GAC) rules [32].

After the assessment of analytical quality parameters for lysozyme detection, the method was applied also to food matrix, in particular by digesting egg white powder and targeting lysozyme's peptides.

LOD was reported at 1.2 µg digested lysozyme in egg powder referring to the peptide having the best response (NLC peptide).

Use of an internal standard (IS) was investigated. MRFA peptide was identified as a possible IS, added to the extracting solvent. Preliminary investigations did not lead to significant improvement of the precision, probably due to manual change of MS/HRMS event as well. Nevertheless, utilization of MRFA as IS could be considered in the future, starting from standardized conditions and taking advantage, for example, of the automated multiplexing acquisition mode, that would enable extremely rapid alternate MS/HRMS acquisition of the analyte and IS.

During the second part of the work, activities focused on investigation of swabbing strategies to obtain peptides from a protein-contaminated surface, performing sampling by a swab and immediately and directly submit it to Swab TS-MS analysis. All the investigations about swabbing strategies were performed by LC-ESI-MS/MS technique, that also constitutes a confirmatory method complementing the rapid AMS screening application.

In this context, two strategies were investigated in order to obtain peptides from protein digestion on the swab. Since the sampling strategy should meet the philosophy of Swab TS-MS, particular attention was paid on the development of in-situ digestion followed by swab sampling of the surface. *In situ digestion/swabbing* method with LC–ESI-MS/MS analysis presented a limit of detection of 0.003 µg/cm$^2$ of egg white powder, corresponding to 82 pg/cm$^2$ of lysozyme. As for Swab TS – MS technique, LOD was estimated at a surface contamination level of 68 µg/cm$^2$ of egg white powder (corresponding to 1.84 µg/cm$^2$ of lysozyme).

The present study represents the starting point of the application of AMS, in particular Swab TS-MS, for the analysis of food allergens. The developed procedure can be exploited for studying new cleaning procedures or for check of those already developed, with the possibility to extend the method toward multiplexing analysis, in order to cover more allergenic proteins and ingredients in a single analysis. This represents one of the major advantages of MS analysis with respect to traditional commercial immunochemical assays, that target a single protein per analysis.

In parallel, Paper Spray–MS (PS-MS) suitability for lysozyme detection was investigated, as a possible alternative to Swab TS application. Detection of lysozyme as entire protein and peptides from tryptic digestion was possible, using proper paper substrate and extracting solvent. Paper spray could be exploited for this application after swab sampling, analyzing eluted sampled solution from swab's tip.

## Bibliography


(1) Sicherer, S. H.; Sampson, H. A. Food Allergy: A Review and Update on Epidemiology, Pathogenesis, Diagnosis, Prevention, and Management. *Journal of Allergy and Clinical Immunology* **2018**, *141* (1), 41–58. https://doi.org/10.1016/j.jaci.2017.11.003.

(2) Urisu, A.; Kondo, Y.; Tsuge, I. Hen's Egg Allergy. *Chem Immunol Allergy* **2015**, *101*, 124–130. https://doi.org/10.1159/000375416.

(3) Iweala, O. I.; Choudhary, S. K.; Commins, S. P. Food Allergy. *Current Gastroenterology Reports*. Current Medicine Group LLC 1 May 1, **2018**. https://doi.org/10.1007/s11894-018-0624-y.

(4) Mendonca, C.; Andreae, D. Food Allergy. *Primary Care: Clinics in Office Practice* **2023**, *50* (2), 205–220. https://doi.org/10.1016/j.pop.2016.04.008.

(5) Sampath, V.; Abrams, E. M.; Adlou, B.; Akdis, C.; Akdis, M.; Brough, H. A.; Chan, S.; Chatchatee, P.; Chinthrajah, R. S.; Cocco, R. R.; Deschildre, A.; Eigenmann, P.; Galvan, C.; Gupta, R.; Hossny, E.; Koplin, J. J.; Lack, G.; Levin, M.; Shek, L. P.; Makela, M.; Mendoza-Hernandez, D.; Muraro, A.; Papadopoulous, N. G.; Pawankar, R.; Perrett, K. P.; Roberts, G.; Sackesen, C.; Sampson, H.; Tang, M. L. K.; Togias, A.; Venter, C.; Warren, C. M.; Wheatley, L. M.; Wong, G. W. K.; Beyer, K.; Nadeau, K. C.; Renz, H. Food Allergy across the Globe. *Journal of Allergy and Clinical Immunology* **2021**, *148* (6), 1347–1364. https://doi.org/10.1016/j.jaci.2021.10.018.

(6) Anvari, S.; Miller, J.; Yeh, C. Y.; Davis, C. M. IgE-Mediated Food Allergy. *Clin Rev Allergy Immunol* **2019**, *57* (2), 244–260. https://doi.org/10.1007/s12016-018-8710-3.

(7) De Martinis, M.; Sirufo, M. M.; Suppa, M.; Ginaldi, L. New Perspectives in Food Allergy. *Int J Mol Sci* **2020**, *21* (4). https://doi.org/10.3390/ijms21041474.

(8) Ortiz, J. C.; Galan-Malo, P.; Garcia-Galvez, M.; Mateos, A.; Ortiz-Ramos, M.; Razquin, P.; Mata, L. Survey on the Occurrence of Allergens on Food-Contact Surfaces from School Canteen Kitchens. *Food Control* **2018**, *84*, 449–454. https://doi.org/10.1016/j.foodcont.2017.09.003.

(9) Cavazza, A.; Mattarozzi, M.; Franzoni, A.; Careri, M. A Spotlight on Analytical Prospects in Food Allergens: From Emerging Allergens and Novel Foods to Bioplastics and Plant-Based Sustainable Food Contact Materials. *Food Chem* **2022**, *388*. https://doi.org/10.1016/j.foodchem.2022.132951.

(10) Galan-Malo, P.; López, M.; Ortiz, J. C.; Pérez, M. D.; Sánchez, L.; Razquin, P.; Mata, L. Detection of Egg and Milk Residues on Working Surfaces by ELISA and Lateral Flow Immunoassay Tests. *Food Control* **2017**, *74*, 45–53. https://doi.org/10.1016/j.foodcont.2016.11.027.

(11) Arrizabalaga-Larrañaga, A.; Ayala-Cabrera, J. F.; Seró, R.; Santos, J. F.; Moyano, E. Ambient Ionization Mass Spectrometry in Food Analysis. In *Food Toxicology and Forensics*; Elsevier, **2020**; pp 271–312. https://doi.org/10.1016/B978-0-12-822360-4.00006-6.

(12) Tsagkaris, A. S.; Nelis, J. L. D.; Ross, G. M. S.; Jafari, S.; Guercetti, J.; Kopper, K.; Zhao, Y.; Rafferty, K.; Salvador, J. P.; Migliorelli, D.; Salentijn, G. I.; Campbell, K.; Marco, M. P.; Elliot, C. T.; Nielen, M. W. F.; Pulkrabova, J.; Hajslova, J. Critical Assessment of Recent Trends Related to Screening and Confirmatory Analytical Methods for Selected Food Contaminants and Allergens. *TrAC - Trends in Analytical Chemistry* **2019**, *121*.. https://doi.org/10.1016/j.trac.2019.115688.

(13) Javanshad, R.; Venter, A. R. Ambient Ionization Mass Spectrometry: Real-Time, Proximal Sample Processing and Ionization. *Analytical Methods* **2017**, *9* (34), 4896–4907. https://doi.org/10.1039/c7ay00948h.

(14) Cooks, R. G.; Ouyang, Z.; Takats, Z.; Wiseman, J. M. Ambient Mass Spectrometry. *Science (1979)* **2006**, *311*, 1566–1570. https://doi.org/10.1126/science.1119426.

(15) Seró, R.; Núñez; Moyano, E. Ambient Ionisation-High-Resolution Mass Spectrometry. Environmental, Food, Forensic and Doping Analysis. *Comprehensive Analytical Chemistry* **2016**, *71*, 51–88. https://doi.org/10.1016/bs.coac.2016.01.003.

(16) Fedick, P. W.; Bain, R. M. Swab Touch Spray Mass Spectrometry for Rapid Analysis of Organic Gunshot Residue from Human Hand and Various Surfaces Using Commercial and Fieldable Mass Spectrometry Systems. *Forensic Chemistry* **2017**, *5*, 53–57. https://doi.org/10.1016/j.forc.2017.06.005.

(17) Kerian, K. S.; Jarmusch, A. K.; Cooks, G. G. Touch Spray Mass Spectrometry for in Situ Analysis of Complex Samples. *Analyst* **2014**, *139* (11), 2714–2720. https://doi.org/10.1039/c4an00548a.

(18) Pirro, V.; Jarmusch, A. K.; Vincenti, M.; Cooks, R. G. Direct Drug Analysis from Oral Fluid Using Medical Swab Touch Spray Mass Spectrometry. *Anal Chim Acta* **2015**, *861*, 47–54. https://doi.org/10.1016/j.aca.2015.01.008.

(19) Jarmusch, A. K.; Pirro, V.; Kerian, K. S.; Cooks, R. G. Detection of Strep Throat Causing Bacterium Directly from Medical Swabs by Touch Spray-Mass Spectrometry. *Analyst* **2014**, *139* (19), 4785–4789. https://doi.org/10.1039/c4an00959b.

(20) Morato, N. M.; Pirro, V.; Fedick, P. W.; Cooks, R. G. Quantitative Swab Touch Spray Mass Spectrometry for Oral Fluid Drug Testing. *Anal Chem* **2019**, *91* (11), 7450–7457. https://doi.org/10.1021/acs.analchem.9b01637.

(21) Yang, B. C.; Wang, F.; Yang, X.; Zou, W.; Wang, J. C.; Zou, Y.; Liu, F. Y.; Liu, H.; Huang, O. P. Medical Swab Touch Spray-Mass Spectrometry for Newborn Screening of Nicotine and Cotinine

in Meconium. *Journal of Mass Spectrometry* **2016**, *51* (12), 1237–1242. https://doi.org/10.1002/jms.3892.

(22) Muggli, T. M.; Schürch, S. Analysis of Pesticide Residues on Fruit Using Swab Spray Ionization Mass Spectrometry. *Molecules* **2023**, *28* (18), 6611. https://doi.org/10.3390/molecules28186611.

(23) Jarmusch, A. K.; Pirro, V.; Logsdon, D. L.; Cooks, R. G. Direct Ion Generation from Swabs. *Talanta* **2018**, *184*, 356–363. https://doi.org/10.1016/j.talanta.2018.02.105.

(24) Pallas, N. R.; Harrison, Y. An Automated Drop Shape Apparatus and the Surface Tension of Pure Water. *Colloids and Surfaces* **1990**, *43*, 169–194. https://doi.org/10.1016/0166-6622(90)80287-E.

(25) Tahery, R.; Modarress, H.; Satherley, J. Density and Surface Tension of Binary Mixtures of Acetonitrile + 1-Alkanol at 293.15 K. *J Chem Eng Data* **2006**, *51* (3), 1039–1042. https://doi.org/10.1021/je050519g.

(26) Han, F.; Yang, Y.; Ouyang, J.; Na, N. Direct Analysis of In-Gel Proteins by Carbon Nanotubes-Modified Paper Spray Ambient Mass Spectrometry. *Analyst* **2015**, *140* (3), 710–715. https://doi.org/10.1039/c4an01688b.

(27) Jin, L.; Yajun, Z.; Wei, M.; Theoneste, M.; Zhiping, Z. Polystyrene-Impregnated Paper Substrates for Direct Mass Spectrometric Analysis of Proteins and Peptides in Complex Matrices. *Analytical Methods* **2018**, *10*, 2803–2811. https://doi.org/10.1039/C8AY01081A.

(28) Zhang, Y.; Ju, Y.; Huang, C.; Wysocki. Vicky H. Paper Spray Ionization of Noncovalent Protein Complexes. *Anal Chem* **2014**, *86*, 1342–1346. https://doi.org/10.1021/ac403383d.

(29) Riboni, N.; Quaranta, A.; Motwani, H. V.; Österlund, N.; Gräslund, A.; Bianchi, F.; Ilag, L. L. Solvent-Assisted Paper Spray Ionization Mass Spectrometry (SAPSI-MS) for the Analysis of Biomolecules and Biofluids. *Sci Rep* **2019**, *9* (1), 10296. https://doi.org/10.1038/s41598-019-45358-x.